Assembly of the light-harvesting chlorophyll antenna in the green alga *Chlamydomonas reinhardtii* requires expression of the *CpFTSY* and *CpSRP43* genes

Referent: Prof. Dr. Bernhard Huchzermeyer

Korreferent: Prof. Dr. Anastasios Melis

Tag der Promotion: 02.04.2012

ABSTRACT

In the course of this Ph.D. research, six putative **t**runcated **l**ight-harvesting **a**ntenna (*tla*) *C. reinhardtii* strains, termed *tla2* through *tla7* were investigated. All six strains showed a pale green, chlorophyll (Chl)-deficient phenotype and had a Chl *a* /Chl *b* ratio that was greater than that of the wild type. Physiological analysis revealed similar quantum yields of photosynthesis, but a higher intensity for the saturation of photosynthesis and greater per chlorophyll productivity in the *tla* strains relative to those in the wild type. Biochemical analysis showed that *tla* strains were deficient in the Chl *a-b* light harvesting complex (LHC). A systematic molecular and genetic analysis revealed a single plasmid insertion in the *tla2* strain, causing a chromosomal DNA rearrangement and deletion of five nuclear genes. The *tla2* strain possessed a Chl antenna size of the photosystems that was only about 65% of that in the wild type. The *TLA2* gene was identified as the *C. reinhardtii* homologue to the *Z. mays* and *A. thaliana CpFTSY* gene, whose occurrence and function in green microalgae has not hitherto been investigated. Functional analysis showed that the nuclear-encoded and chloroplast-localized CrCpFTSY protein specifically operates in the assembly of the peripheral components of the Chl *a-b* light-harvesting antenna. By contrast, in higher plants, a *cpftsy* null mutation inhibits the assembly of both the LHC and photosystem complexes, thus resulting in seedling lethal phenotypes. The *tla3* strain also carried a single plasmid insertion in the genomic DNA. The *tla2* strain possessed a Chl antenna size of the photosystems that was about 45% of that in wild type, i.e., more severely affected than the *tla2* strain. It did not assemble $PSII_\alpha$ supercomplexes and only smaller $PSII_\beta$-size units were present. The *TLA3* gene was identified as the *C. reinhardtii* homologue to the *Z. mays* and *A. thaliana CpSRP43* gene, whose occurrence and function in green microalgae has not previously been investigated. Both CpFTSY and CpSRP43 proteins are components of the chloroplast Signal Recognition Particle (CpSRP), whose function is the assembly of transmembrane complexes. Molecular analysis of the *tla4-tla7* strains revealed that they also are either $\Delta cpftsy$ or $\Delta cpsrp43$ disrupted mutants, suggesting that the activity of the CpSRP pathway exerts a dominant influence on the size of light-harvesting antenna. The greater than wild type per chlorophyll productivity of the *tla* mutants suggested that highly-conserved *CpFTSY* and *CpSRP43* genes can be used as tools by which to generate *tla* type strains for improved solar energy conversion efficiency and photosynthetic productivity in plants and algae under mass culture and bright sunlight conditions.

KURZZUSAMMENFASSUNG

In dieser Arbeit wurden sechs durch Plasmidinsertion generierte C. reinhardtii Mutanten untersucht mit Veränderungen in der Lichtsammelantenne (truncated light-harvesting antenna; tla), namentlich *tla2 – tla7*. Alle sechs Stämme zeigen einen hellgrünen, schwach pigmentierten Phänotyp mit einem hohen Chl a/Chl b Verhältnis. Eine physiologische Analyse ergab, dass die Quantenausbeute der Photosynthese jeweils dem Wildtyp ähnelte. Jedoch erreichten die *tla* Mutanten Lichtsättigung erst bei höheren Lichtintensitäten, wobei sie aber eine potentiell höhere Produktivität pro Chlorophyll aufwiesen. Molekulare und genetische Analyse von *tla2* haben gezeigt, dass ein einziges Plasmid in die genomische DNS insertiert wurde, was eine chromosomale Umordnung zur Folge hatte, wobei fünf Gene gelöscht oder unterbrochen wurden. Durch Komplementierung des *tla2* Stammes konnte gezeigt werden, dass das Gen CrCpFTSY, das bisher noch nicht in Grünalgen experimentell untersucht wurde, für den *tla2* Phänotyp verantwortlich ist. Biochemische Analysen des *tla2* Stammes zeigten eine geringere Menge an Lichtsammelproteinen im Vergleich zum Wildtyp, und spektroskopisch wurde die Anzahl von Chlorophyllmolekülen pro Reaktionszentrum auf 65% der Anzahl vom Wildtyp bestimmt. Es konnte gezeigt werden, dass das CrCpFTSY Protein für den Aufbau des Lichtsammelapparates benötigt wird, aber im Gegensatz zu den *Δcpftsy* Mutanten von höheren Pflanzen nicht für den korrekten Zusammenbau der Photosysteme essentiell ist. Im *tla3* Stamm ist ebenfalls ein einziges Plasmid in das Genom integriert. Das *TLA3* Gen wurde als ein Homolog zum A. thaliana *CpSRP43* Gen identifiziert, das zuvor noch nicht in Grünalgen untersucht wurde. Auch im *tla3* Stamm wurde eine starke Abnahme der Lichtsammelproteine beobachtet. Messungen ergaben, dass die Lichtsammelantenne nur noch ca. 45% des Wildtyps umfasst. Spektroskopisch konnten keine PSIIα Supercomplexe, sondern nur noch kleinere $PSII_\beta$ nachgewiesen werden. Untersuchungen an den Stämmen tla4-tla7 zeigten, dass diese entweder *Δcpftsy* oder *Δspsrp43* Mutanten sind. Das lässt vermuten, dass der chloroplastidäre Signal Recognition Particle Weg (CpSRP) zur Integration von Transmembranproteinen einen dominanten Einfluss auf die Größe der Lichtsammelantenne hat. Auf Grund der höheren Photosyntheseleistung pro Chlorophyll könnten die im Pflanzenreich hoch konservierten Gene, *CpFTSY* und *CpSRP43*, Anwendung zur Generierung von *tla* Stämmen zur Steigerung der Solarenergieumwandlung und Photosyntheseleistung in Massenkulturen unter hoher Lichteinstrahlung finden.

KEYWORDS

Photosynthesis, light-harvesting antenna, chloroplast signal recognition pathway

SCHLAGWORTE

Photosynthese, Lichtsammelantenne, Chloroplast-signal-recognition Weg

TABLE OF CONTENTS

INTRODUCTION

Photosynthesis

Photosynthesis is defined as the biological process by which organisms absorb and convert the electromagnetic wave energy of the visible and near infrared regions of the solar spectrum into chemical energy. The evolution of photosynthesis on earth can be divided into two main types, H_2O-oxidizing "oxygenic" photosynthesis, and anoxygenic photosynthesis, where solar energy is converted in the absence of H_2O-oxidation. The overall reaction of photosynthesis in H_2O-oxidizing organisms can be summarized as:

$$CO_2 + 2NADPH + 3\ ATP + 2H^+ + 2H_2O \rightarrow (CH_2O) + 2NADP^+ + 3ADP + 3P_i + H_2O \quad (1)$$
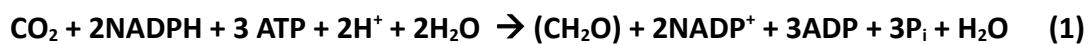
where high potential energy electrons for the generation of reductant (NADPH) and energy for the generation of ATP power are derived from the light reactions of photosynthesis; and where the carbon reactions of photosynthesis convert this primary forms of energy into carbohydrate equivalents (CH_2O).

In oxygenic photosynthesis, electrons for the generation of NADPH are derived from H_2O according to the reaction:

$$2H_2O \rightarrow 4e^- + 4H^+ + O_2 \quad (2)$$

where O_2 is released into the atmosphere as a waste by-product, and where the potential energy of the electrons is elevated in upon consuption of sunlight energy in photosystem-II and photosystem-I. Oxygen accumulated in the atmosphere over 2.5 billions of years in oxygenic photosynthesis is now is vital to all aerobic life forms on earth. By photosynthesis significant amounts of solar energy are stored into chemical energy, and this is our source of food and fiber for most biological activity and life on earth.

Evolution of photosynthesis

Photosynthesis has probably evolved around 3.2 to 3.5 billion years ago, relatively shortly after the first life forms appeared, about 4 billion years ago. These early forms of photosynthesis were anoxygenic, while oxygenic photosynthesis evolved significantly later, about 2.4 billion years ago (Buick 2008), presumably after electron donors like hydrogen and hydrogen sulfide were depleted. About 1.2 billion years ago, with the event of the incorporation of an ancient symbiotic cyanobacterium into a eukaryote, the first eukaryotic

algae evolved (Rodríguez-Ezpeleta et al., 2005). The descendents of this symbiotic cyanobacterium became the chloroplasts in land plants, which evolved about 0.5 billion years ago.

Oxygenic photosynthesis

Cyanobacteria, algae and plants are capable of performing oxygenic photosynthesis. The reaction has two distinct components, namely the light-reactions and the carbon-reactions of photosynthesis. The light-reactions convert the energy of absorbed photons into chemical energy in form of the energy carrying molecules such as nicotinamide adenine dinucleotide phosphate (NADPH) and adenosine triphosphate (ATP). The energy stored in NADPH and ATP is used by the carbon reactions of photosynthesis to reduce CO_2 and to form organic molecules. The light-reactions are highly conserved in all organisms of oxygenic photosynthesis, as are the two photosystems that perform it. However, there are substantial variations in the light-harvesting pigments content, composition and organization between taxonomically different organisms, and also between the two photosystems.

The light reactions of oxygenic photosynthesis

The light reactions reaction of oxygenic photosynthesis take place in the thylakoid membrane and involve the function of four protein holocomplexes, namely photosystem II (PSII), cytochrome b_6f complex, photosystem I (PSI), and ATP synthase. In cyanobacteria the thylakoid membrane derives from the cell's plasma membrane. In algae and plants, the thylakoid membrane is contained within the chloroplast. In all systems, the thylakoid membrane fully encloses an interior space called "the lumen", and separates the lumen from the outside surrounding "stroma phase". The thylakoid membrane can be arranged in stacks, called grana, which are rich in PSII, the interconnecting non-stacked thylakoids called stroma-exposed thylakoids, which are enriched in PSI and the ATP-synthase.

There are two different mechanisms of the light-dependent reactions in oxygenic photosynthesis, linear electron flow and cyclic electron flow.

The light-reactions of photosynthesis drive energy-poor electrons from H_2O to $NADP^+$ via sunlight energy consumption at PSII and PSI. Light absorption and utilization at PSII causes an electron of a tetrapyrrole pigment molecule to attain an elevated energy state. This electron then is transferred through the electron transport chain to the cytochrome b_6f

complex. This electron transport process, and the energy released from it, helps a proton accumulation to occur in the lumen of thylakoids, resulting in a substantial ΔpH across the thylakoid membrane. Peter Mitchell's chemiosmotic hypothesis (Mitchell, 1961) explained how the energy contained within the ΔpH drives the endergonic function of the ATP synthase, resulting in the generation of ATP. Electrons from the cytochrome b_6f complex are further transported to PSI, were the energy of another photon is utilized to elevate the potential energy of the electrons to a much higher level, sufficient to reduce the iron-sulfur protein "ferredoxin". Reduced ferredoxin serves as the ubiquitous reductant in the photosynthetic apparatus, driving the reduction of $NADP^+$ and, to a lesser extent, the reduction of inorganic nitrogen and sulfur compounds into bio-organic molecules. The primary electron acceptor from reduced ferredoxin is, however, nicotinamide adenine dinucleotide phosphate ($NADP^+$), which is reduced to NADPH and thus stores energy originating from the absorbed photons in a chemical form useful to metabolic processes in the chloroplast / cell. As mentioned earlier, electron supply for the process of photosynthetic electron transport is provided by H_2O at PSII, where water is oxidized to release O_2, with protons (H^+) deposited in the lumen, which further increase the value of the proton gradient. The energy stored in the proton gradient is utilized by the ATP synthase to drive incorporation of inorganic phosphate (P_i) into adenosine diphosphate (ADP), thus forming ATP, this process of light depended ATP, in a process referred to as photophosphorylation.

Photosystem II

Photosystem II is a light-driven water:plastoquinone oxidoreductase. It occurs in the appressed thylakoid membrane regions of chloroplasts as a homodimeric protein-cofactor complex with a molecular weight of about 600 kDa. It encompasses at least 22 protein subunits containing at least 99 cofactors per monomer, among these there are 37 chlorophyll a and 12 beta-carotene molecules (Glick and Melis 1988; Barber, 2003; Ferreira et al., 2004; Guskov et al., 2009) Figure 1 shows the structure of PSII-core complex, the chlorophyll molecules and carotenoids are highlighted. The main protein subunits of the PSII-core complex are D1 (encoded by the Cp *psbA* gene), D2 (*psbD* gene), CP47 (*psbB* gene), and CP43 (*psbC* gene). Chlorophyll-proteins CP47 and CP43 are essential for PSII assembly and bind 16 and 14 Chl a molecules respectively and most of the β-carotene in PSII, they function as the internal light-harvesting antenna for PSII (Ferreira et al., 2004). The excitation

energy absorbed by these pigments is transferred to the reaction center (RC) Chl *a* molecule, which is contained by the reaction center D1 and D2 proteins. These proteins bind all the co-factors needed for the PSII electron transport reactions from H_2O to PQ.
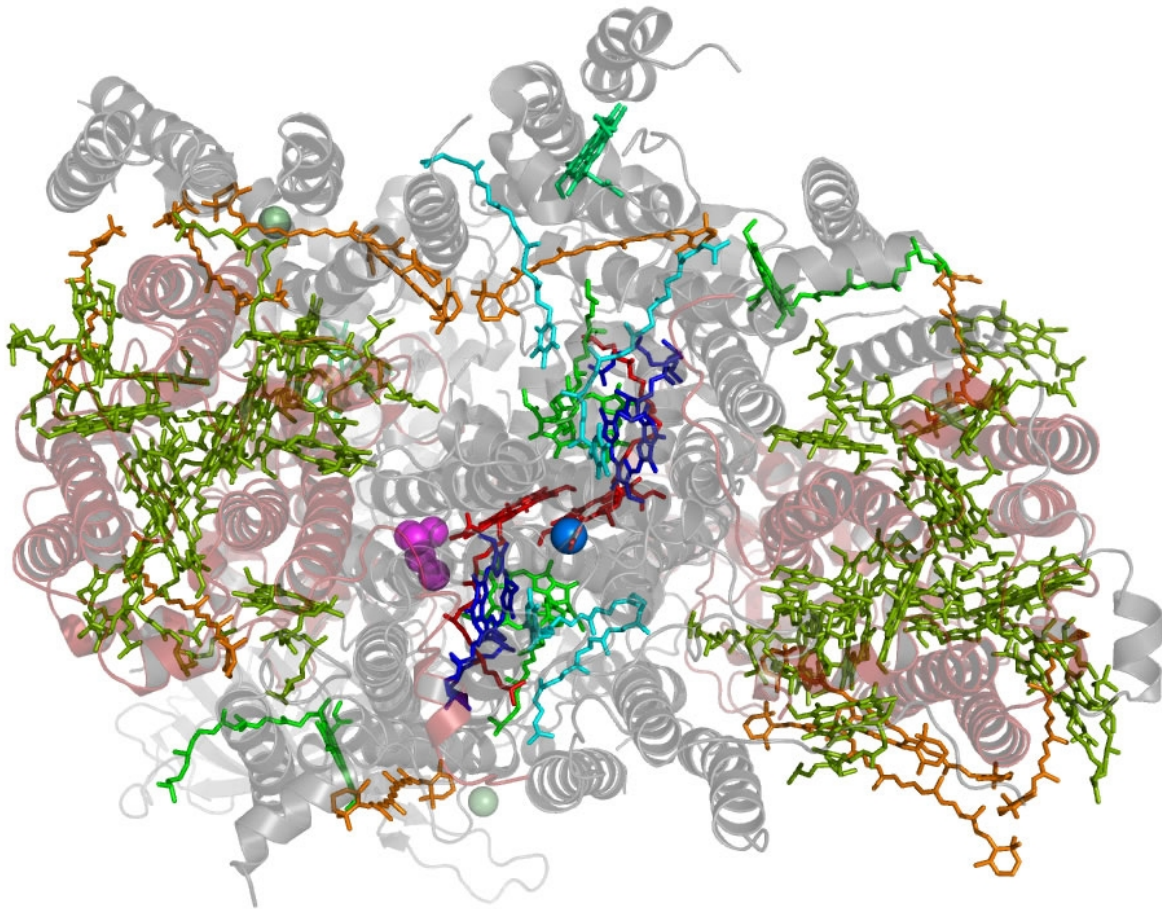
Figure 1: PSII monomer structure. The internal antenna proteins CP43 and CP47 are shown in pale red, the Chl *a* molecules bound to them are shown in moss-green and the carotenoids in orange. P680 is shown in red; Phe: blue; Chl bound to D1 and D2 in lightgreen. The Mn-cluster of the OEC is shown in purple. In total PSII binds 35 Chl *a* molecules functioning as the internal light-harvesting pigments. Structural information by Guskov et al., 2009.

In a temporal sequence of events, excitation energy from the internal light-harvesting antenna (CP43 or CP47) is transferred to the reaction center pair of Chl *a* molecules (P680). The energy of the excited state in P680, namely P680*, is utilized to physically move an electron, within a few picoseconds, from P680 to the adjacent pheophytin (Phe) molecule, also bound to the D1 protein, thus constituting the endergonic "charge separation" reaction and forming two charged radicals: P680$^{\bullet+}$ and Phe$^{\bullet-}$. This initial

charge separation reaction converts the electromagnetic energy of a photon into chemical energy. After the initial charge separation reaction, $P680^{\bullet+}$ and electrons from $Phe^{\bullet-}$ are transferred to the primary plastoquinone electron acceptor (Q_A) to form Q_A^- in a reaction that takes place in the picosecond time scale, thereby separating the two photochemical charges from each other both in an energetic and spatial sense. From the D2 bound semiquinone anion species Q_A^-, the electron is transferred to the secondary plastoquinone electron acceptor (Q_B) to form Q_B^- (Q_B is bound by D1), After a second photochemical turnover, Q_B^- is further reduced to Q_B^{2-}. Two protons from the stroma are then used to protonate Q_B^{2-} to form plastohydroquinone (PQH_2), which has a low-affinity for the D1-QB-binding site, becomes dissociated from the D1 protein and is released into the grana thylakoid membrane lipid bilayer driven by diffusion to the cytochrome b_6f complex for a subsequent oxidation.

To fill the electron gap at $P680^{\bullet+}$, water is oxidized at the Mn-containing site of PSII that is attached to the lumen side of the D1 and D2 protein. The water oxidation process is catalyzed by a cluster of four Mn and one Ca atoms (Nixon and Diner, 1992). The mechanism of this reaction is not completely understood. Kok et al. (1970) presented evidence to support a model for a 4-step oxidation cycle in which two H_2O molecules are oxidized simultaneously, following the sequential absorption-utilization of four photons by the PSII RC. In the interim, the positive charges resulting from the photochemical cycles are stored on Mn, until all four Mn atoms are oxidized, upon which the catalytic oxidation of $2H_2O$ molecules is enabled.

Photosystem I

Photosystem I is a light-driven plastocyanin:ferredoxin oxidoreductase. It comprises at least 12 protein subunits, and more then 110 co-factors including the PSI-core light-harvesting antenna pigments of 95 chlorophyll *a* molecules (Glick and Melis 1988) most of which are bound to the heterodimeric core complex of PSI consisting of the PsaA and PsaB subunits (Amunts et al., 2010). Figure 2 shows a PSI reaction center in association with light-harvesting proteins. By analogy with PSII, the charge separation reaction in PSI occurs at a pair of chlorophyll molecules (P700) after receiving excitation energy from the internal light-harvesting antenna of PSI. The primary electron acceptor is a bound chlorophyll molecule (A_0). The Following the charge separation reaction between P700 and A_0 ($P700^+ A_0^-$) the

electron is passed on to a phylloquinone (A_1) and via three cubane-type iron sulfur clusters (F_X, F_A and F_B) to ferredoxin (FD), a soluble protein on the stromal side of the thylakoid membrane. Ferredoxin functions as a high potential energy electron carrier, and serves as an electron donor via the enzyme ferredoxin-NADP$^+$ reductase, to generate NADPH. Reduced ferredoxin also serves as a reductant in the conversion of nitrite to ammonia for amino acid synthesis, and in the reduction of sulfate to sulfide for cysteine and methionine biosynthesis. The electron gap at P700$^+$ is filled by electrons originating from PSII (linear electron flow) via the reduced form of the Cu-containing electron carrier Plastocyanin.
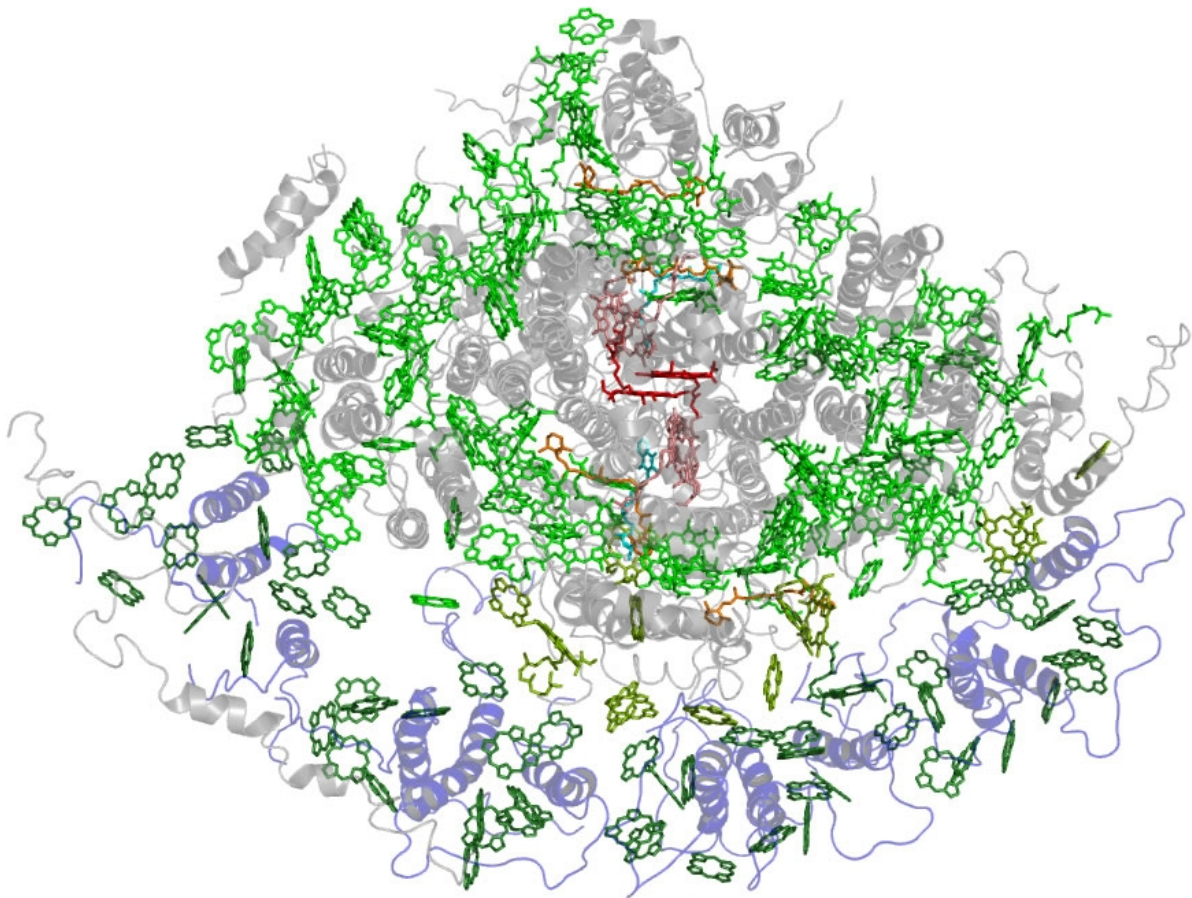
Figure 2: PSI-LHCI super complex structure. The reaction center proteins are shown in gray, the light-harvesting proteins in light blue. The light-harvesting proteins bind only to one side of the PSI complex. P700, A_0 and A_1 are shown in red, Chl molecules bound to the reaction center complex are show in light-green, and those bound to the light-harvesting complexes in dark green. Chl molecues in between the core complex and the light-harvesting proteins which could not clearly be assigned are shown in moss-green. Structural information by Amunts et al., 2010.

Peripheral light-harvesting Chl antenna complexes

Photosynthesis depends on the absorption of sunlight by pigment molecules localized both in the photosystem-core and in peripheral light-harvesting Chl antenna complexes. In higher plants and green algae, a completely functional but minimal PSI unit encompasses the PSI-core of 95 Chl *a* molecules, while the PSII-core functions with a minimal number of 37 Chl *a* molecules (Glick and Melis, 1988; Zouni et al., 2001). Increasing the capacity of the photosynthetic apparatus to absorb sunlight entails the addition of peripheral light-harvesting pigment-proteins associated with each photosystem-core complex. This auxiliary peripheral to the photosystems antenna contains Chl *a* and Chl *b* molecules. An enlarged Chl antenna size, often exceeding 200 Chl molecules for each photosystem, is thought to afford a competitive survival advantage to the organism in an environment where sunlight is often the growth-limiting factor (Kirk, 1994). The PSI-core and PSII-core are essentially the same in all H_2O-oxidizing photosynthetic organisms. However, taxonomically different species evolved a variety of different strategies and peripheral pigment-proteins to be associated with PSI and PSII. These light-harvesting antenna protein complexes from so called super-complexes with the photosynthetic reaction centers. The photosystem-peripheral light-harvesting complexes serve as auxiliary antennae for the collection of sunlight energy and as a conducting medium for excitation energy migration towards a photochemical reaction center (Smith et al., 1990).

Proteins of the peripheral light-harvesting complex in plants and green algae belong to the same large family, which presumable arose by multiple gene duplication and fusion events (Montané and Kloppstech, 2000). They share a general structure of three transmembrane helices with the N-terminus being exposed in the soluble phase on the stromal side of the thylakoid membrane, while the C-terminus is in the lumen. These pigment-proteins each contains 10-15 Chl *a* and Chl *b* molecules and 3-4 xanthophylls (Liu et al, 2004; Pan et al, 2011; Castelletti et al, 2003; Croce et al, 2002). PSI and PSII assemble separate light-harvesting holocomplexes, each encoded for and defined by a different set of genes. The *LHCA* gene subfamily encodes for proteins of the light-harvesting complex I (LHCI) associated with PSI, while the *LHCB* gene subfamily encodes for proteins of the light-harvesting complex II (LHCII) associated with PSII (Jansson et al. 1992).

Light-harvesting complex of photosystem II

The peripheral light-harvesting complex of photosystem II in higher plants consist of six distinct pigment-containing proteins, namely LHCB1-6. Multiple copies of genes usually encode these proteins. In *Arabidopsis thaliana,* for example, the LHCB1 protein is encoded by five copies of the *LHCB1* gene (Elrad and Grossman, 2004). Within the LHCB1-6 proteins there are two groups, the minor and major light-harvesting proteins, distinguished by their relative abundance in the thylakoid membrane (Harrison and Melis, 1992). The minor proteins, namely LHCB4-6, are found in close proximity to the PSII-core (Fig. 3). They do not from higher-order complexes with each other and are thus monomeric. Usually one of each minor light-harvesting proteins is found per PSII reaction center. The major light-harvesting proteins, LHCB1-3, form hetero trimers with each other. Compared to the minor antenna they are more loosely associated with to the PSII-core and their abundance can vary substantially depending on environmental conditions. Biochemical quantification of the LHCB proteins, in association with a precise measurement of the Chl *a* and Chl *b* molecules contained in a PSII holocomplex, helped define a stoichiometry of $(LHCB1)_9$ $(LHCB2)_3$ $(LHCB3)_2$ $(LHCB4)_2$ $(LHCB5)_1$ $(LHC6)_1$ per PSII complex in barley chloroplasts (Harrison and Melis 1992).

The light-harvesting complex of PSII in the model green algae *Chlamydomonas reinhardtii* is also composed of minor and major light-harvesting Chl-proteins. However, *C. reinhardtii* has a different set of genes encoding for these light-harvesting proteins. Two genes encode for the minor light-harvesting antenna proteins, LHCB4 and LHCB5, thus *C. reinhardtii* is missing the LHCB6 protein found in higher plants (Elrad and Grossman, 2004). The major light-harvesting proteins are encoded by nine genes, *LHCBM1-LHCBM6, LHCBM8, LHCBM9* and *LHCBM11* (Elrad and Grossman, 2004).

The LHCII assembly takes place in a stepwise fashion. A newly assembled PSII-core first acquires a partial complement of the peripheral light-harvesting antenna, increasing its Chl content from 37 to about 120-130 chlorophyll molecules per reaction center. This structural configuration constitutes the so-called called $PSII_\beta$ form of PSII. It is normally found in the stroma-exposed thylakoid membranes (Melis, 1991). Addition of trimeric light-harvesting protein complexes to $PSII_\beta$ converts the latter to the fully pigmented $PSII_\alpha$ supercomplex, possessing a fully developed LHCII with up to 250 Chl *a* and Chl *b* molecules.

The stacked membranes of grana thylakoids are the locus of PSII$_\alpha$ (Melis, 1991). This stepwise process of LHCII assembly is reversible and helps facilitate the PSII$_\alpha$ disassembly that occurs during the repair of PSII from a frequently-occurring photodamage (Guenther and Melis, 1990; Melis 1999).
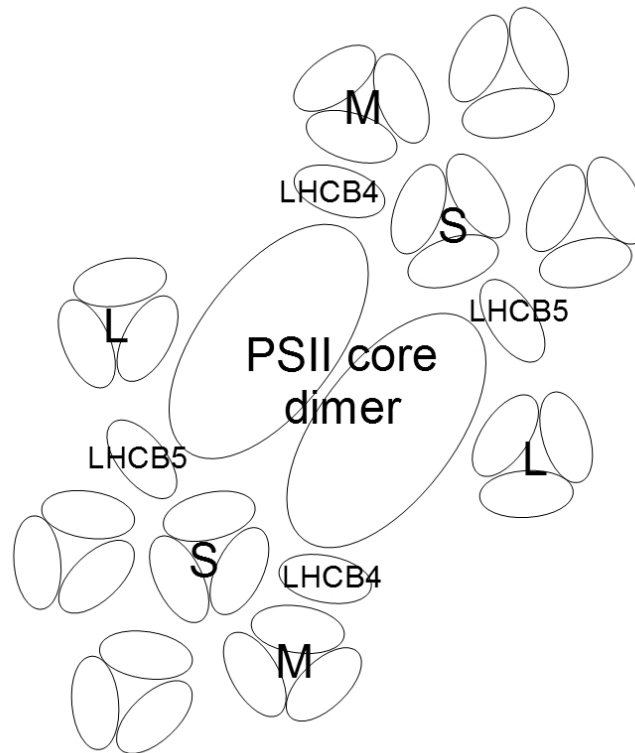
Figure 3: Model of *C. reinhardtii* PSII-LHCII super-complex. One of each minor lightharvesting proteins (LHCB4 and LHCB5) is bound to a PSII monomer. The major lightharvesting Chl-proteins form heterotrimer complexes named, S, M and L. Each PSII-core monomer binds 37 Chl *a* molecules. Each heterotrimer LHC-II complex binds about 40-45 Chl *a* and Chl *b* molecules. Spectroscopic measurements have show that there must be more trimeric light-harvesting complexes in this model shown without label, to bring the number of Chl molecules found in association with a PSII monomer to about 250-300 (Ley and Mauzerall, 1982; Smith et al., 1990; Harrison and Melis, 1992)

Light-harvesting complex of photosystem I

The light-harvesting complex associated with photosystem I (LHCI) in higher plants is composed of four proteins, namely LHCA1-4. LHCA1 and LHCA4 can from heterodimers (Croce et al., 2002), while LHCA2 and LHCA3 can from either homodimers or heterodimers (Castelletti et al., 2003). The proteins of LCHI in *Chlamydomonas reinhardtii* are encoded by

nine genes, *LHCA1-LHCA9*. These light-harvesting proteins bind to specific locations on the periphery of the PSI-core complex (Amunts et al., 2010) (Fig. 4). Stoichiometric consideration, in combination with a measured PSI holocomplex Chl antenna size of 200 Chl *a* and Chl *b* molecules, suggest that about 8 copies of the LHCI proteins must participate in the formation of the peripheral light-harvesting complex of PSI (Smith et al., 1990).
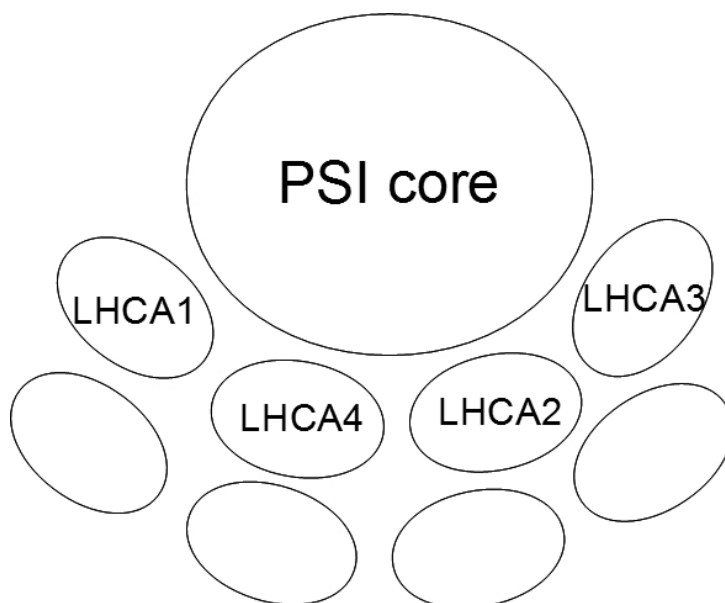
Figure 4: PSI-LHCI supercomplex. The light-harvesting proteins bind on one specific side of the PSI core protein. Each PSI-core monomer binds 95 Chl *a* molecules. Each LHC-I protein binds about 13-15 Chl *a* and Chl *b* molecules. In total there are about 8 LHC-I proteins associated with one PSI reaction center

Physiological variations in the size of the light-harvesting complexes

Given the modular composition and assembly of the photosystems, it is understood that the size of the peripheral light-harvesting complexes is not fixed but could vary substantially depending on the genetic, developmental, and even environmental light conditions. With constraints imposed by the genetics of the system, the Chl antenna size appears to be regulated in photosynthetic organisms inversely to the level of irradiance (Smith et al., 1990; Ballottari et al., 2007). A smaller PS absorption cross-section under high-light helps to limit the rate of excitation trapping and charge separations in each reaction center, helping to conserve resources and leading to less photodamage and photoinhibition

events in the chloroplast (Ballottari et al., 2007). The Chl antenna size regulatory mechanism is highly conserved and functions in all organisms of oxygenic and anoxygenic photosynthesis (Anderson 1986, Nakada et al., 1995, Escoubas et al., 1995, Huner et al., 1998, Yakovlev et al., 2002, Masuda et al., 2003).

Adjustments in the antenna size of PSII are implemented mainly by the removal or addition of the trimeric LHCB subunits (Mawson et al., 1994; Ballottari et al., 2007). While under low light conditions these peripheral trimers are abundant in the LHCII, they are depleted under high irradiance growth conditions (Mawson et al., 1994; Web and Melis, 1995; Ballottari et al., 2007). Experimental evidence has shown up to 300 chlorophyll molecules associated with PSII under low-light growth, whereas as few as ~60 molecules per PSII reaction center were measured under high light conditions in green microalgae (Ley and Mauzerall, 1982; Smith et al., 1990; Harrison and Melis, 1992).

The light-harvesting antenna complex of PSI can also vary with the light intensity during growth. A maximum of ~ 250 molecules of Chl molecules per PSI was measured under low light growth conditions and a minimum of ~100 Chl molecules was reported under high irradiation growth (Ley and Mauzerall, 1982; Smith et al., 1990).

Protein import and routing in the chloroplast

The chloroplast of higher plants and green algae contains about 3,000 different proteins. About 100 of these proteins, depending on the species, are encoded by the chloroplast genome (Sugiura, 1989), whereas the vast majority of the chloroplast proteome is encoded in the nucleus. The products of these nuclear encoded genes carry a so-called transit peptide composed of 30-130 amino acids on the amino-terminal of the protein. This sequence targets the nuclear-encoded protein to the chloroplast. The post-translational import of the nuclear-encoded and cytosol-synthesized precursor protein through the outer and inner envelope membranes of the chloroplast is mediated by the 'translocon at the outer envelope membrane of chloroplasts' (Toc) and the 'translocon at the inner envelope membrane of chloroplasts' (Tic) (Jarvis and Soll, 2002; Jarvis and Robinson 2004). Upon import in the stroma, the transit peptide is cleaved off by an ATP-dependent ClpC protease. Depending on the final destination of the protein, it either takes its final conformation (stroma targeted), or is further targeted to the internal thylakoid membrane compartments

of the chloroplast. Proteins that are targeted to the thylakoid lumen are processed by the Twin-Arginine Translocation (TAT) pathway, or by a pathway similar to the secretory (SEC) pathway of bacteria. Both pathways require an additional target peptide that is unmasked after the chloroplast transit peptide is cleaved off (Hageman et al., 1986; Smeekens et al., 1986; Ko and Cashmore, 1989; Chaddock et al., 1995). The SEC pathway uses an ATP-driven translocation complex to facilitate the transport through the membrane, similar to the SEC translocase found in bacteria (Yuan et al., 1994; Laidler et al., 1995; Schuenemann et al., 1999). The TAT pathway derives its name from a twin-arginine motif in the translocation signal peptide (Chaddock et al., 1995). In contrast to the SEC translocase, the TAT-pathway is capable of transporting proteins in its folded configuration across the thylakoid membrane (Hynds et al., 1998; Clark and Theg, 1997). The translocation of proteins via the TAT pathway is thought to be dependent on the pH gradient across the thylakoid membrane as indicated by *in vitro* experiments (Mould and Robinson, 1991; Klösgen et al., 1992; Cline et al., 1992), hence the TAT pathway is sometimes referred too as the ΔpH-dependent pathway. However, *in vivo* studies with *C. reinhardtii* could not demonstrate any ΔpH dependence (Finazzi et al., 2003).

In higher plants the light-harvesting proteins and some PSII- and PSI-core proteins are integrated into the thylakoid membrane via a pathway similar to the signal recognition partial (SRP) pathway in bacteria (Pool, 2005). The chloroplast signal recognition particle pathway (CpSRP) is capable of co-translational and post-translational insertion into the lipid bilayer of thylakoid membrane proteins. The co-translational function is essential for the insertion of proteins encoded by the chloroplast genome like the PSII reaction center D1 protein (Nilsson and van Wijk, 2002; Zhang and Aro, 2002; Pilgrim et al, 1998; Dewez et al. 2009). It involves the chloroplast signal recognition particle protein CpSRP54, the chloroplast SRP integrase (ALB3) and the SEC translocase CpSECY (Zhang et al, 2001; Klostermann et al., 2002; Pasch et al., 2005). Mechanistically, CpSRP54 binds to a newly synthesized protein and guides it to ALB3 and CpSECY for co-translational integration into the thylakoid membrane.

The post-translational integration of thylakoid membrane proteins requires two proteins forming the signal recognition particle (CpSRP), namely CpSRP54 and CpSRP43, a signal recognition receptor, namely CpFTSY, and the integrase ALB3. CpSRP43 is a chaperon to prevent and also reverse aggregation of light-harvesting proteins after import into the

chloroplast (Falk and Sinning, 2010). It is reported to recognize a specific motif between the transmembrane helices 2 and 3 of light-harvesting proteins termed L18 motif (DeLille et al, 2000; Tu et all 2000). CpSRP54 binds to the sequence of the third transmembrane helix of light-harvesting proteins (High et al., 1997), but also recognizes a chromo protein domain on CpSRP43, a protein domain often found in protein-protein interactions (Jonas-Straube et al, 2001; Goforth et al, 2004). The chloroplast signal recognition receptor, CpFTSY, recognizes this complex presumable by interaction with CpSRP54 (Moore et al., 2003) and forms a membrane bound complex (Moore et al., 2003). This large complex is thought to diffuse along the thylakoid membrane until it reaches ALB3. Upon hydrolysis of guanosine triphosphate (GTP) catalyzed by the GTPase domains in CpSRP54 and CpFTSY, the target protein becomes integrated into the thylakoid membrane (Tu et al., 1999). Some transmembrane proteins, if not most, are integrated into the thylakoid membrane independently of nucleoside triphosphates, pH gradient, or any other known pathway for protein integration (Michl et al., 1994; Kim et al., 1998; Mant et al., 2001; Woolhead et al., 2001) and hence a spontaneous integration of these proteins into the thylakoid membrane is postulated.

Knockout mutants of the *CpSRP*-pathway genes

CpSRP gene knockout mutants have been identified and studied in higher plants, specifically *Arabidopsis thaliana* and *Zea mays,* and to a lesser extend in the green algae *Chlamydomonas reinhardtii*. The mutants and their phenotypes are summarized in Table I. The c*psrp43* mutant of *Arabidopsis thaliana* showed a lower Chl content to about 50% of the wild type, as well as significantly lower levels of the light-harvesting proteins (Klimyuk et al, 1999; Amin et al, 1999). Photosystem reaction center and light-harvesting proteins, as well as other chloroplast proteins were lower in abundance in first true leaves of a c*psrp54* mutant of *A. thaliana*, but the protein levels were restored after 3-4 days of cultivation (Pilgrim et al, 1998).

An *Arabidopsis thaliana* T-DNA knockout mutant of c*pftsy* was missing most of the light-harvesting proteins, but was also deficient in PSI and PSII-core and reaction center proteins from the thylakoid membrane (Asakura et al., 2008). The *cpftsy* mutants in both Arabidopsis and maize (i.e., higher plants) were seedling lethal (Asakura et al., 2004; Asakura et al., 2008).

The *Arabidopsis thaliana* mutant of *alb3* had a drastic chlorophyll-deficiency, down to about 5% of that in the wild type and was also seedling lethal, apparently due to the inability to assemble functional photosystems (Sundberg et al., 1997; Asakura et al., 2008).

The genome of *Chlamydomonas reinhardtii* encodes for two ALB3-like proteins, namely *ALB3.1* and *ALB3.2*. The incorporation of the peripheral light-harvesting complexes into the thylakoid membrane but also the correct assembly of D1 into PSII depends on *ALB3.1* (Bellafiore et al., 2002; Ossenbühl et al., 2004). In contrast to the *alb3* mutant in *Arabidopsis thaliana*, the *alb3.1* mutant of *Chlamydomonas reinhardtii* is able to grow photo-autotrophically (Bellafiore et al., 2002). ALB3.2 has been studied by RNA interference and appears to function in the assembly of PSI and PSII as evident by a decreased abundance to 25-50% of wild type levels, while other thylakoid membrane proteins were less affected (Göhre et al., 2006).

Mutated protein	Species	Mutant synonym	Chl content	Affected chloroplast proteins	Viability	References
CpSRP54	*A. thaliana*	*ffc*	25% in first true leaves	reduction of most LHC's, PSI and PSII	yes	(Pilgrim et al, 1998)
CpSRP43	*A. thaliana*	*cao, chaos*	50%	recuction of most LCH's, normal PSI and PSII	yes	(Klimyuk et al, 1999; Amin et al, 1999)
CpSRP54/CpSRP43	*A. thaliana*	*ffc/cao*	15%	strong reduction of LHC's, PSI and PSII	yes	(Amin et al, 1999)
CpFTSY	*A. thaliana*	*cpftsy*	6-7%	strong reduction of LHC's, PSI and PSII	seedling lethal	(Asakura et al., 2008)
CpFTSY	*Z. mays*	*csr1*	12%	strong reduction of LHC's, PSI and PSII	seedling lethal	(Asakura et al., 2004)
ALB3	*A. thaliana*	*alb3*	5%	strong reduction or absence of LHC's, PSI and PSII	seedling lethal	(Sundberg et al., 1997; Asakura et al., 2008)
Alb3.1	*C. reinhardtii*	*ac29*	30%	strong reduction of LHC's, PSI and PSII affected to a lesser extend.	retarded growth	(Bellafiore et al., 2002; Ossenbühl et al., 2004)
Alb3.2 (RNAi)	*C. reinhardtii*	*alb3.2*	25%-50%	strong reduction of PSI and PSII, LHC's affected to a lesser extend	lethal	(Göhre et al., 2006)

Table I: Knockout mutants or RNAi down regulation of CpSRP proteins from the literature. Chlorophyll content is given relative to the wild type.

Genes involved in the assembly of the light-harvesting Chl antenna in *Chlamydomonas reinhardtii*

In addition to *ALB3.1* there are independently-known genes that play a role in defining the size of the light-harvesting complex in the green algae *Chlamydomonas reinhardtii*, namely *TLA1 and NAB1* (Polle et al., 2003; Mussgnug et al., 2005; Tetali et al, 2007; Mitra and Melis, 2010). The nucleic acid-binding protein NAB1 binds to the mRNA of the major *LHCB* genes in the cytosol and, thereby, inhibits and represses their translation (Mussgnug et al., 2005). Consequently, a deletion of the *NAB1* gene de-represses *LHCB* translation, leading to a larger light-harvesting antenna size phenotype in NAB1-minus mutants.

A mutant with a substantially down-regulated expression of the *TLA1* gene showed a lighter green phenotype and a truncated light-harvesting Chl antenna size for both photosystems (Polle et al. 2003). TLA1 is highly conserved gene and its protein is found among many eukaryotes, but it is not present in prokaryotes. The tentative function assigned to TLA1 is to help define the relationship between nucleus and organelles, with emphasis on the chloroplast in photosynthetic tissues, perhaps affecting size and number of organelles in the cell by an as yet unknown mechanism (Tetali et al., 2007; Mitra and Melis, 2010). (Tetali et al., 2007; Mitra and Melis, 2010).

RESULTS

The *tla2* mutant

Characterization of the *tla2* mutant: pigment content and composition

Cells of the *tla2* strain, when cultivated as single cell colonies on agar, displayed light green coloration than their wild type counterparts (Fig. 5). Biochemical analysis showed that, on a per cell basis, the *tla2* strain accumulated only about 20-25% of the chlorophyll present in the wild type. It also showed an elevated Chl *a* / Chl *b* ratio, suggesting lower amounts of the Chl *a-b* light-harvesting complex in the mutant (Table II). The cellular content of Chl in wild type and *tla2* was measured upon growth under two different light conditions: low light (30 µmol photons m^{-2} s^{-1}) and medium light (450 µmol photons m^{-2} s^{-1}) (Table II). Four wild type strains were used as controls for this analysis. Strain CC125 is the parental wild type strain of CC425 (*CW15*, *ARG7*). Strain 4A+ (*ARG7*) is the wild type strain of *ARG7* strains used for the back crosses. CC503, which was applied in the *C. reinhardtii* genome sequencing (Merchant et al., 2007). All wild type controls contained about 2.5 fmol Chl per cell under low light, and had a Chl *a*/Chl *b* ratio ranging between 2.7 and 3.0. The wild type Chl content per cell was lower when grown under medium light. In the wild type strains, it was about 1.7 fmol Chl per cell. A lower Chl/cell under medium light growth conditions is a compensatory response of the photosynthetic apparatus to the level of irradiance, seeking to balance the light and carbon reaction of photosynthesis (Greene et al., 1988; Smith et al., 1990).
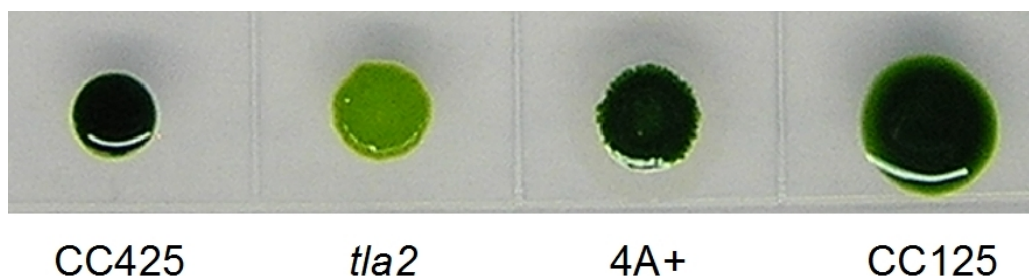
Figure 5: Single-cell colonies of *Chlamydomonas reinhardtii* wild type and *tla2* mutant grown on agar. Note the dark green coloration of the wild type strains, as compared to the light green coloration of the *tla2* mutant.

Low light [80 µmol photons m^{-2} s^{-1}]

Strain	Chl/Cell [fmol]	Chl *a*/Chl *b*	Car/Cell [fmol]	Car/Chl
4A+	2.57±0.43	2.72±0.07	1.07±0.17	0.42±0.00
CC-125	2.66±0.13	3.00±0.03	1.11±0.06	0.42±0.00
CC-503	2.36±0.05	2.73±0.05	0.93±0.04	0.39±0.01
CC-425	2.33±0.10	2.86±0.04	0.95±0.04	0.41±0.01
C1	1.93±0.17	2.87±0.02	0.67±0.16	0.42±0.00
C2	1.55±0.04	3.01±0.03	0.67±0.00	0.43±0.01
C3	1.06±0.01	3.35±0.16	0.54±0.01	0.51±0.00
C4	0.61±0.09	3.92±0.09	0.42±0.05	0.68±0.02
tla2	0.46±0.04	9.60±0.98	0.38±0.00	0.82±0.06

Medium light [450 µmol photons m^{-2} s^{-1}]

Strain	Chl/Cell [fmol]	Chl *a/b*	Car/Cell [fmol]	Car/Chl
4A+	1.66±0.37	2.45±0.09	0.85±0.17	0.51±0.01
CC-125	1.85±0.49	2.75±0.14	1.01±0.33	0.54±0.04
CC-503	1.68±0.33	3.08±0.12	0.84±0.13	0.50±0.03
CC-425	1.35±0.19	2.85±0.04	0.74±0.10	0.55±0.01
C1	1.03±0.04	2.71±0.09	0.56±0.03	0.54±0.02
C2	0.71±0.07	3.62±0.11	0.52±0.03	0.74±0.03
C3	0.51±0.07	4.36±1.05	0.43±0.07	0.85±0.07
C4	0.35±0.05	6.49±0.56	0.34±0.04	0.97±0.02
tla2	0.33±0.04	7.92±0.83	0.30±0.03	0.90±0.01

Table II. Chlorophyll and carotenoid content and pigment ratios for wild type, *tla2* mutant, and *tla2*-complemented strains (C1-C4) of *Chlamydomonas reinhardtii* (n=3-5; means ± SD).

The *tla2* mutant displayed a substantially lower Chl content per cell under both irradiance-growth conditions, equal to about 20% of that in the corresponding wild type controls: under low-light growth, it was about 0.5 fmol Chl/cell and under medium-light it was 0.3 fmol Chl/cell. The Chl *a/*Chl *b* ratio in the *tla2* mutant was substantially greater than that of the wild type, and in the range of (8-10):1, reflecting absence of the auxiliary Chl *b*

and possibly of a truncated light-harvesting Chl antenna size in this strain. The total carotenoid (Car) content in the *tla2* mutant was lower relative to that in the wild type, albeit not in proportion to that of Chl. Consequently, the Car/Chl ratio was about 0.4-05:1 in the wild type strains and 0.8-0.9:1 in the *tla2* mutant.

Functional properties and Chl antenna size analysis of wild type and *tla2* mutant

The functional properties of photosynthesis and the Chl antenna of the *tla2* mutant were assessed from the light-saturation curve of photosynthesis, i.e., from the relationship between light intensity and photosynthetic activity measured under *in vivo* conditions (Melis et al., 1999; Polle et al., 2000; Polle et al., 2003). Light saturation curves of photosynthesis were measured with wild type and *tla2* following cell acclimation to photoautotrophic growth at medium irradiance (growth at 450 μmol photons m^{-2} s^{-1}). At zero incident intensity, the rate of oxygen evolution has measured to be negative (Fig. 6), reflecting oxygen consumption by the process of cellular respiration (absence of photosynthesis). Measured on a per Chl basis, the rate of dark respiration of the *tla2* mutant was about 50% greater than that of the wild type (Fig. 6). This higher rate of respiration is partially due to the lower Chl content per cell in the mutant. However, rates of respiration on a per cell basis were lower in the mutant, down to about 30% of those of the wild type (Table III).

In the light-intensity region of 0-400 μmol photons m^{-2} s^{-1}, the rate of photosynthesis increased as a linear function of light intensity, both in the wild type and *tla2* mutant (Fig. 6). These linear portions of the light saturation curves were about parallel to one-another, suggesting similar quantum yields of photosynthesis for the two strains. This is an important consideration, as it shows that the *tla2* mutation did not interfere with the high innate quantum yield of photosynthesis. The rate of photosynthesis in the wild type saturated at about 500 μmol photons m^{-2} s^{-1} (Fig. 6, solid circles) whereas that of the mutant continued to increase with light intensity through the 2,000 μmol photons m^{-2} s^{-1} level. Statistically, the light-saturated rate (P$_{max}$) for the wild type was about 100 mmol O$_2$ (mol Chl)$^{-1}$ s^{-1}, whereas P$_{max}$ for the *tla2* mutant was about 150 mmol O$_2$ (mol Chl)$^{-1}$ s^{-1} (Table III).
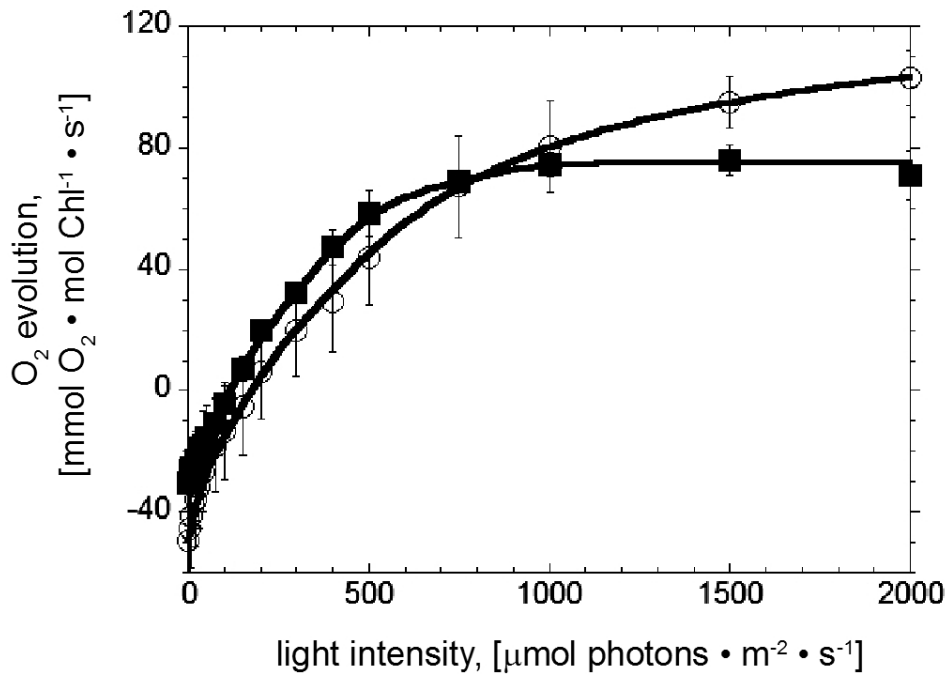
Figure 6: Light-saturation curves of photosynthesis obtained with the *C. reinhardtii* wild type (solid squares) and the *tla2* mutant (open circles). The initial slopes of both curves are similar, suggesting equal quantum yield of the photosynthesis. The light-saturated rate P_{max} was greater in the *tla2* mutant than in the wild type, suggesting a greater productivity on a per Chl basis in the *tla2* than in the wild type.

The light-saturated rate of photosynthesis is a measure of the overall photosynthetic capacity (P_{max}) (Powless and Critchley, 1980). A large wild-type light-harvesting Chl antenna saturates photosynthesis at about 500 μmol photons m^{-2} s^{-1} (Fig. 6). A much higher light intensity of bright sunlight, >2000 μmol photons m^{-2} s^{-1}, was needed to saturate photosynthesis in the *tla2* mutant. Important in the context of this work is the light intensity required to bring about the rate of photosynthesis to the half saturation point. The half-saturation intensity for the wild type was measured to be about 210 μmol photons m^{-2} s^{-1}, while for the *tla2* mutant it was 380 μmol photons m^{-2} s^{-1}. Since there is a reciprocal relationship between the half-saturation intensity of photosynthesis and the Chl antenna size, it may be concluded that photosystems (PSII & PSI) in the *tla2* mutant collectively possess only about 55% the Chl antenna size found in the corresponding wild type. Such differences in the half-saturation intensity and P_{max} are typical among fully pigmented and truncated Chl antenna microalgae (Melis et al., 1999; Polle et al., 2000; Polle et al., 2003).

A more precise determination of the functional Chl antenna of PSI and PSII units in

wild type and the *tla2* mutant was conducted by the spectrophotometric and kinetic method developed in this lab (Melis, 1989). The number of Chl molecules associated with each photosystem is given in Table III, measured in photoautotrophically grown cells under 450 μmol photons m^{-2} s^{-1}. The number of Chl molecules of PSII$_\alpha$ and PSII$_\beta$ was determined to be 250 and 90 for the wild type, respectively. These numbers were lowered to 160 and 90 for the *tla2* mutant. The proportional abundance of PSII$_\alpha$ and PSII$_\beta$ changed as a result of the mutation from 60:40 (PSII$_\alpha$: PSII$_\beta$) in the wild type to 45:55 in the mutant. Thus, an average of 190 Chl molecules is associated with the reaction centers of PSII in the wild type, while the average PSII antenna size of the *tla2* mutant was lowered to 120 Chl molecules (63%). The number of Chl molecules associated with a PSI reaction center was determined to be 210 for the wild type and 120 for the *tla2* mutant. Thus, the PSI antenna size of the *tla2* mutant was only about 60% of that in the wild type.

Parameter measured	WT	*tla2*
Respiration [mmol O$_2$ • (mol Chl)$^{-1}$ • s^{-1}]	30.2$\pm$11.9	49.1$\pm$15.2
Respiration [amol O$_2$ • cell^{-1} • s^{-1}]	55.8$\pm$26.3	16.2$\pm$5.4
Quantum yield, relative units	100$\pm$25	108$\pm$17
P$_{max}$ [mmol O$_2$ • (mol Chl)$^{-1}$ • s^{-1}]	106.3$\pm$12.8	152.3$\pm$18.0
P$_{max}$ [amol O$_2$ • cell^{-1} • s^{-1}]	196.2$\pm$46.2	50.3$\pm$7.3
P$_{max}$ / Respiration, relative units	3.5$\pm$1.9	3.1$\pm$1.1
Half-saturation intensity, [μmol photons m^{-2} s^{-1}]	210	380
Functional PSII$_\alpha$ Chl antenna size	249$\pm$27	160$\pm$7
Functional PSII$_\beta$ Chl antenna size	90$\pm$30	90$\pm$12
Fraction of PSII$_\alpha$ [%]	61$\pm$1	46$\pm$1
Average PSII Chl antenna size	190$\pm$20	120$\pm$9
Functional PSI Chl antenna size	180$\pm$9	123$\pm$5

Table III. Photosynthesis, respiration, and photochemical apparatus characteristics of wild type (WT) and the *tla2* mutant of *Chlamydomonas reinhardtii* grown photo-autotrophically under medium light [450 μmol photons m^{-2} s^{-1}] conditions. Photosystem Chl antenna size and reaction center concentrations were measured spectrophotometrically (Melis, 1998). (n=3; means ± SD).

To investigate if the loss of photosystems and light-harvesting antenna affects photoautotrophic growth a growth curve was measured of *tla2* in comparison with the wild type under medium-light (450 µmol photons m^{-2} s^{-1}) conditions (Fig. 7). To determine the doubling time the first six points have been used, to prevent slower growth rates at higher cell densities to influence the calculation. The doubling time of the wild type at this light intensity was determined to be 6.3±0.1 h, whereas the *tla2* mutant doubled every about 7.2±0.3 h. This difference is consistent with the difference in the rate of oxygen evolution between the two strains at 450 µmol photons m^{-2} s^{-1} (Fig. 6).
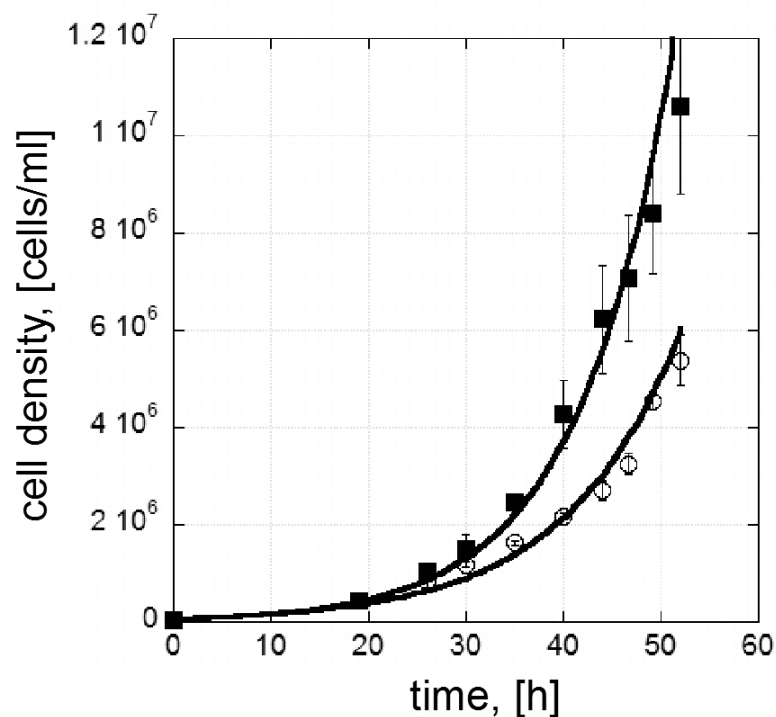
Figure 7: Photoautrotrophic growth curves obtained under medium light (450 µmol photons m-2 s-1) with the *C. reinhardtii* wild type (solid squares) and the *tla2* mutant (open circles). Doubling times were determined to be 6.3±0.1 h for the wild type and 7.2±0.3 for the *tla2* mutant.

The above functional and antenna analysis provided a foundation upon which the *tla2* strain was deemed to be a good candidate for the identification of gene(s) impacting the Chl antenna size of the photosystems. Accordingly, a detailed molecular and genetic analysis was undertaken to map the plasmid insertion site and to test for plasmid and lesion co-segregation in the *tla2* mutant, prior to gene cloning.

Southern blot analysis of wild type and *tla2* mutant

To determine the copy number of pJD67 insertions and their integrity in the *tla2* mutant, Southern blot analysis of the *tla2* genomic DNA was undertaken. A map of the linearized pJD67 plasmid, restriction sites on the pJD67 vector that were employed for the Southern blot analysis, the position of probes and their DNA hybridization regions are shown in Fig. 8A. Probes (1 through 6) were designed to various parts of the inserted pJD67 vector, as shown in Fig. 8A, and used to probe genomic DNA samples of *tla2,* its host wild type strain CC425, and a positive control (pJD67 transformant *tla3* strain). Probes were selected for their specificity, with probe 1 being specific to the origin of replication of the pJD67 vector. Probe 2 covered the antibiotic resistance *bla* gene. Probe 3 was designed to hybridize to the intergenic region between the 3' end of the *bla* gene and the *ARG7* promoter region. Probe 4 covered both a plasmid specific sequence and the 5' end of the *ARG7* promoter region. The latter is present in both, the transforming plasmid and in the genomic DNA of the parental CC425 strain, as part of the endogenous inactive *ARG7* gene. Probe 5 was designed to the 5' coding region of the *ARG7* gene, whereas probe 6 is specific to the 3' end of the *ARG7* gene. While Probes 1, 2 and 3 are specific to the pJD67 sequence, probes 4, 5 and 6 contain sequences that are also present in the *C. reinhardtii* host strain CC425 and thus at least one hybridization signal is expected to be generated by these latter probes.
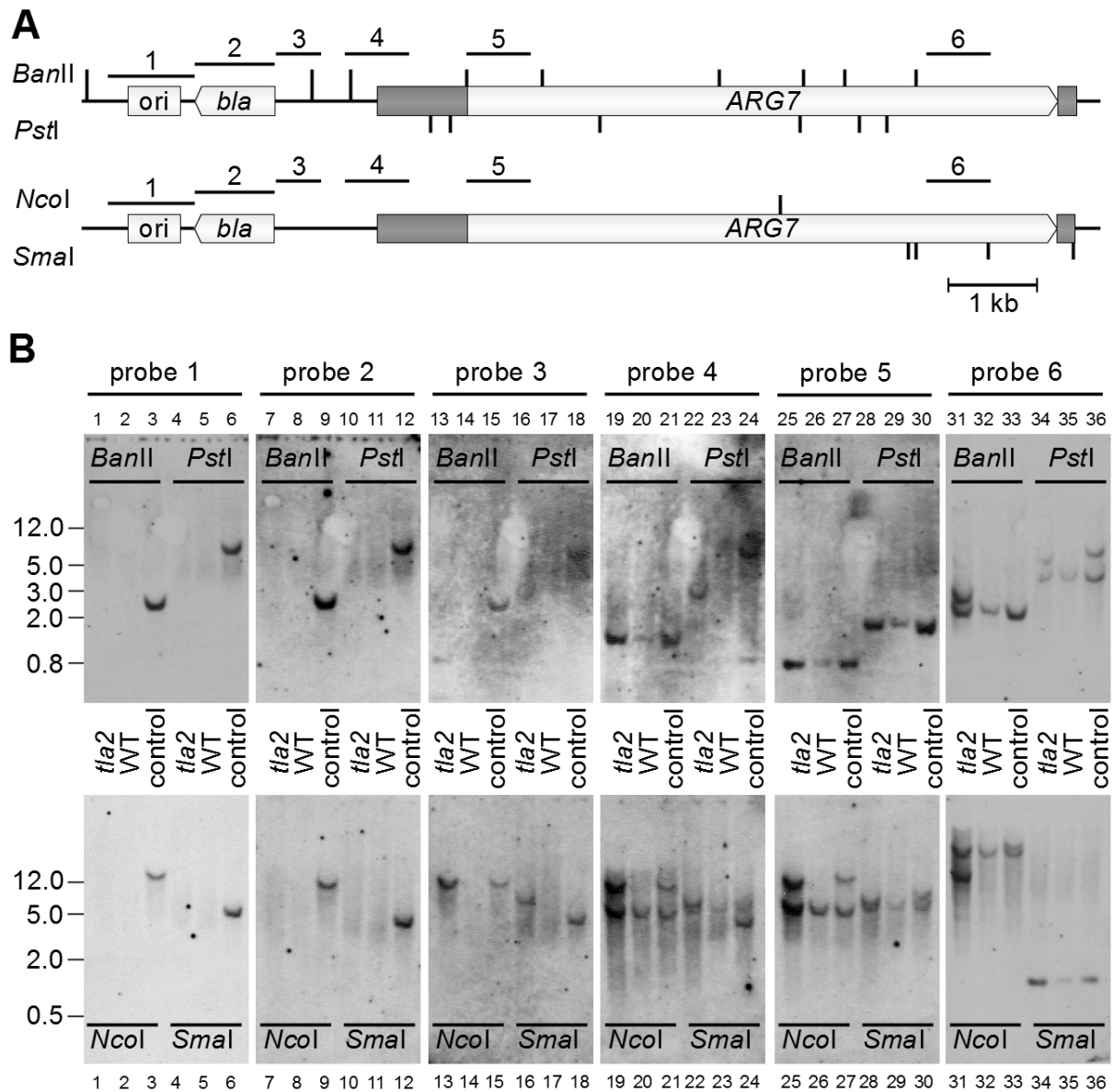
Figure 8: Southern blot analysis to define copy number and integrity of inserted pJD67 plasmid into the genomic DNA of *Chlamydomonas reinhardtii* insertional transformant. Wild type, *tla2*, and *tla3* (an unpublished truncated antenna mutant isolated in this lab) strains were used in this analysis. **A.** Schematic map of pJD67. Dark gray boxes indicate the promoter and terminator region of the *ARG7* gene. These regions and the *ARG7* gene are not plasmid specific but are also present in the host strain. Isolated genomic DNA was digested by *Ban*I, *Pst*I, *Nco*I and *Sma*I. The location of probes 1-6, used for the Southern blot analysis, are marked with black lines. **B.** Developed films of hybridized Southern blots. Each column indicates the probe used for hybridization and consist of a set of four genomic DNA digests, *Ban*I and *Pst*I in the upper row, *Nco*I and *Sma*I in the lower row. The digested genomic DNA was loaded as follows: 1: *tla2*; 2: CC-425; 3: positive control (*tla3*). Marker sizes indicate electrophoretic mobility in kb.

Genomic *C. reinhardtii* DNA was digested by various restriction enzymes and size fractionated via agarose gel electrophoresis. Transfer to a positive-charged nylon membrane and hybridization reactions were carried out as shown in Fig. 8B. When tested with probe 1 or probe 2, *tla2* genomic DNA digests did not generate a hybridization signal (Fig. 8B, lane 1 and 7). Absence of the *ori* and *bla* regions of the pJD67 plasmid from the *tla2* DNA is consistent with the notion that the 5' end of the inserted pJD67 plasmid is missing from the *tla2* mutant. When tested with probe 3, a single hybridization band was detected, indicating a single insertion of the pJD67 vector into the genomic DNA of *tla2* (Fig. 8B, lane 13 and 16). This finding was confirmed by using probes 4, 5 and 6. In theory, if *tla2* genomic DNA is hybridized with probes 4, 5 or 6, two distinct hybridization bands should be generated; one band originating from the exogenous pJD67 plasmid and one from the endogenous inactive *ARG7* gene. This was found to be the case for digests with *Nco*I and *Sma*I using probe 4 and 5 (Fig. 8B, lanes 19 and 22 lower panel), and for *Ban*II, *Pst*I and *Nco*I digests upon using probe 6 (Fig. 8B, lanes 31 and 34). When probes 4 and 5 were used on *Ban*II and *Pst*I genomic DNA digests, only one hybridization band was detected. This is because these restriction enzymes generate fragments of about the same molecular weight from both the endogenous DNA sequence and the exogenously inserted pJD67 plasmid sequence (Fig. 3A). The corresponding restriction fragments using probe 5 were found to be 0.8 kb for the *Ban*II digest and 1.6 kb for the *Pst*I digest. The same applies to the fragment generated upon *Sma*I digest (0.8 kb) using probe 6. Using Probe 4 on *Ban*II digests creates a fragment that is 1316 bp in size for the pJD67 insertion, and 1307 bp for the endogenous *ARG7* gene sequence, as determined by a virtual digest of the published genome sequence (Merchant et al., 2007). These similar sizes could not be resolved on the agarose gel used for the Southern blot analysis, thus only a single hybridization band could be detected. In brief, the Southern blot analysis conducted here showed that genomic DNA of the *tla2* mutant contains a single copy of the pJD67 insertion from which about 2.5 kb of its 5' end, including the *ori* and *bla* regions have been deleted.

Mapping the pJD67 insertion site in the *tla2* genomic DNA

The Southern blot analysis revealed that the plasmid specific *ori* and the *bla* loci at the 5' end of the pJD67 plasmid are not present in the *tla2* mutant. However, the downstream 5' plasmid specific sequence was retained in the insertion site of the *tla2*

mutant, based on the fact that probe 3 generated a signal in the Southern blot of *tla2* genomic DNA (Fig. 8B, lanes 13 and 16). By PCR analysis, using the same fixed-position reverse primer and shifted forward primer, it could be determined to a 20 bp accuracy, how much of the pJD67 vector has been retained in the *tla2* mutant insert site. Subsequently, TAIL-PCR (Liu et al., 1995) was employed to amplify genomic DNA flanking sequence on the 5' of the insertion. The locus of the insertion was found to be within the coding sequence of a predicted gene Cre05.g239000 on the *C. reinhardtii* chromosome #5. Efforts to complement the mutant with BAC clones containing Cre05.g239000, namely BAC 28L08 and 21D17 failed; consequently the pJD67 insertion site in the *tla2* mutant was further investigated. Analysis by TAIL-PCR, starting amplification upstream of the insertion site in the genomic DNA of the *tla2* mutant and towards the insertion indicated that a 358 kb genomic DNA fragment flipped its orientation by 180 degrees (5' to 3') in the *tla2* mutant. This unexpected finding was confirmed by Southern blot analyses using various restriction enzymes and two probes on both sides of the 5' and 3' of the flipped genomic DNA region (Fig. 9A, white and black bars). Restriction enzymes and probes were selected so that both probes would hybridize to DNA fragments of different sizes in genomic DNA digests of the wild type but would hybridize on the exact same fragment using genomic DNA digests of the *tla2* mutant (Fig. 9A). In this approach, wild-type genomic DNA digests were expected to generate 3.7 and 15.0 kb (*Sac*I), 3.4 and 3.0 kb (*Fsp*I) DNA fragments using the 5' (Fig. 9A, white bar) and 3' probe (Fig. 9A, black bar) for hybridization respectively. Using these probes on *tla2* mutant genomic DNA digests, they are expected to hybridize to the exact same DNA fragment, 5.9 and 5.5 kb upon digestion with *Sac*II and *Fsp*I, respectively.
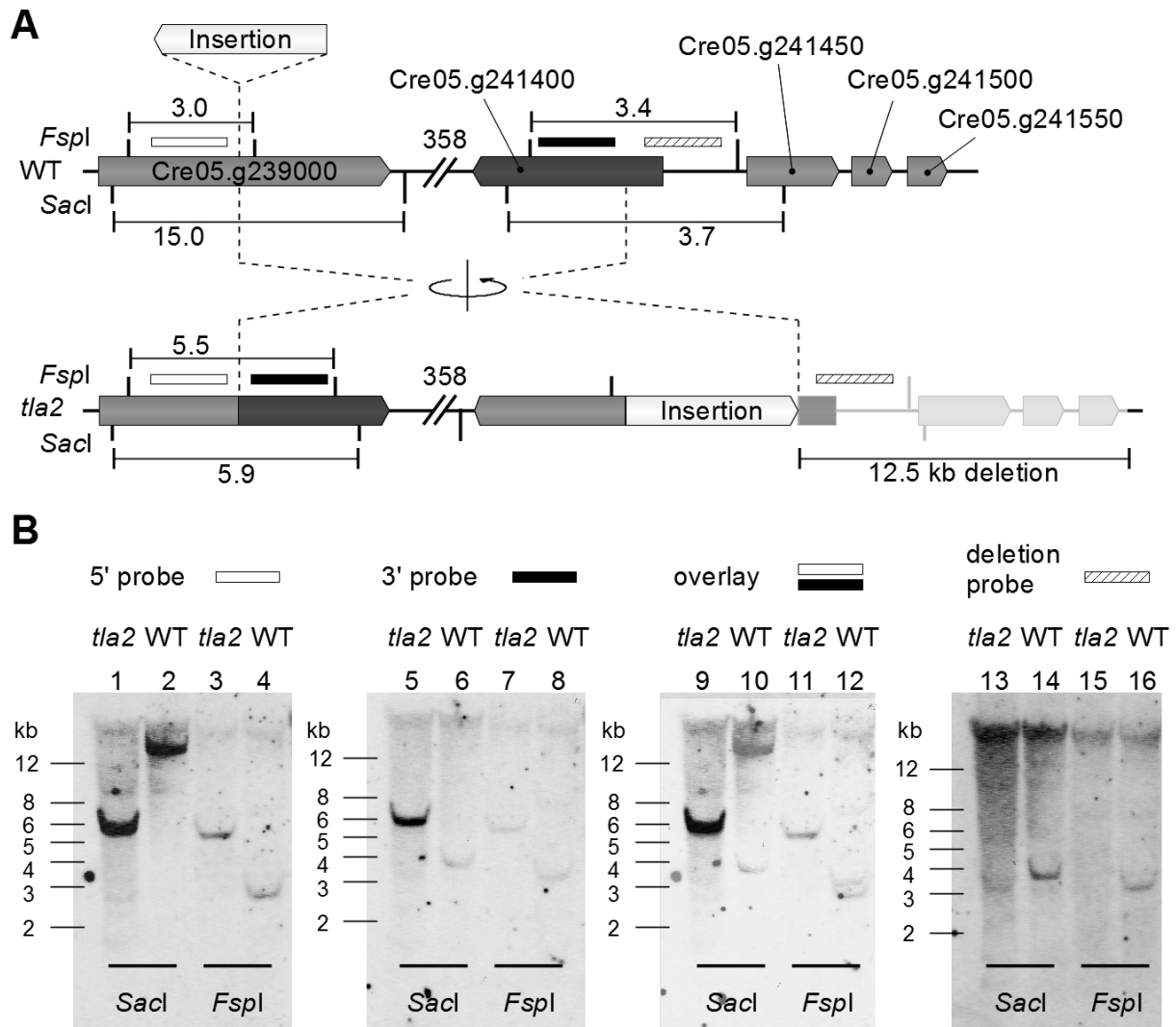
Figure 9: DNA insertional mutagenesis-induced reorganization of the genomic DNA in the *tla2* strain. **A.** Schematic comparing the genomic DNA on chromosome 5 in wild type (upper map) and *tla2* mutant (lower map). Arrows mark Genes and their orientation. Dashed lines indicate the rearrangement of the genomic DNA in the *tla2* mutant. Genes that are deleted in the *tla2* mutant are grayed-out. Probes used for hybridization are marked with bars: white bar - 5'probe, hatched bar - 3' probe and black bar - deletion probe. The expected size of fragments generated upon digestion with *Fsp*I and *Sac*I are marked in kb. **B.** Southern hybridized blots. Probes used for hybridization are indicated on top of each panel. Restriction enzymes used for digestion and the genomic DNA sample are indicated in the bottom of the blot. Individual lanes are numbered 1-16. The marker on the left indicates the electrophoretic mobility in kb.

Southern blots probed with the 5' and 3' end probe generated a single band in each lane of the expected size (Fig. 9B, lanes 1-8). The overlay of both blots (Fig. 9B, lanes 9-12) showed that the hybridization signals for the *tla2* genomic digests are indeed at the exact

same spot for both blots, while the wild type genomic DNA digests with *Sac*I and *Fsp*I showed two separate hybridization signals. These results provide evidence that a 358 kb fragment of genomic DNA was broken off and subsequently reinserted in the opposite orientation (180 degree flip) during the process of the pJD67 insertion.

Further genomic DNA PCR analysis using various primers downstream from the flipped genomic DNA region revealed that a stretch 12.5 kb was deleted in the *tla2* mutant (Fig. 9A). Included in this region were three predicted genes, namely Cre05.g241450, Cre05.g241500 and Cre05.g241550. To strengthen this finding, a probe in the putative deleted region was designed and was used in Southern blot DNA hybridization reactions (Fig. 9B, lanes 13-16). The probe clearly hybridized to fragments of wild type genomic DNA digested at expected sizes, 3.7 and 3.4 kb for *Sac*I (Fig. 9B, lane 14) and *Fsp*I (Fig. 9B, lane 16) digests, respectively. However, it failed to generate significant hybridization signals with the *tla2* genomic DNA digests (Fig. 9B, lanes 13 and 15).

This detailed PCR and Southern blot analysis revealed that, in addition to the 180 degree flip of a 358 kb genomic DNA fragment, four predicted genes in the *tla2* mutant are non-functional either because of disruption or deletion, namely Cre05.g239000, Cre05.g241450, Cre05.g241500, and Cre05.g241550.

Point of pJD67 insertion is linked with the *tla2* phenotype

Genetic crosses were used to test if the point of pJD67 insertion is directly responsible for the *tla2* phenotype. This is an important consideration, as the *tla2* lesion could have occurred inadvertently in a locus distinct and far away from the pJD67 insertion site. To eliminate background mutations that do not contribute to the phenotype of *tla2,* progeny of the fourth cross of the original *tla2* strain with strain AG1-3.24 (*arg7*-) were used in the below genetic crosses and PCR analysis.

Ten complete tetrads were plated on non-selective media containing arginine (TAP+ARG) and on plates selective for intact *ARG7* gene within the insertion, supplemented with no arginine (TAP only). Fig. 10 shows one typical tetrad analysis from such genetic crosses. When daughter cells were grown on TAP+ARG plates, the tetrad included two viable dark-green and two viable pale-green colonies (Fig. 10, upper panel). The dark green daughter cell colonies had a wild type Chl *a/*Chl *b* ratio (Chl *a/*Chl *b* = ~2.7:1). A high Chl

*a/*Chl *b* ratio (~9:1) was measured for the pale green daughter cell colonies. A 2:2 wild type to *tla2* phenotype distribution was found among the progeny of all tetrads that were tested, providing strong evidence that a single genetic locus is causing the *tla2* phenotype. When plated on TAP-only agar plates (absence of arginine), the dark green daughter cells could not grow, apparently because they lacked a functional *ARG7* gene and, therefore, lack arginine autotrophy (Fig. 10, middle panel). Cells, able to grow on selective media were exclusively pale green progeny, suggesting a linkage between the *tla2* phenotype and the inserted pJD67 plasmid.
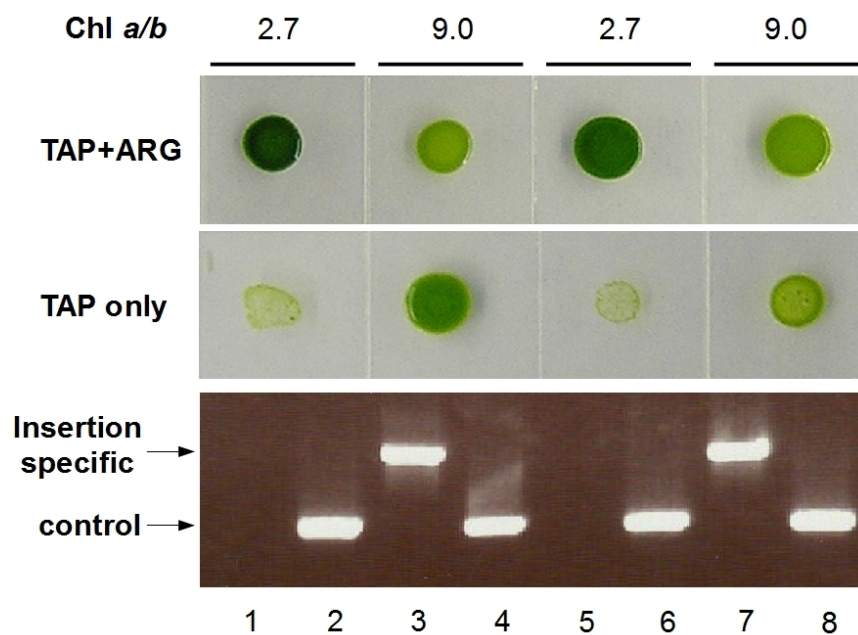
Figure 10: Genetic cross analysis of *tla2* with AG1-3.24 (*arg2*) strain. One representative tetrad from a single cross is shown, plated on non-selective TAP+ARG media (top panel) or selective TAP-only media (middle panel). The Chl *a*/Chl *b* ratio of these progeny is shown at the top of the panels. The lower panel shows the result of PCR reactions, two lanes per progeny: the PCR reaction using an insertion specific primer-set was loaded on lanes 1, 3, 5, 7, and a positive control PCR on lanes 2, 4, 6, 8.

To further show that the insertion locus is co-segregating with the *tla2* phenotype we used genomic DNA PCR analysis. A forward primer in predicted Cre05.g239000 ORF and a reverse primer in the pJD67 sequence were employed. This combination of primers would generate a product only in the daughter cells of a genetic cross that actually carried the pJD67 insertion. As a positive control, a set of primers was used from a genomic DNA region of *C. reinhardtii* not affected by the insertion. Fig. 10 (lower panel) shows that dark green

daughter cells failed to generate a pJD67-specific product (lanes 1 and 5) whereas they generated a product from the control primers (lanes 2 and 6). Pale green daughter cells, on the other hand, generated both an insertion-specific (lanes 3 and 7) and a control-specific product (lanes 4 and 8). These findings were observed with all tetrads examined. The results of the PCR analysis are consistent with the genetic analysis and strongly suggest that a single locus is causing the *tla2* phenotype and, furthermore, that it is linked with the pJD67 insertion site.

Cloning of the *TLA2* gene

Using information from the sequenced *C. reinhardtii* genome and the BAC-end DNA we searched for BAC clones comprising the five deleted genes in the *tla2* mutant. Two BAC clones, namely 28L06 and 21D17, were identified and shown to contain Cre05.g239000. Two other BAC clones, namely 08N24 and 36L15 were identified and shown to contain the genes Cre05.g241400 and **Cre05.g241450**. We could not find a BAC clone that comprises genes Cre05.g241500 and Cre05.g241550. Each of the four identified BAC clones was used along with pBC1 (conferring paromomycin resistance) in a co-transformation approach to complement the *tla2* strain. Transformants that grew on a paromomycin plate were screened for strains with a complemented *tla2* phenotype. This was done upon measurement of the Chl/cell and the Chl *a/*Chl *b* ratio of the transformant colonies. Transformation with BAC clones 28L06 and 21D17 failed to generate any complemented strains. However, BAC clones 08N24 and 36L15 both successfully complemented the *tla2* phenotype in about 50% of the co-transformed algae. The latter showed a dark green coloration and a low Chl *a/*Chl *b* ratio phenotype. BAC clones 08N24 and 36L15 contain two predicted *C. reinhardtii* genes, Cre05.g241400 and Cre05.g241450. These two genes were tested separately, as cDNA constructs, for their ability to complement the *tla2* phenotype. For this purpose, the corresponding start and stop codon of the full length mRNA of both genes was identified by 5' and 3' RACE. Both cDNAs were then cloned separately into pSL18 (confers paromomycin resistance) for transformation of the *tla2* mutant. Transformation with Cre05.g241400 cDNA did not yield any complemented strains, while the cDNA construct of gene **Cre05.g241450** yielded complements in which the wild type phenotype was recovered to various degrees. These results suggested that deletion of gene Cre05.g241450 is responsible for the *tla2* phenotype. Gene Cre05.g241450 is predicted to

encode a putative FTSY precursor protein with a chloroplast-targeted transit peptide. A putative CpFTSY protein has not been previously reported or characterized in *Chlamydomonas reinhardtii*.

The *CpFTSY* gene of *C. reinhardtii* is 6578 bp long and consists out of 13 exons and 12 introns. The *CpFTSY* mRNA is 1814 bp in length with a 5' and 3' UTR of 189 and 479 bp, respectively. The gene encodes for a protein of 381 amino acids including a putative 36 amino acid long chloroplast target peptide as determined by ChloroP (http://www.cbs.dtu.dk/services/ChloroP/) and TargetP (http://www.cbs.dtu.dk/services/TargetP/) (Fig. 11). The mature protein of 345 amino acids with a molecular weight of 38.2 kD shares significant sequence homology with the SRP54_N helical bundle domain from amino acid 33-105 and the SRP54 type GTPase domain (amino acids: 126-333) as determined by Pfam (http://pfam.sanger.ac.uk). These domains are universally conserved in SRP receptor proteins (Luirink and Sinning, 2004) suggesting that Cre05.g241450 encodes for the CpFTSY protein in the model green algae *C. reinhardtii.*

MQTTVGRKCVASSAAGRSRNVTVFRRCSRGGPVKVV ANAGGEAGPGFLQRLGRVIKEKAAGDFDR FFAGTSKTRE RLGLVDEMLALWSLEDYEDSLEELEEVLISADFGPRTALKIVDRIREGVKAGRVKSAEDIRASLKAAIVEL LTAR GRSSELKLQGR PAVVLIVG VNGAGKT TTVGKIA YKYGKEGAKVFLIPGDTFRAAAAEQLAEWSRRAGATIGAFRE GARPQAVIASNLDDLRQRTCKDASDVYDLILV DTAGR LHTAYKLMEELALCKAAVSNALPGQPDETLLVLDGTTG LNMLNQAKEFNEAVRLSGLIL TKLD GTARGGAVVSVVDQLGLPVKFIGVGETAEDLQPFDPEAFAEALFP KVKEP ATAGTK
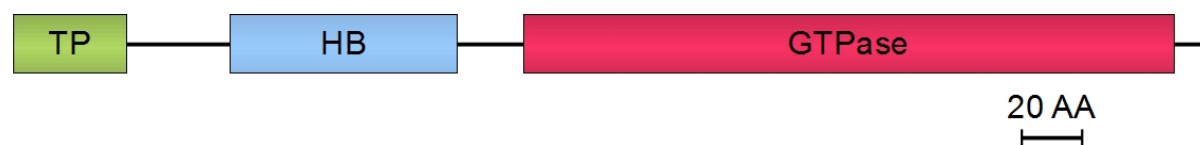
Figure 11: (Upper) Amino acid sequence of the *Chlamydomonas reinhardtii* FTSY protein. Domains of the CrCpFtsY protein are defined as follows: Amino acids 1-36: Transit peptide (green font). Amino acids 66-147: Helical bundle domain (Pfam), SRP54-type-protein (blue font). Amino acids 162-370: GTPase domain (Pfam), SRP54-type protein (red font). Amino acids 164-183: P-loop nucleotide binding motif, (pre) (red, gray-shaded font). Amino acids 170-176, 258-262 & 322-325: Homologous nucleotide binding (red, black-background font). (Lower) Domain presentation of the CrCpFTSY protein. TP: chloroplast transit peptide. HB: Helical bundle domain. GTPase: GTPase domain.

Homology of the putative CrCpFTSY with other CpFTSY proteins

A ClustalW analysis and comparison of the putative CrCpFTSY with the known CpFTSY proteins of *Arabidopsis thaliana* (GenBank accession # NP_566056) and *Zea mays* (GenBank

accession # NP_001105732) was undertaken (Fig. 12). The comparative amino acid sequence analysis showed 46.1% identity and 61.9% similarity of the CrCpFTSY to AtCpFTSY and 50.5% identity and 65.5% similarity to ZmCpFTSY, strengthening the notion of a chloroplast localization and function for the CrCpFTSY identified in this work. Furthermore, a ClustalW amino acid sequence analysis of the putative CrCpFTSY identified in this work with the cytoplasmic SRα subunit homologue of the signal recognition receptor (GenBank Accession # XP_001692081) showed dissimilarity between these proteins, both in terms of amino acid sequence alignment and in terms of length between the two polypeptides (Appendix C).

```
AtCpFTSY      ---GSGMKETAAAKFGERQHMDSPDLGTDDDDKAMACSAG---PSGFFTRLGRLIKEKAK  54
ZmCpFTSY      MAAPSHVLPFLSPAGGCAASSARAHSGYRAGLLRCSAAAG---QAGFFTRLGRLIKEKAK  57
CrCpFTSY      MQTTVGRKCVASSAAGRSRNVTVFRRCSRGGPVKVVANAGGEAGPGFLQRLGRVIKEKAA  60
                 :.   *                 .      .  **    .**:  ****:*****

AtCpFTSY      SDVEKVFSGFSKTRENLAVIDELLLFWNLAETDRVLDELEEALLVSDFGPKITVRIVERL  114
ZmCpFTSY      SDVEKLFSGFSKTRENLSVVDELLTYWNLADTDRVLDDLEEALLVSDFGPKISFRIVDTL  117
CrCpFTSY      GDFDRFFAGTSKTRERLGLVDEMLALWSLEDYEDSLEELEEVLISADFGPRTALKIVDRI  120
              .*.::.*:* *****.*.::**:*  *.*  : :  *::***.*: :****: :.:**: :

AtCpFTSY      REDIMSGKLKSGSEIKDALKESVLEMLAKKNSKTELQLGFRKPAVIMIVGVNGGGKTTSL  174
ZmCpFTSY      REEIRDGKLKSGAEIKAALKRCILELLTSKGGNSELNLGFRKPAVIMIVGVNGGGKTTSL  177
CrCpFTSY      REGVKAGRVKSAEDIRASLKAAIVELLTARGRSSELKLQGR-PAVVLIVGVNGAGKTTTV  179
              **  :   *::**. :*: :** .::*:*: :. .:**:*  * ***::****** .****::

AtCpFTSY      GKLAHRLKNEGTKVLMAAGDTFRAAASDQLEIWAERTGCEIVVAEGDKAKAATVLS----  230
ZmCpFTSY      GKLAYRFKNEGVKVLMAAGDTFRAAARDQLEVWAERTGSEIVIDNDKKAQPPAVLS----  233
CrCpFTSY      GKIAYKYGKEGAKVFLIPGDTFRAAAAEQLAEWSRRAGATIGAFREGARPQAVIASNLDD  239
              **:*::   :**.**:: .******** :**  *:.*:*. *   .    ..: *

AtCpFTSY      --KAVKRGKEEGYDVVLCDTSGRLHTNYSLMEELIACKKAVGKIVSGAPNEILLVLDGNT  288
ZmCpFTSY      --QAVKRGKREGFDVVLCDTSGRLHTNYGLMEELVSCKKVLAKALPGAPNEILLVLDGTT  291
CrCpFTSY      LRQRTCKDASDVYDLILVDTAGRLHTAYKLMEELALCKAAVSNALPGQPDETLLVLDGTT  299
               : . :.  : :*::* **:***** * ***** **  .:.: :.* *:* ******.*

AtCpFTSY      GLNMLPQAREFNEVVGITGLILTKLDGSARGGCVVSVVEELGIPVKFIGVGEAVEDLQPF  348
ZmCpFTSY      GLNMLQQAREFNDVVGVTGFILTKLDGTARGGCVVSVVDELGIPVKFIGVGEGMEDLQPF  351
CrCpFTSY      GLNMLNQAKEFNEAVRLSGLILTKLDGTARGGAVVSVVDQLGLPVKFIGVGETAEDLQPF  359
              ***** **:***:.* ::*:*********:**** *****::**.*****::**:********  ******

AtCpFTSY      DPEAFVNAIFS-----------  359
ZmCpFTSY      DAEAFVEAIFP-----------  362
CrCpFTSY      DPEAFAEALFPKVKEPATAGTK  381
              *.***.:*:*.
```

Figure 12: CLUSTAL 2.1 multiple sequence alignment of AtCpFTSY, ZmCpFTSY and CrCpFTSY. The comparative amino acid sequence analysis showed 46.1% identity and 61.9% similarity between the three proteins, strengthening the notion of a chloroplast localization and function for the CrCpFTSY identified in this work.

Complementation of the *tla2* strain with the CpFTSY cDNA

Complementation of the *tla2* strain with a wild type CpFTSY cDNA resulted in the isolation of several transformant lines, which showed various degrees of wild type recovery in their phenotype. The phenotypic complementation ranged anywhere between that of wild type and *tla2* mutant. Some successfully transformed lines failed to rescue the mutation altogether. This variable effectiveness in the *tla2* complementation is attributed to cDNA insertions in different regions of the chromosomal DNA in *Chlamydomonas*, many of which are either slow transcription zones, or are subject to epigenetic silencing. Four *tla2*-complemented lines were chosen for further detailed characterization, namely C1, C2, C3 and C4. Of those, C1 had a phenotype closest to the wild type, both in terms of the Chl/cell and Chl *a/*Chl *b* ratio (Table II). It was the strongest complemented line out of the four lines investigated. It has a Chl *a/*Chl *b* ratio of 2.7 - 2.9 under either low or medium light conditions, which is in the same range as that of the wild type. The Chl/cell content of C1 was slightly lower under low light compared to the wild type strains with about 1.9 fmol Chl per cell. Under medium light this difference was exacerbated, with C1 cells containing about 1.0 fmol Chl, i.e., only about 60% of that in the wild type. However, under both low-light and medium-light growth conditions the Chl/cell in C1 is substantially greater than in the *tla2* mutant. C2, C3 and C4 lines were shown to be partially complemented strains of the *tla2* mutant, with C2 having the highest and C4 the lowest Chl/cell, while the numbers for C3 were found to be in-between those of C2 and C4. This gradient of complementation from C1 to C4 applied to all photochemical apparatus parameters measured (Table II).

To further characterize the phenotype of the *tla2* mutation in relation to wild type, Western blot analyses with specific PSII and LHC-II antibodies were undertaken (Fig. 13) using cells grown photoautotrophically under medium light. Lanes were loaded on an equal cell basis, except for the wild type where 25% (about equal reaction centers) and 12% cells were loaded additionally. All LHC-II proteins were either substantially lowered or not detected in the *tla2* mutant. LHCB1 and LHCB2 were lowered to about 10% of the wild type levels, while LHCB3 was not detectable in the *tla2* mutant. The minor antenna protein LHCB4 was reduced to less then 5% of the wild type levels and no cross-reaction signal could be observed using an antibody raised against LHCB5. The PSII reaction center protein D2 also showed a lower abundance on a per cell basis, down to about 20-25% of the wild type.

However, loss of the peripheral Chl *a-b* antenna binding proteins is proportionally higher than the lowering of the photosystem reaction center proteins, consistent with the notion of a truncated light-harvesting antenna phenotype in the *tla2* mutant. Fig. 13 further shows that the PSI reaction center protein PSAL is also lowered to about the same level as D2 (down to about 25% of that in the wild type). The same outcome pertains to the large subunit of RuBisCo (RBCL). The β subunit of the ATP-synthase (ATPβ) on the other hand was affected to a lesser extend by the loss of the CpFTSY protein in the *tla2* mutant (Fig. 13).
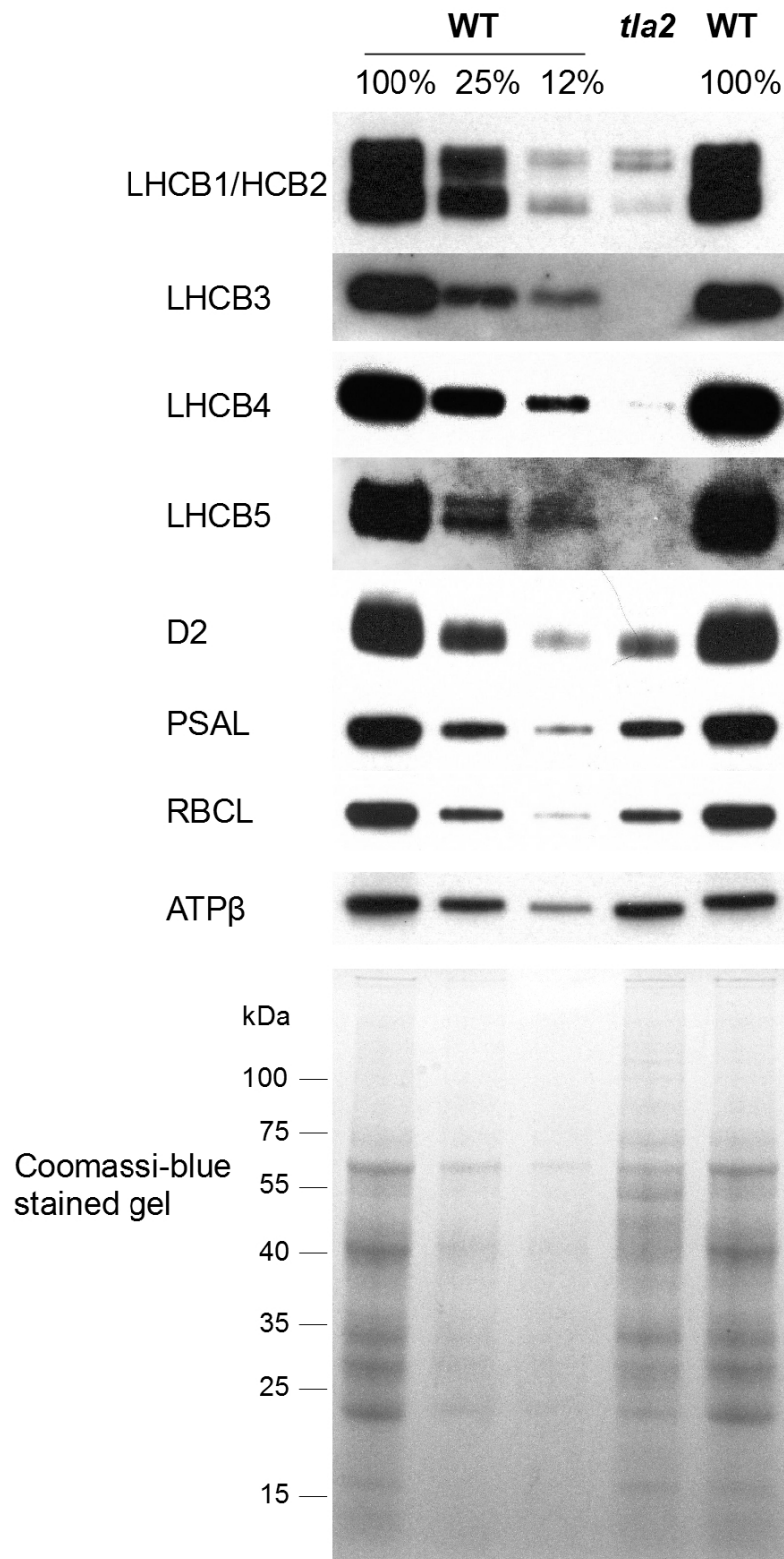
Figure 13: Western blot analysis of the light-harvesting antenna proteins of PSII in wild type and the *tla2* mutant. **A.** Immuno-detection of proteins with specific polyclonal antibodies against the light harvesting proteins LHCB1/LHCB2, LHCB3, LHCB4 and LHCB5, the PSII reaction center protein D2, the PSI reaction center protein PSAL, RuBisCo and the β subunit of the ATP synthase are shown. **B.** Coomassie-blue stained SDS-PAGE analysis of the samples shown in A.

To test the level of CpFTSY protein expression in the wild type and *tla2* complementary lines, Western blot analyses were conducted with specific polyclonal antibodies, directed against the recombinant CpFTSY protein of *C. reinhardtii*. No cross-reaction between CpFTSY-specific antibodies and a protein band at around 39 kD could be detected in the *tla2* cell extracts, proving that *tla2* is a true knock-out mutant of CpFTSY (Fig. 14A). In the C4 complement, levels of the CpFTSY protein content were below 10% of those in the wild type, while C3 and C2 contain about 25% and 50% of the wild type CpFTSY protein, respectively. The C1 complemented line was found to over-express the CpFTSY protein, as evident by the short film exposure time in Fig. 14A. It was estimated that the C1 complemented line cells accumulate more than a 5-fold greater amounts of the CpFTSY protein than the wild type. However, this over-expression of the CpFTSY protein in the C1 complemented line did not increase the pigmentation per cell in this strain, nor did it lower the Chl *a/*Chl *b* ratio to a value beyond that of the wild type. This finding suggests that wild type levels of the CpFTSY protein are sufficient to meet all needs of the *C. reinhardtii* chloroplast and that levels of the CpFTSY protein in the wild type are not the limiting step in either the accumulation of Chl/cell or enhancement of the PS Chl antenna size.

Intermediate between wild type and *tla2* values of the Chl/cell and the Chl *a/*Chl *b* ratio were observed in the C2-C4 transformants. These intermediate values correlated with the degree of complementation and with the level of expression of the CpFTSY protein in these complemented lines. Accordingly, levels of expression for the CpFTSY protein, the Chl/cell and the reciprocal of the Chl *a/*Chl *b* ratio were in the order C1>C2>C3>C4 (see Fig. 14A and Table II).

Under low-light heterotrophic growth, the PSII reaction center proteins CP43 and PSBO accumulated in the *tla2* mutant to about 50% of the wild type level, while the major PSII Chl *a-b* light-harvesting antenna protein LHCB1 was lowered to a mere 10% of the wild type (Fig. 14A). The latter is consistent with the low pigmentation and also with the high Chl *a/*Chl *b* ratio of the *tla2* mutant. The PSI reaction center protein PSAL was also found to be lower in abundance, down to about 10% in the *tla2* mutant relative to the wild type. The different relative abundance of PSI and PSII in the *tla2* mutant compared to the wild type under heterotrophic, low light growth versus photoautotrophic, medium light growth can be explained as a consequence of the changed light and growth conditions that prevail, rather

than to a direct consequence of the *tla2* mutation. The level of these proteins was restored in the C1 complemented line, while the other complemented lines showed intermediate protein contents directly correlating with the CpFTSY expression in these strains.
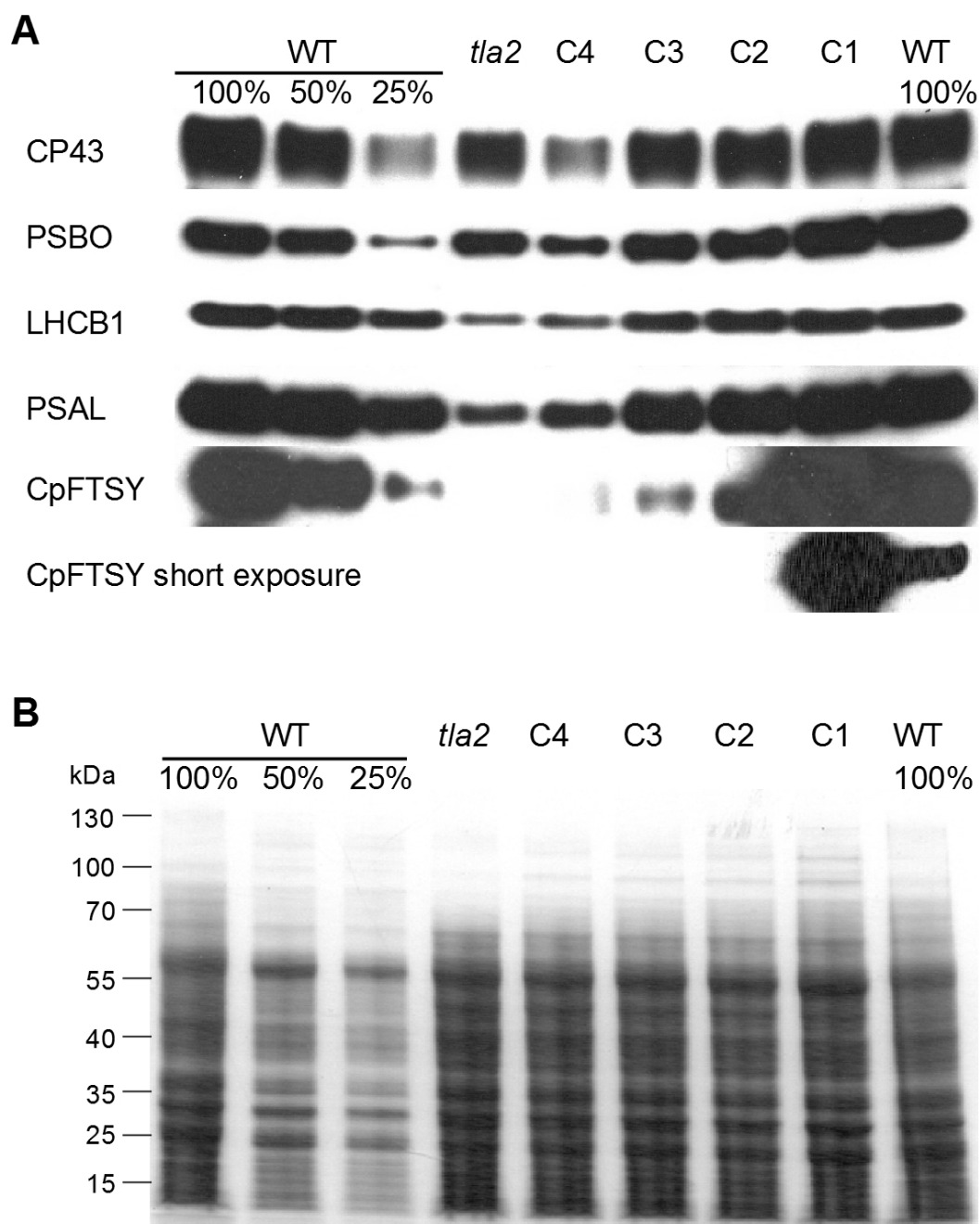
Figure 14: Western blot analysis of *C. reinhardtii* total cell protein extracts isolated from wild type, the *tla2* mutant strain, and *tla2* lines C1, C2, C3, and C4 complemented with a wild type copy of the *CrCpFTSY* gene. **A**. Immuno-detection of CrCpFTSY and specific thylakoid membrane proteins was performed with polyclonal antibodies against PSII subunits CP43 and PSBO, Photosystem I subunit PSAL and LHC-II subunit LHCB1. Loading of lanes was based on Chl and corrected for the Chl content per cell so as to load proteins on an equal cells basis. **B.** Coomassie-blue stained SDS-PAGE analysis of the samples shown in A.

CpFTSY is localized in the chloroplast stroma

Two protein-targeting programs, namely TargetP and ChloroP, predicted chloroplast targeting of the precursor CpFTSY protein. The analysis with TargetP included a reliability score, which was rather low in the case of the CpFTSY apo-protein indicating a weak prediction. However, both programs predicted that the first 36 amino acids probably act as the chloroplast transit peptide. To investigate if the CpFTSY protein is indeed chloroplast localized, an intact chloroplast enriched fraction was isolated from *C. reinhardtii* and probed by Western blot analysis (Fig. 15). Included in this analysis were proteins from total cell extract, thylakoid membrane fraction, soluble fraction of whole cells, and intact chloroplasts. For the total cell extract and the chloroplast-enriched fraction equal amounts of chlorophyll was loaded. The Western blot analysis results showed that the amount of the CpFTSY protein was about the same in total cell and chloroplast extracts (Fig. 15A). CpFTSY antibody cross-reaction could be detected in the membrane fraction, whereas a strong CpFTSY cross-reaction was noted with proteins in the soluble extracts of *C. reinhardtii*. These results are consistent with predictions made on the basis of bioinformatic software analysis (DAS, HMMTOP, PredictProtein, SOSUI, TMHMM, TMpred and TopPred) assigning soluble properties to the CpFTSY protein. A similar profile was noted in Western blots of the above-mentioned protein extracts, probed with specific polyclonal antibodies raised against the CpSRP54 protein of *C. reinhardtii* (Fig. 15A). The latter is postulated to function in tandem with the CpFTSY protein (see Discussion section). Fig. 15A also shows Western blot analysis results of the above mentioned protein extracts with specific polyclonal antibodies raised against the D1 and PSBO proteins of PSII, the latter serving as controls for the purity of the fractions that were employed in the localization of the CpFTSY protein.
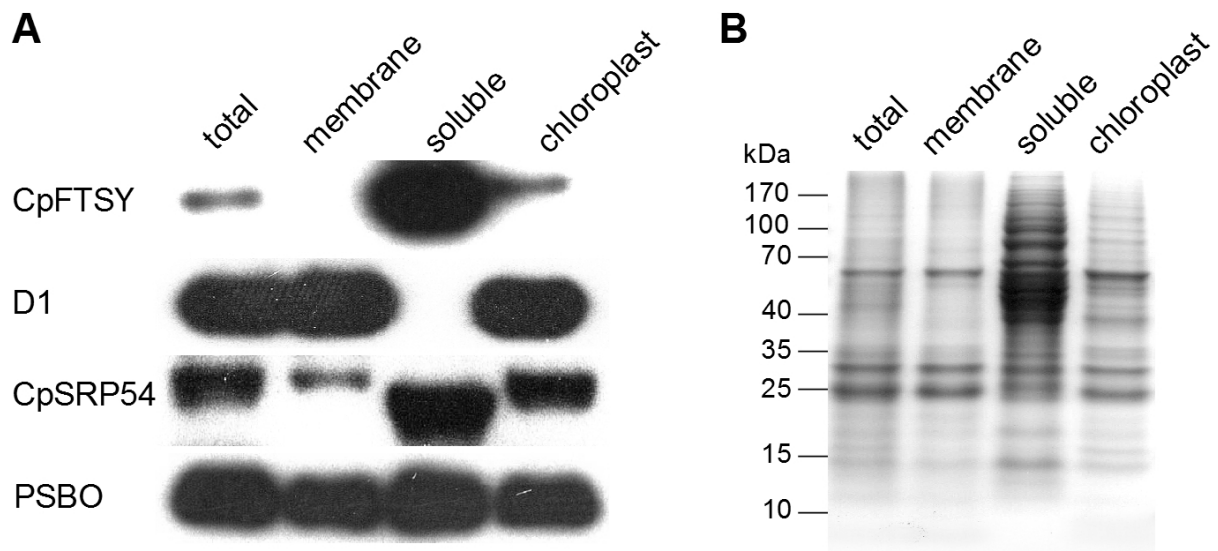
Figure 15: Cell fractionation and localization of the CpFTSY protein. **A.** Immunoblot analysis of wild-type total cell protein extract (1.5 µg Chl loaded), total membrane extract (1.5 µg Chl loaded), total soluble fraction (75 µg of protein loaded), and isolated chloroplast extract (1.5 µg Chl loaded). Western blot analysis was conducted with specific polyclonal antibodies raised against the CrCpFTSY, CrCpSRP54, PSBO or D2 proteins. **B.** Coomassie-blue stained SDS-PAGE analysis of the samples shown in A.

Chlorophyll-protein analysis of wild type and *tla2* mutant by non-denaturing Deriphat-PAGE

The pale green phenotype of the *tla2* mutant, its low Chl content per cell, the higher than wild type Chl *a*/Chl *b* ratio, and the lower content of thylakoid membrane proteins (PSII-RC, LHCB1, PSI-RC) all indicate alterations in the organization of the photosynthetic apparatus and in the light harvesting antenna of this strain. Further insight of these changes was afforded by non-denaturing Deriphat-PAGE analysis. In photosynthetic organisms the photosystems are organized in large complexes (holocomplexes) with the PS-core and LHC tightly coupled and integral to the thylakoid membrane. However, the subcomplexes can be separated by non-denaturing deriphat PAGE (Peter and Thornber, 1991). We used this method with thylakoid membrane preparations from *tla2*, its complemented C1-C4 lines and a wild type control. Four different pigment-containing protein complexes could be distinguished in the PAGE analysis of the wild type: large complexes, migrating to about 660 kDa, PSI and PSII complexes, including their light harvesting antennae, PSII dimers (~500 kDa), PSII monomers (~250 kDa) and LHC-II trimers at around 70 kD (Fig. 16A). In the *tla2*

mutant most of these Chl-protein native bands were substantially reduced or absent. PSII-LHC-II super-complexes and PSII dimers could not be detected on the green native gels. On the other hand, the intensity of the PSII monomer band did not change significantly in the *tla2* mutant relative to the wild type (lanes loaded on a per cell basis). In the *tla2* complemented lines the green band attributed to PSII monomers stayed at about the same level, while all other green bands increased in their intensity in parallel with the degree of *tla2*-CpFTSY complementation.

A two-dimensional analysis of the protein complexes resolved by the native page was also undertaken (Fig. 16B). Putative proteins were identified based on their molecular weight in the 2-dimensional SDS-PAGE. Results obtained from the two-dimensional denaturing SDS-PAGE analysis were consistent with the notion of substantial depletion of the LHC from the *tla2* mutant. The analysis further revealed that the abundance of the ATP synthase in *tla2* thylakoids was also slightly lowered by the mutation since the alpha and beta subunits of this complex were not as abundant as those in the wild type (Fig. 16B).
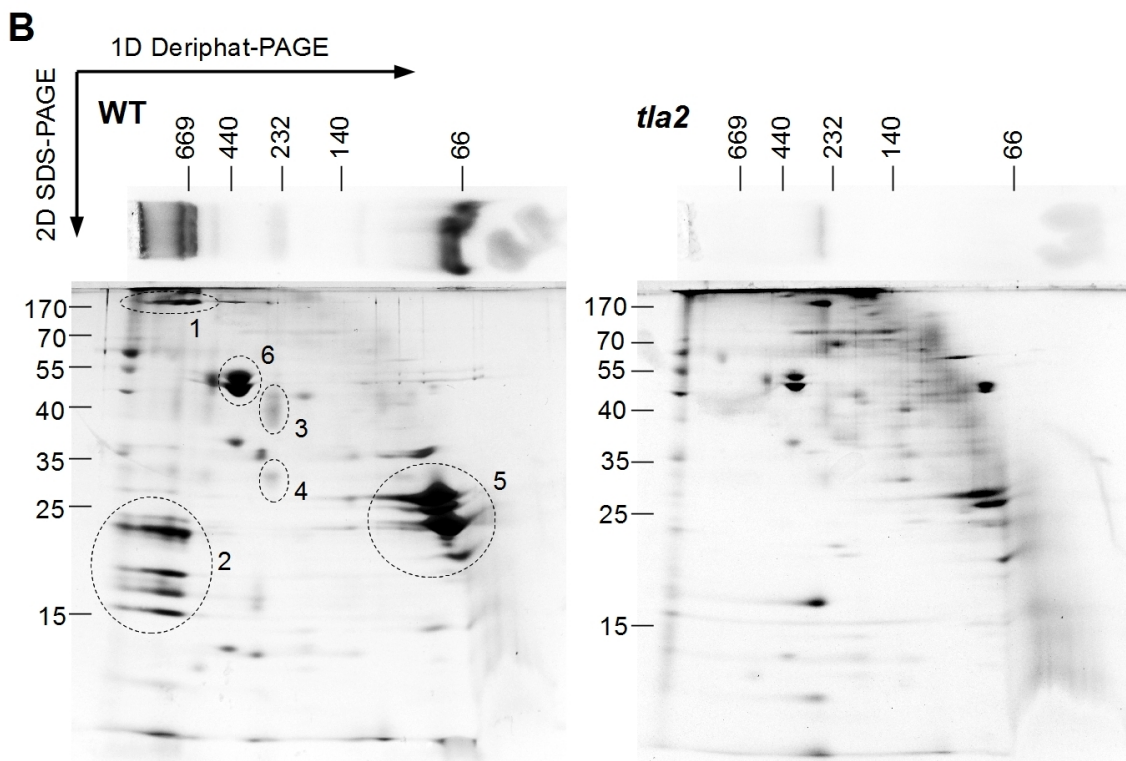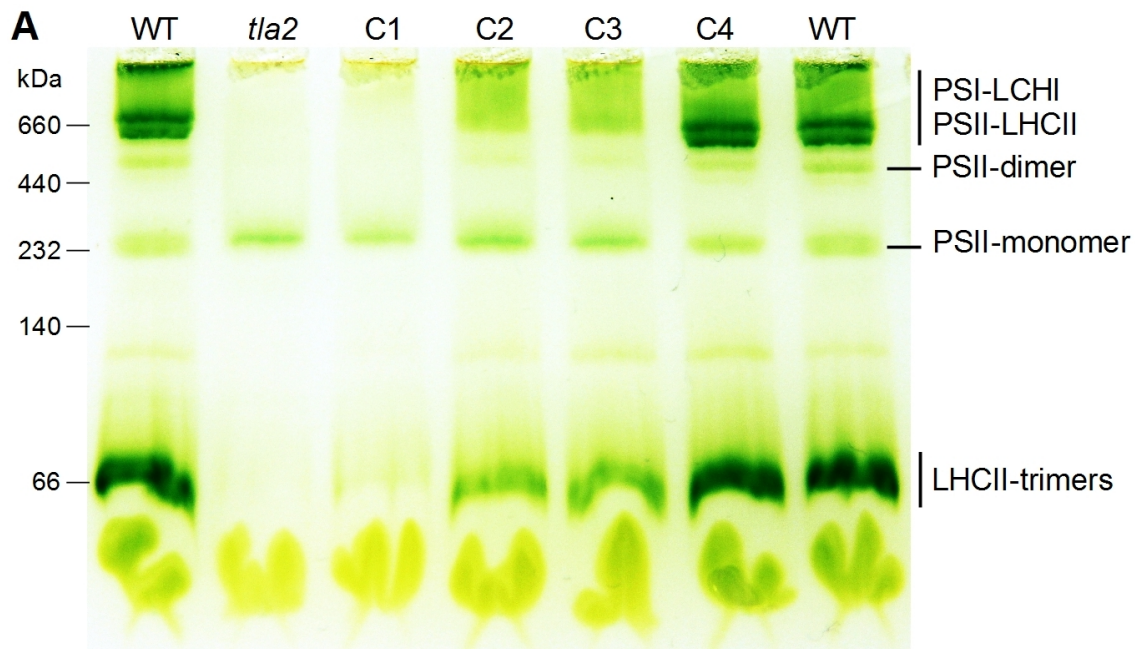
Figure 16: Analysis of photosynthetic complexes from thylakoid membranes, resolved by nondenaturing deriphat PAGE and denaturing second dimension electrophoresis. Samples tested were from wild type, *tla2* mutant, and *tla2* lines C1, C2, C3, and C4 complemented with a wild type copy of the *CrCpFTSY* gene. **A.** Pigment-protein complexes resolved by nondenaturing deriphat-PAGE. Protein complexes were identified by their molecular mass of the first nondenaturing and second denaturing dimension. Masses of the marker on the left are given in kDa. **B.** Silver nitrate stained second denaturing dimension from wild type and *tla2*. 1: PSI reaction center proteins PSAA and PSAB dimer, 2: LHCI proteins, 3: PSII reaction center proteins CP43 and CP47, 4: PSII reaction center proteins D1 and D2, 5: LCHII proteins, 6: α and β subunit of the ATP-synthase. Molecular size markers are given in kDa.

44

The *tla3* mutant

tla3 phenotype

The *tla3* strain, when cultivated on agar, displayed a light yellow-green coloration, compared to the dark green of the wild type strains (Fig. 17). Measurements of pigment content showed that cells of the *tla3* mutant contain only about 15% of the chlorophyll present in wild type strains (Table IV). While the Chl *a* content in the *tla3* mutant is about 30% of the wild type, Chl *b* content dropped to about 5%. This disproportional loss of Chl *b* compared to Chl *a* changed the Chl *a* / Chl *b* ratio in the *tla3* mutant to about 13:1, while this ratio in the wild types is normally ranging between 2.7-3.0:1. An elevated Chl *a* / Chl *b* ratio suggests that the peripheral Chl *a-b* light harvesting antenna complexes are substantially depleted in abundance, i.e., they do not assemble to form large arrays of antennae as those found in the wild type. Accordingly, this strain is a putative truncated light-harvesting antenna (*tla*) mutant. The total carotenoid per cell content in the *tla3* mutant was also lowered to about 35% of that in the wild type.

CC425   4A+   *tla3*

Figure 17: Single-cell colonies of *Chlamydomonas reinhardtii* wild type and *tla3* mutant grown on agar. Note the dark green coloration of the wild type strains, as compared to the pale green coloration of the *tla3* mutant.

Low light [80 μmol photons m^{-2} s^{-1}]
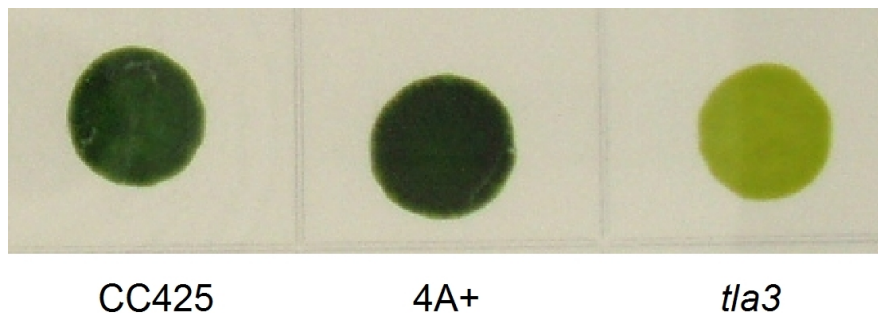
Strain	Chl/Cell [fmol]	Chl a/Cell [fmol]	Chl b/Cell [fmol]	Chl a/Chl b	Car/Cell [fmol]	Car/Chl
4A+	2.57±0.43	1.84±0.32	0.73±0.11	2.72±0.07	1.07±0.17	0.42±0.00
CC125	2.66±0.13	1.95±0.10	0.71±0.03	3.00±0.03	1.11±0.06	0.42±0.00
CC504	2.36±0.05	1.69±0.04	0.67±0.01	2.73±0.05	0.93±0.04	0.39±0.01
CC425	2.33±0.10	1.69±0.07	0.64±0.03	2.86±0.04	0.95±0.04	0.41±0.01
C1	1.26±0.35	0.91±0.25	0.36±0.10	2.77±0.02	0.70±0.15	0.56±0.04
C2	1.59±0.10	1.17±0.05	0.42±0.05	3.08±0.22	0.67±0.02	0.42±0.01
C3	0.81±0.02	0.61±0.02	0.19±0.00	3.59±0.03	0.54±0.04	0.67±0.03
C4	0.45±0.02	0.38±0.02	0.07±0.00	6.64±0.07	0.40±0.01	0.89±0.03
tla3	0.38±0.03	0.34±0.01	0.04±0.00	12.70±1.72	0.37±0.01	0.97±0.01

Table IV: Chlorophyll and carotenoid pigment content and ratios for wild type, *tla2* mutant, and *tla2*-complemneted strains of *Chlamydomonas reinhardtii* (n=3-5; means ± SD).

To investigate if the functional light-harvesting Chl antenna size of the photosystems of the *tla3* mutant is indeed smaller compared to the wild type, the light-saturation curve of photosynthesis was measured under *in vivo* conditions with photoautotrophically grown cells. The dark respiration rate of the cells, measured at 0 light intensity, was about 30 mmol O_2 (mol Chl)$^{-1}$ s^{-1} in the wild type and 62 mmol O_2 (mol Chl)$^{-1}$ s^{-1} in the *tla3* mutant (Fig. 18). When normalized to a per cell basis, wild type cells respired at about 56 amol of O_2 per second, while the *tla3* mutant consumed only 21 amol of O_2 per second. This phenomenon of a lower respiration rate per cell for *tla* type mutants has been observed previously with the *tla2* strain (Kirst et al., 2012) and may be explained to be a consequence of the slower supply of respiratory substrate in these mutants.

In the light intensity range of 0-400 μmol photons m^{-2} s^{-1}, photosynthetic activity increased as a function of the light intensity. The increase was linear for *tla3* and wild type, and both strains showed similar initial slopes, suggesting the same quantum yields of photosynthesis. This initial slope is shown in the results of Fig. 18, specifically in the region between 20-200 μmol photons m^{-2} s^{-1} light intensity, where there is a linear regression in for both strains. The slope of these linear regressions was measured to be 0.56 and 0.57 in

relative units for the *tla3* and wild type, respectively. Identical initial slopes in the light-saturation curves indicate that the quantum yield of photosynthesis for *tla3* and wild type is essentially the same. It may be concluded that the mutation in *tla3*, and the putative truncated Chl antenna size did not interfere with the quantum yield efficiency of the photosynthetic apparatus.
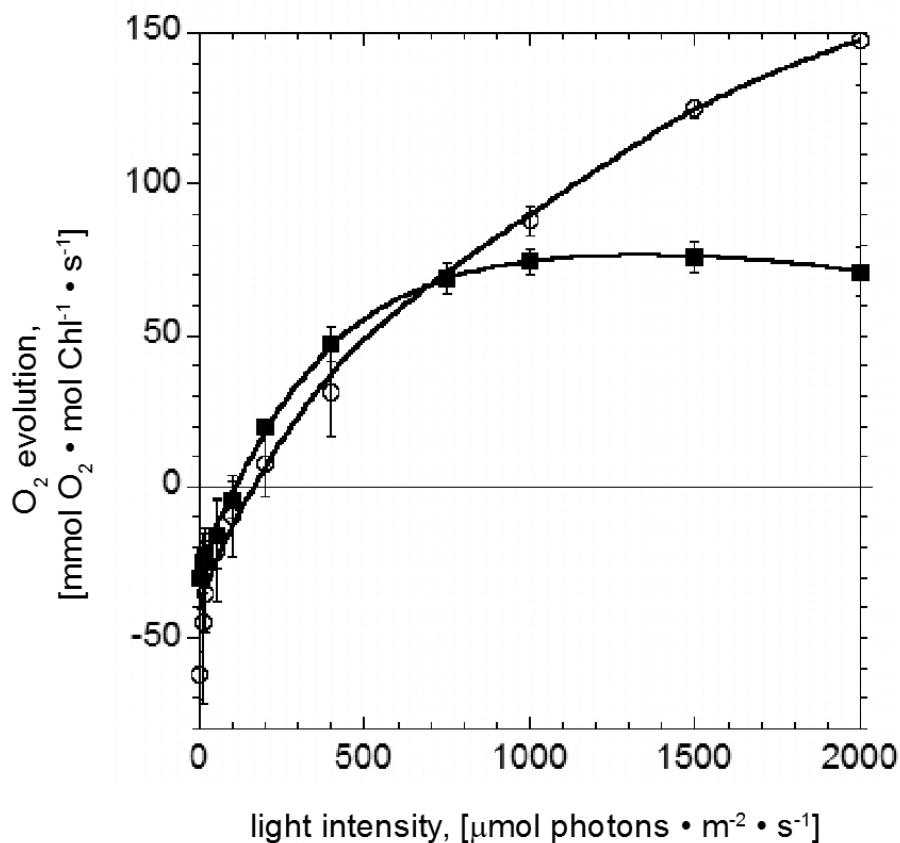
Figure 18: Light-saturation curves of photosynthesis obtained with the *C. reinhardtii* wild type (solid squares) and the *tla3* mutant (open circles). The initial slopes of both curves are similar, suggesting equal quantum yield of the photosynthesis. The light-saturated rate P_{max} was tow fold higher in the *tla3* mutant than in the wild type, suggesting a greater productivity on a per Chl basis in the *tla3* than in the wild type.

Photosynthetic activity in the wild type saturated at about 500 μmol photons m^{-2} s^{-1}. Higher light intensities did not bring about any further increase in the rate (Fig. 18). The light-saturated rate of photosynthesis minus respiration is defined as P_{max}, equal to about 100 mmol O_2 (mol Chl)$^{-1}$ s^{-1} in the wild type (Table V). The photosynthetic activity of the *tla3* mutant continued to increase beyond 500 μmol photons m^{-2} s^{-1} and did not quite saturate, even at light intensities corresponding to bright sunlight at about 2,000 μmol photons m^{-2} s^{-1}.

47

For the purposes of this work, P_{max} in the *tla3* mutant was defined as the rate of O_2 evolution achieved at 2,000 μmol photons m^{-2} s^{-1}. (P_{max}=210 mmol O_2 (mol Chl)$^{-1}$ s^{-1}). The rate of photosynthesis in the light-saturation measurement is based on the chlorophyll content of the samples. Hence, P_{max} provides a measurement of the productivity of chlorophyll in the two strains. On this basis, *tla3* outperforms the wild type by about 100%, 210 compared to 106 mmol O_2 (mol Chl)$^{-1}$ s^{-1} for *tla3* and wild type, respectively (Table V). However, the maximal photosynthetic activity of *tla3* on a per cell basis was measured to be about 35% of that in the wild type, (P_{cell} = 69 amol O_2 cell^{-1} s^{-1} for the *tla3,* compared to 196 amol O_2 cell^{-1} s^{-1} for the wild type. This observation suggests fewer thylakoid membranes and/or photosynthetic electron transport chains in the mutant.

Parameter measured	WT	*tla3*
Quantum yield, relative units	100±25	102±20
Respiration [mmol O_2 • (mol Chl)$^{-1}$ • s^{-1}]	30.2±11.9	62.2±8.0
Respiration [amol O_2 • cell^{-1} • s^{-1}]	55.8±26.3	20.6±5.4
P_{max} [mmol O_2 • (mol Chl)$^{-1}$ • s^{-1}]	106.3±12.8	209.7±16.7
P_{max} [amol O_2 • cell^{-1} • s^{-1}]	196.2±46.2	69.3±6.6
P_{max} / Respiration, relative units	3.5±1.9	3.4±0.7
Half-saturation intensity, [μmol photons m^{-2} s^{-1}]	210	>600
Functional PSIIα Chl antenna size	333±27	-
Functional PSIIβ Chl antenna size	119±31	94±5
proportion of PSIIα [%]	59±1	-
Average PSII Chl antenna size	245±30	94±5
Functional PSI Chl antenna size	230±26	120±10

Table V: Photosynthesis, respiration, and photochemical apparatus characteristics of wild type (WT) and the *tla2* mutant of *Chlamydomonas reinhardtii* grown phototrophically under medium light [459 μmol photons m^{-2} s^{-1}]. Photosystem Chl antenna size and reaction center concentrations were measured spectrophotometrically (Melis, 1998). (n=3; means ± SD).

The half-saturation intensity of the wild type was determined to be about 200 µmol photons m^{-2} s^{-1}, whereas the half-saturation intensity of *tla3* was estimated to be greater than 600 µmol photons m^{-2} s^{-1}. Because of the reciprocal relation of the half-saturation intensity to the collective size of the light-harvesting antenna of both photosystems, it can be estimated that the size of the light-harvesting antenna of the photosystems in the *tla3* mutant is about 1/3rd of that in the wild type. This observation suggests that, in addition to a diminished amount of thylakoid membranes and/or photosynthetic electron transport chains, there is a substantially smaller Chl antenna size in the mutant.

To measure precisely the Chl molecules functionally associated with each photosystem, the kinetic-spectrophotometric method of Melis (1989) was applied. The number of Chl molecules associated with the reaction center of PSI and PSII was measured in cells grown photoautotrophically under a medium light intensity (450 µmol photons m^{-2} s^{-1}). The wild type showed biphasic PSII conversion kinetics, attributed to the two populations of PSII$_\alpha$ and PSII$_\beta$ units (Melis and Homan, 1976; Melis and Duysens, 1979) having a large and a smaller light-harvesting Chl antenna size, respectively. The Chl (*a* and *b*) molecules associated with these two forms of PSII were measured to be 333 and 119, respectively (Table V). It was further determined that the ratio of PSII$_\alpha$: PSII$_\beta$ was about 60:40 in the wild type. Thus, the average number of Chl molecules associated with a PSII reaction center in the wild type was calculated to be 245, consistent with earlier measurements from this lab (Polle et al., 2003). The PSII conversion kinetics of the *tla3* strain showed a single Q$_A$ reduction phase, thus only one type of PSII unit is present in the *tla3* mutant. The functional light-harvesting Chl antenna size of PSII in the *tla3* strain was measured to be 95 Chl molecules, which is about 38% of the wild type Chl antenna size. The light-harvesting antenna of PSI contained 230 and 120 Chl molecules for the wild type and *tla3* mutant, respectively, a reduction to about 50% of the wild type antenna.

To investigate the abundance of the proteins associated with the Chl *a-b* light-harvesting complex in wild type and *tla3* mutant, Western blots analysis of total cell protein extracts was undertaken. *C. reinhardtii* proteins were probed with specific polyclonal antibodies raised against the *A. thaliana* light-harvesting proteins 1-5 (Fig. 19). For better comparison of the results, the wild type lanes were loaded in three different concentrations, equal cell basis (100%), 25% cells (about equal reaction center basis) and 8% cells.

Antibodies against the major light-harvesting proteins LHCB1 and LHCB2 cross-reacted with specific proteins in *C. reinhardtii*. The abundance of the latter was lower to about 5-10% in the *tla3* mutant as compared to the wild type. The protein band cross-reacting with the anti-LHCB3 was not detectable in the *tla3* mutant. The protein bands cross-reacting with the minor light-harvesting antenna proteins LHCB4 and LHCB5 where both reduced to about 5% or less in the *tla3* mutant. The PSBD PSII reaction center protein was lowered to about 35% in the mutant, relative to the wild type. The PSI reaction center protein PSAL was also lower in abundance to about 15-20%.
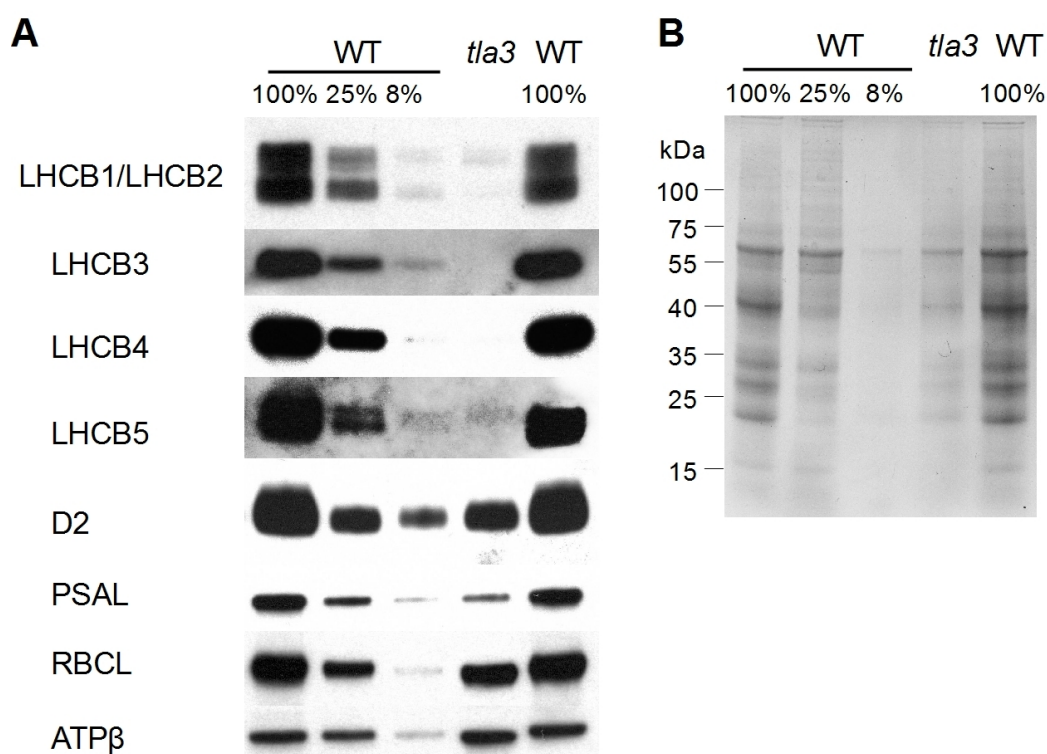
Figure 19: Western blot analysis of the light-harvesting antenna proteins of PSII in wild type and the *tla3* mutant. **A.** Immuno-detection of proteins with specific polyclonal antibodies against the light harvesting proteins LHCB1/LHCB2, LHCB3, LHCB4 and LHCB5, the PSII reaction center protein D2, the PSI reaction center protein PSAL, RuBisCo (RBCL) and the β subunit of the ATP synthase are shown. **B.** Coomassie-blue stained SDS-PAGE analysis of the samples shown in A.

These results clearly show that loss of the light-harvesting proteins is proportionally greater than the loss of reaction centers, confirming the truncated light-harvesting antenna size phenotype at the protein level. The abundance of the large subunit of RuBisCo (RBCL) and the β subunit of the ATP-synthase (ATPβ) were not affected by the mutation (Fig. 19).

Collectively, the above analysis strongly suggested that the *tla3* strain has a *bona fide* truncated Chl antenna size; raising the question of the gene(s) that was/were interfered with to arrive at this phenotype. Accordingly, a gene cloning analysis was undertaken.

Southern blot analysis

Southern blot analyses were employed to determine the copy number of inserted pJD67 plasmids into the genomic DNA of the *tla3* mutant. For this analysis, different probes covering the entire pJD67 sequence were used. The horizontal bars in Fig. 20A, numbered 1-6, depict the location of the six probes and their binding location along the length of the pJD67 plasmid, linearized with *Hind*III. Figure 20A, vertical bars, show the location of restriction sites on the pJD67 vector for the enzymes used to digest the genomic DNA. If a single plasmid was inserted into the genomic DNA of *tla3,* then one hybridization signal would be expected to be generated with probes 1-3, while probes 4-6 would generate two separate hybridization signals, one originating from the inserted pJD67 plasmid, the other from the endogenous inactive *ARG7* gene and its promoter and terminator regions (dark gray areas). These two hybridization signals can be distinguished from one another from their fragment size in Southern blots of genomic DNA, whereby the DNA fragment containing the endogenous gene would have the same size in both wild type and *tla3* mutant, whereas a hybridization signal corresponding to a different fragment size in the mutant would be originating from the inserted plasmid.

The Southern blot analyses using probes 1, 2 and 3 generated a single hybridization band with the *tla3* genomic DNA and none with the wild type genomic DNA (Fig. 20B), indicating a single insertion of the pJD67 plasmid in the *tla3* strain. When probes 4, 5 and 6 were used with wild type genomic DNA digests, a single hybridization band was detected, identifying the fragment size of the endogenous *ARG7* target sequence. An additional hybridization band of different size was detected with the *tla3* genomic DNA digests. It should be noted that probe 6 used on *tla3* genomic DNA digested with *Sma*I generates a single hybridization band of about 700 bp in size because the restriction sites of *Sma*I in this area of the *ARG7* gene are close together and generate the same fragment size for plasmid DNA and endogenous *ARG7* gene DNA (Fig. 20A). However, the hybridization signal intensity in the lane loaded with *tla3* genomic DNA digest (Fig. 20B, probe 6, *Sma*I, *tla3*) is greater compared to that of the wild type (Fig. 20B, probe 6, *Sma*I, WT), indicating that the *ARG7*

51

DNA target is more abundant in the *tla3* sample, as would be expected if an insertion of pJD67 DNA took place.

A

B
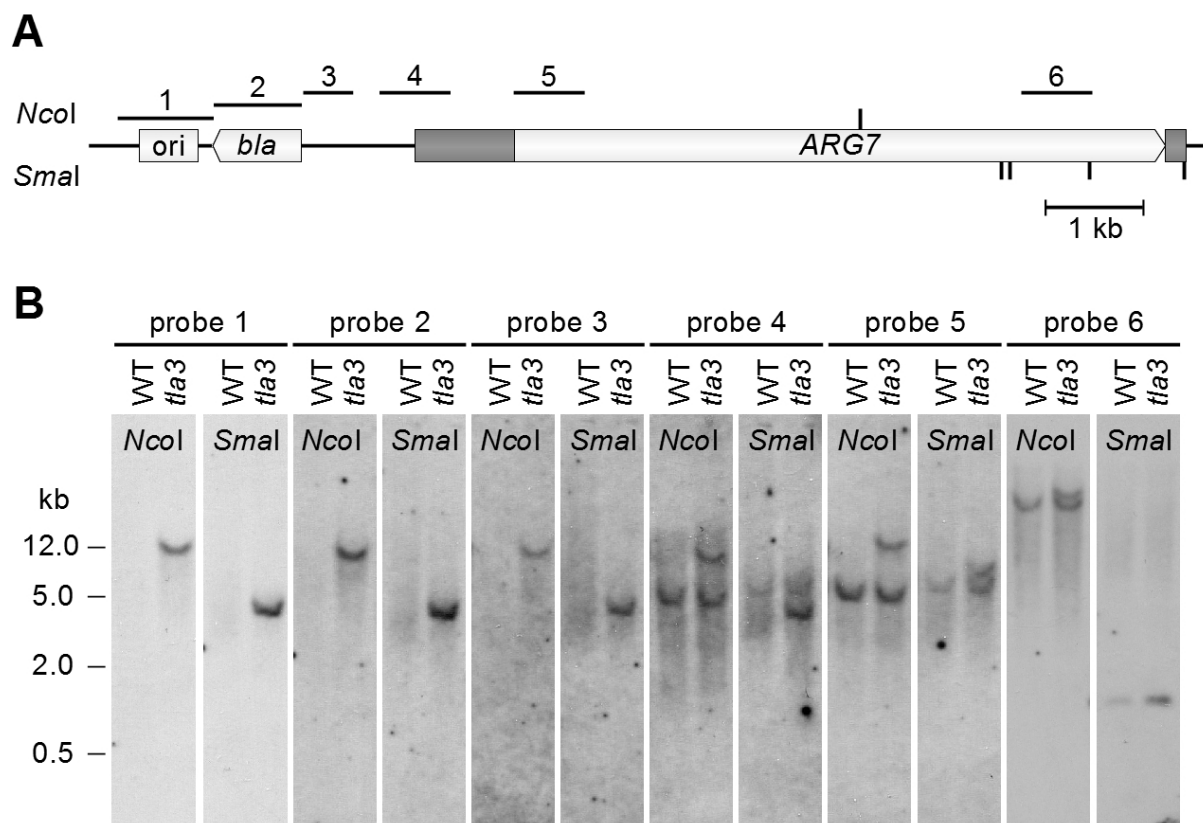
Figure 20: Southern blot analysis to define copy number and integrity of inserted pJD67 plasmid into the genomic DNA of *Chlamydomonas reinhardtii* insertional transformant. Wild type and *tla3* strains were used in this analysis. **A.** Schematic map of pJD56. Dark gray boxes indicate the promoter and terminator region of the *ARG7* gene. These regions and the *ARG7* gene are not plasmid specific but are also present in the host strain. Isolated genomic DNA was digested by *Nco*I and *Sma*I. The location of probes 1-6, used for the Southern blot analysis, are marked with black lines. **B.** Developed films of hybridized Southern blots. Each column indicates the probe used for hybridization and consist of a set of two genomic DNA digests, *Nco*I and *Sma*I. Marker sizes indicate electrophoretic mobility in kb.

In this Southern blot analysis, no more then one hybridization signal could be detected from the pJD67 plasmid, indicating a single pJD67 insertion into the genomic DNA of *tla3*. The Southern blots also provided information about the integrity of the inserted plasmid DNA. Every one of the probes 1-6, designed to hybridize to the pJD67 sequence in the *tla3* mutant, generated an insertion specific hybridization signal with *tla3* genomic DNA digests. This observation suggests that all parts of the plasmid are present in the *tla3* mutant.

In a *Hind*III linearized plasmid, as the one shown in Fig. 20A, the *Chlamydomonas* genomic DNA sequence flanking the insertion would begin upstream from the origin of replication of the pJD67 plasmid and on the other side of the insertion downstream from the *ARG7* terminator. A consequence of such a plasmid insertion would be that probes 1-5 would hybridize to the same fragment size if *tla3* DNA were to be digested by *Nco*I, because the *Nco*I restriction site within the pJD67 sequence is further down stream of all these 5 probes. The same applies to *Sma*I digests. In the case of a *Hind*III linearized pJD67 plasmid, the minimal fragment size would be at least 7.6 kb and 9.1 kb for *Nco*I and *Sma*I digests, respectively.

For Southern blots with *Nco*I digested genomic DNA, probes # 1 through 4 generated a hybridization signal of about 12 kb (Fig. 20B). However, probe # 5 hybridized to a slightly larger DNA fragment of 13-14 kb. The observation that probe #5 hybridized to a different DNA fragment than probes # 1 through 4 was more obvious when the genomic DNA was digested with *Sma*I. Probes # 1 through 4 hybridized to a fragment that is about 4 kb in size, while probe # 5 recognized a fragment of about 6 kb. Moreover, the fragment size recognized by probes 1-4 is smaller than the minimum expected size if an intact *Hind*III linearized plasmid was integrated into the genomic DNA of *tla3*. Specifically, these probes hybridized to a fragment of about 4 kb in size, which is about 5 kb smaller then the actual expected size. This analysis suggested that the pJD67 plasmid was rearranged during the process of insertional mutagenesis, whereby a portion of its 5' end, including the *ori* and *bla* regions of the plasmid, separated from the *ARG7* gene and was inserted at a different site in the *Chlamydomonas* genomic DNA. In that case there would be two different partial insertions, one would contain the origin of replication and the *bla* gene, the other would contain the partial insertion with the *ARG7* gene. To investigate the possibility of two partial insertions in the *tla3* mutant, multiple TAIL PCRs were performed to amplify sequence flanking the *Hind*III site of the plasmid. The resulting sequences of this analysis revealed that the plasmid DNA is still intact at the *Hind*III site. This would suggest that the inserted pJD67 plasmid in the *tla3* mutant has not been linearized at the *Hind*III site or has been re-annealed upon integration. It can be concluded that only one plasmid was inserted into the genomic DNA of the *tla3* strain, that spontaneously broke apart between probes 4 and 5 in the process of insertion but is intact at the *Hind*III site.

Mapping the pJD67 plasmid insertion site in the *tla3* strain

For flanking sequence analysis, it is necessary to map the location of insertion and the structure of the inserted plasmid to an accuracy of 100 bp. To this end, genomic DNA PCR analyses were undertaken, using the same forward primer and several reverse primers designed to correspond to DNA regions between probe 4 and probe 5. Figure 21A shows a map of the pJD67 sequence between the *bla* and *ARG7* gene and the location of the primers used for this analysis. For the reverse primers 1 through 4, a PCR product was generated using genomic DNA of the *tla3* strain as a template (Fig. 21B). However, reverse primers 5 through 8 failed to generate any PCR product. This analysis defined that the break point in the pJD67 plasmid has occurred between reverse primer 4 and reverse primer 5 (Fig. 21), which is 650 to 750 bp within the *ARG7* gene promoter.
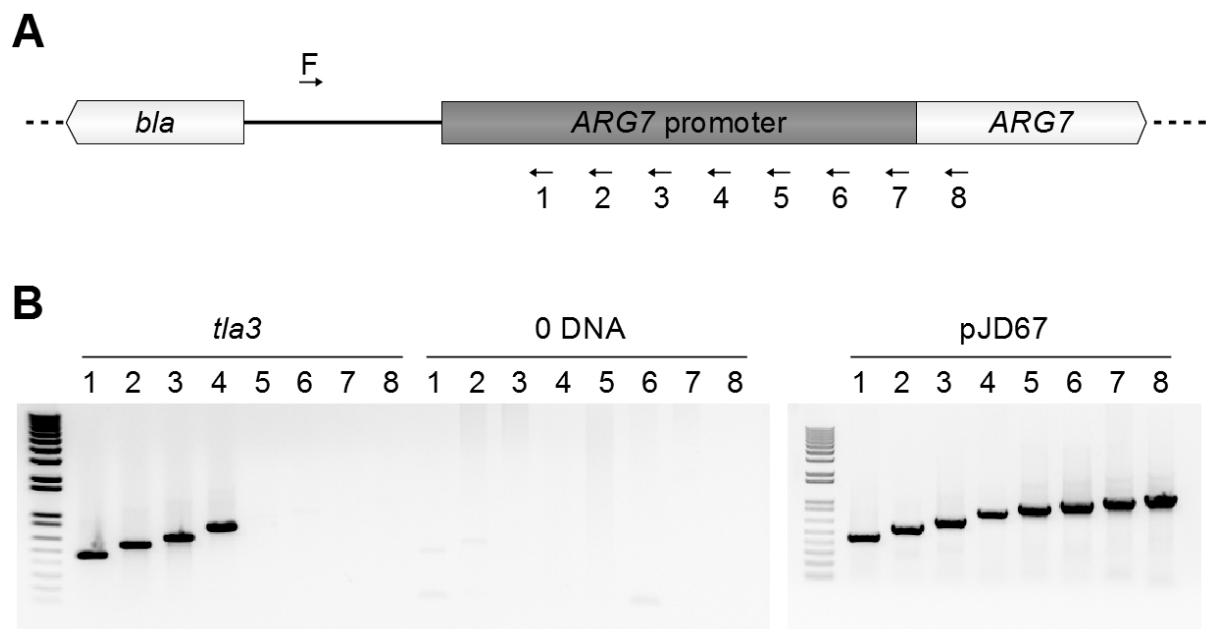
Figure 21: Genomic DNA PCR analysis to map the Insertion in *tla3*. **A.** Map of the pJD67 sequence between the *bla* and *ARG7* gene and the location of the primers. **B.** PCR reactions on *tla3* genomic DNA, 0 DNA control and positive control using pJD67. Primers further downstream of reverse primer 4 can not generate a product on *tla3* genomic DNA indicating the break point of the inserted plasmid being between primer 4 and primer 5.

Cloning the flanking sequence of the *tla3* insertion

On the basis of the above findings, TAIL PCR was attempted with a beginning point located in the *ARG7* promoter region, about 100 bp upstream of the break point in the *ARG7* promoter of the inserted plasmid. In this approach, a mix of two products is expected, one from the endogenous *ARG7* promoter and one from pJD67 sequence. After cloning the PCR products into *E. coli*, 50 clones were sequenced to determine if any of then contained the sequence flanking the pJD67 insertion. However, all clones sequenced contained exclusively sequences flanking the endogenous *ARG7* promoter but not that of the insertion. The negative result could be attributed to a greater efficiency in amplifying the flanking sequence of the endogenous *ARG7* promoter, but not that of the insert. To increase the chances of cloning the flanking sequence of the plasmid insertion site, the DNA adapter method was employed (Fig. 22). Based on the Southern blot results, it was expected that *Sma*I or *Xma*I (neoschizomer of *Sma*I) digests would generate a fragment of about 4 kb containing about 3.7 kb plasmid DNA and about 200-300 bp of upstream flanking sequence. The latter would be sufficient to locate the insertion site (Fig. 22A). The *tla3* genomic DNA was digested by *Xma*I, generating an overhang (Fig. 22B). An adapter with the matching overhang was ligated to the fragment, and using nested PCRs with forward primers in the pJD67 specific region and reverse primers in the adapter region, the sequence flanking the pJD67 insertion was specifically amplified (Fig. 22C). The insertion site was thus localized in scaffold #32 within the fourth intron of predicted gene Cre32.g781800 (Fig. 23). PCR analysis was employed to screen the insertion site for possible deletions. This analysis revealed that a predicted gene immediately upstream, namely Cre32.g781750, was deleted in the *tla3* mutant. Bioinformatic analysis showed that predicted gene Cre32.g781750 has homology to the *CpSRP43* gene in higher plants.
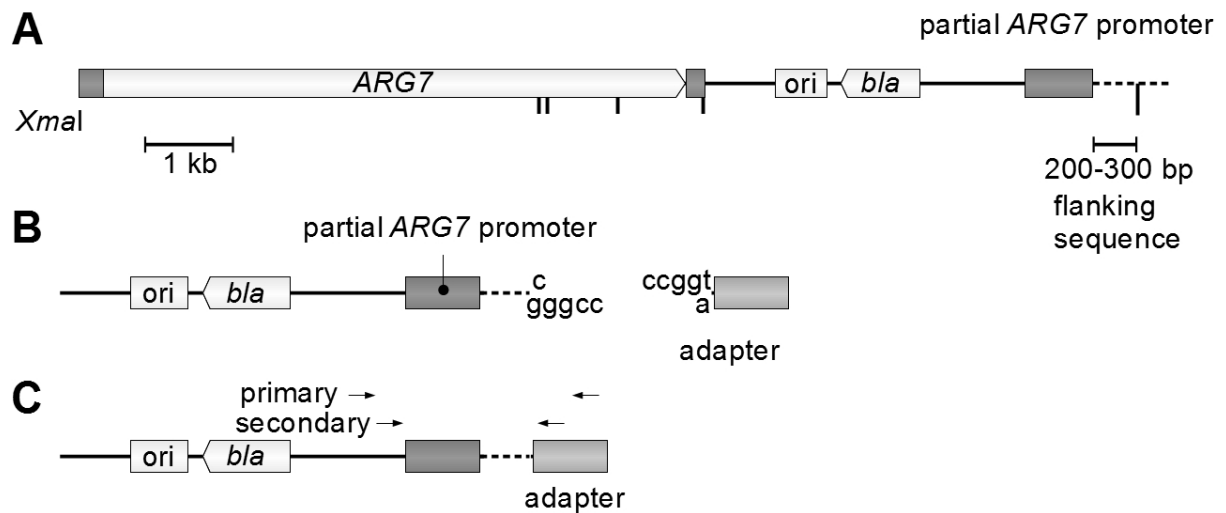
Figure 22: Flanking sequence cloning of the *tla3* insertion using the adapter method. **A.** Map of the pJD67 insertion based on the information of Southern blots and PCR mapping. **B.** *Xma*I digest of genomic DNA and ligation to the adapter with a matching overhang. **C.** Map of location of the nested PCR primers to amplify the flanking sequence.

Figure 23: Map of the Insertion site in the Tal3 mutant. The grayed out areas are deleted in the *tla3* mutant including the *CpSRP43* homologue Cre32.g781750.

Complementation of *tla3*

The cDNA of the genes Cre32.g781800 and Cre32.g781750 was cloned into the *C. reinhardtii* over-expression vector pSL18. After *Kpn*I linearization, the constructs were transformed separately into the *tla3* strain. The pSL18-Cre32.g781800 construct failed to rescue the mutation, as it did not generate any complemented strains. The pSL18-Cre32.g781750 construct yielded several complemented strains with various degrees of recovery of the dark-green coloration, ranging anywhere from dark-green wild-type coloration to pale-green *tla3*-type of coloration (Fig. 24). On the basis of the successful complementation of the *tla3* mutant with the Cre32.g781750 gene, it was concluded that the *tla3* mutant phenotype was caused by a knockout of the *Chlamydomonas* homologue of

the *CpSRP43* gene known from higher plants (Klimyuk et al, 1999; Amin et al, 1999). Four complemented *tla3* lines were selected randomly to measure pigment content and composition properties. All complemented lines, namely tla3-comp1 through tla3-comp4, showed various degrees of restoration the Chl *a*/Chl *b* ratio, as they also showed a significantly greater amount of pigmentation per cell than the un-complemented *tla3* mutant (Table IV). However, none of the four selected complemented lines that were analyzed here had as high a Chl content and as low a Chl *a* / Chl *b* ratio as the wild type. The most promising of the complemented strains, C2 (Fig. 24) accumulated chlorophyll on a per cell basis equal to only about 60% of that in the wild type.
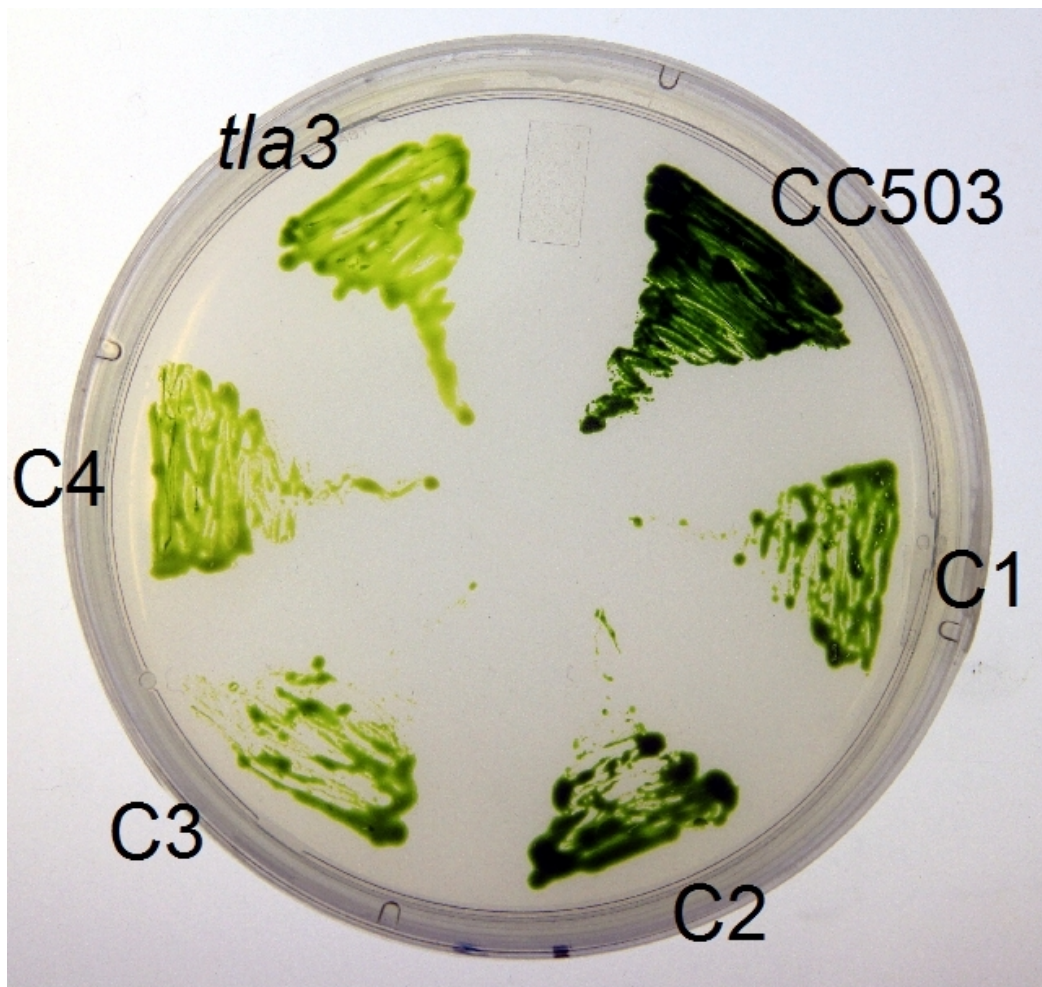
Figure 24: Colonies of *Chlamydomonas reinhardtii* wild type CC503, *tla3* mutant and the complemetary lines C1 through C4 grown on agar. Note the dark green coloration of the wild type, the pale green coloration of the *tla3* mutant and the intermediate phenotypes of the complements.

The genomic DNA of the *CpSRP43* gene in *C. reinhardtii,* from start to stop codon was found to be 4,988 bp long and contains 12 exons. The gene encodes for a protein of 430 amino acids, of which the first 37 amino acids are predicted, on the basis of ChloroP (http://www.cbs.dtu.dk/services/ChloroP/), and also on the basis of TargetP (http://www.cbs.dtu.dk/services/TargetP/) to serve as a chloroplast targeting sequence and transit peptide (Fig. 25). The mature protein of 393 amino acids contains four protein domains, determined by Pfam (http://pfam.sanger.ac.uk), three chromodomains (CD), CD1 from amino acids 27-76, CD2 from amino acids 214-266, CD3 from amino acid 305-324 and an ankyrin-repeat-domain of three repeats (amino acids 80-171).
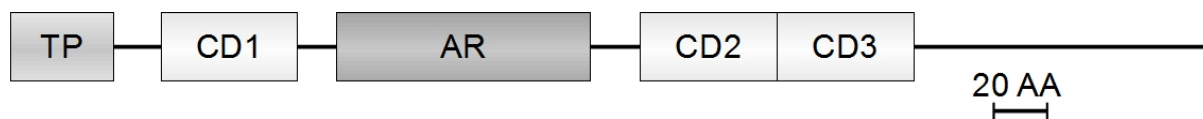
Figure 25: The *Chlamydomonas reinhardtii* CpSR43 protein schematic. TP: Chloroplast transit peptide. CD1 , CD2 and CD3: chromodomains. AR: ankyrin domain.

tla4, *tla5*, *tla6* and *tla7* mutants

Four additional *tla* mutant strains with a high Chl *a/* Chl *b* ratio have been isolated in the course of screening several DNA insertional mutagenesis libraries of *Chlamydomonas reinhardtii*, namely *tla4*, *tla5*, *tla6* and *tla7*. In addition to a high Chl *a/* Chl *b* ratio (Table VI), *tla4* through *tla7* were found to contain less Chl per cell, compared to a wild type (Table VI) and thus have a pale green phenotype similar to the *tla2* and *tla3* mutants described earlier in this Thesis.

Low light [80 µmol photons m^{-2} s^{-1}]

Strain	Chl/Cell [fmol]	Chl *a*/Chl *b*
4A+	2.57±0.43	2.72±0.07
CC125	2.66±0.13	3.00±0.03
CC504	2.36±0.05	2.73±0.05
CC425	2.33±0.10	2.86±0.04
tla2	0.46±0.04	9.60±0.98
tla3	0.38±0.03	12.70±1.72
tla4	0.45±0.02	9.83±1.02
tla5	0.40±0.01	11.02±1.34
tla6	0.39±0.02	10.74±1.92
tla7	0.41±0.04	10.01±1.21

Table VI: Chlorophyll pigment content and ratio for wild types and *tla* type mutants of *Chlamydomonas reinhardtii* selected in the screening process (n=3-5; means ± SD).

Genetic analysis of *tla4*

To determine if the pJD67 insertion is linked with the *tla4* phenotype, the mutant was backcrossed to an arginine requiring wild type strain AG1-3.24 (*arg7*). Ten complete tetrads (Fig. 26, TAP+ARG, columns A-J) were plated on non-selective media (TAP+ARG) and on media selecting for a functional *ARG7* gene provided by the pJD67 insertion (Fig. 26, TAP-only, columns A-J). When grown on the non-selective media (TAP+ARG), the tetrads showed a combination of dark green and pale green phenotype colonies. The dark green colonies were measured to have a Chl *a/* Chl *b* ratio of about 2.5-2.7, while the pale green had a Chl *a/* Chl *b* ratio around 10 (Table VI). All tetrads tested displayed a 2:2 wild type (dark green) to *tla4* (pale-green) phenotype segregation, suggesting that the *tla4* phenotype is caused by a single genetic locus. When plated on the selective media (TAP-only), the dark green colonies could not grow, while the pale green progeny grew, proving arginine autotrophy. The co-segregation of the *tla4* phenotype and the arginine autotrophy strongly suggest a linkage between the *tla4* phenotype and the inserted plasmid pJD67, which provided a functional *ARG7* gene to the cells of the pale green colonies.
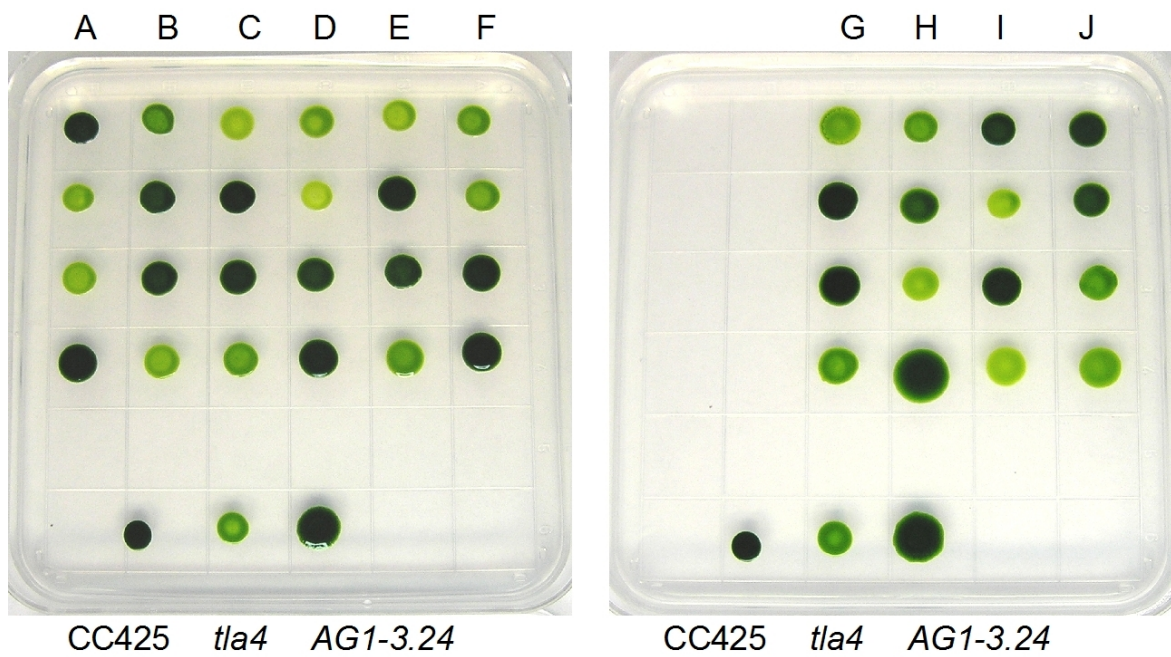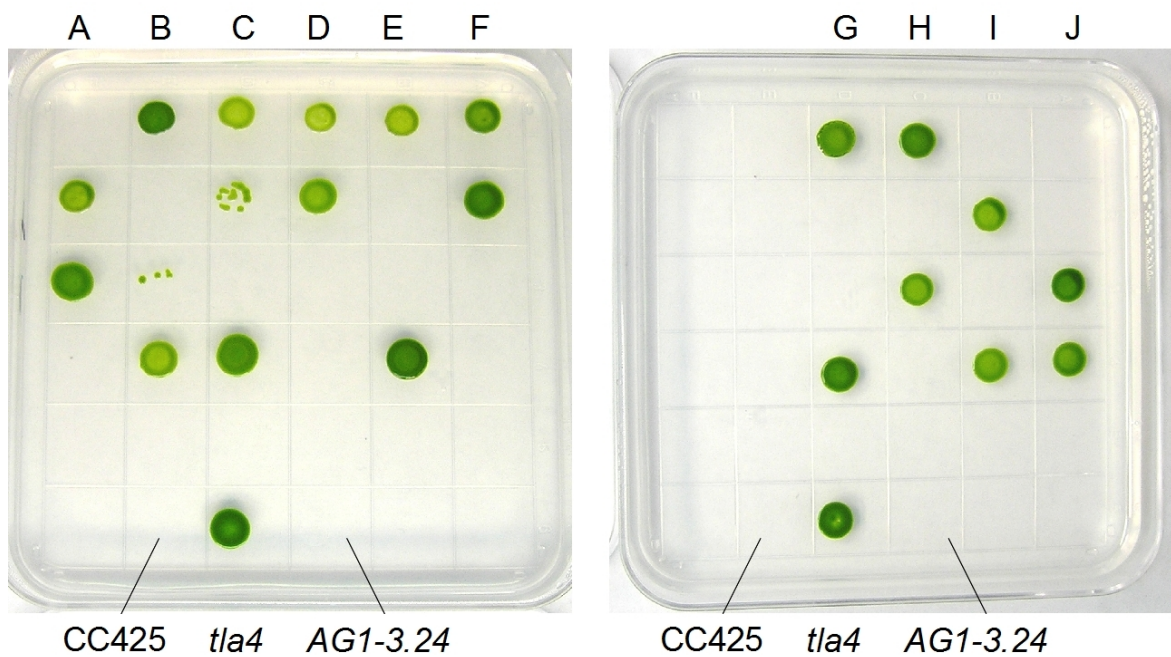
Figure 26: Genetic cross analysis of *tla4* with AG1-3.24 (*arg2*) strain. Ten complete tetrads, columns A-J, were plated on non-selective media TAP+ARG (upper panel) and on media selecting for a functional *ARG7* gene provided by the pJD67 insertion (lower panel). The dark green colonies were measured to have a Chl *a*/Chl *b* ratio between 2.5 and 2.7 while the dark green colonies had a ratio around 9.

Analysis of CpSRP genes in the *tla4* through *tla7* mutant strains

The studies of the *tla2* and *tla3* mutant strains showed that genes of the chloroplast signal recognition pathway have an effect on the pigmentation and the Chl *a/* Chl *b* ratio. Knockout of the CpSRP genes in *Chlamydomonas*, unlike those in higher plants, permitted photoautotrophic growth and did not result in a lethal phenotype. To investigate whether CpSRP genes were knocked-out in any of the four mutants, systematic PCR analysis of the genomic DNA in the *tla4-7* strains was undertaken. Figure 27 shows representative PCR results using primer sets in each of the four CpSRP genes, namely *CpSRP43*, *ALB3.1*, *CpFTSY* and *CpSRP54*. The genomic DNA PCR analysis reproducibly failed to generate a product from the *tla4* genomic DNA with primers selected from within the *CpFTSY* gene, suggesting that the *CpFTSY* gene is either deleted or substantially disrupted. Genomic DNA of *tla5* and *tla6* could not amplify the *CpSRP43* gene by PCR, and genomic DNA of the *tla7* strain failed to generate a PCR product from the *CpFTSY* gene. Thus, *tla4* and *tla7* are putative *cpftsy* mutants, and *tla5* and *tla6* are putative *cpsrp43* mutants.
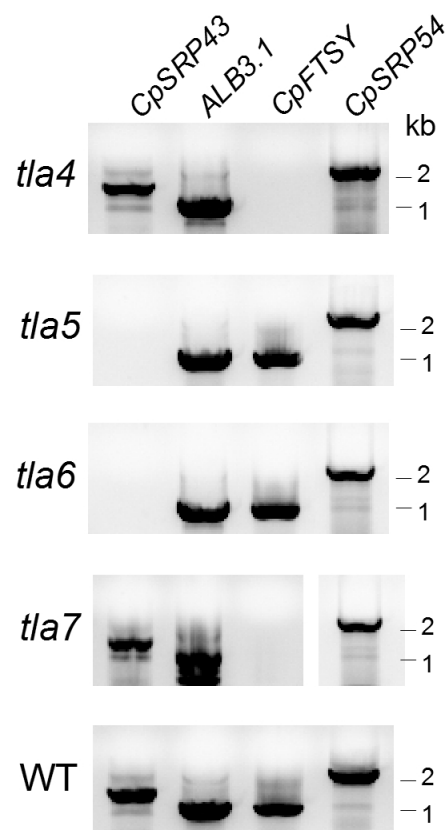
Figure 27: Representative PCR results using primer sets in each of the four CpSRP genes, namely *CpSRP43*, *ALB3.1*, *CpFTSY* and *CpSRP54* on genomic DNA from *tla4* through *tla7* and the wild type

Complementation of the mutants *tla4-tla7*

To further strengthen the notion that CpSRP genes were mutated in the *tla4-7* strains, and are thus responsible for the pale green phenotypes, each of these mutant lines was complemented with a cDNA construct containing the putative knocked-out gene. Strains *tla4* and *tla7* were successfully transformed with the cDNA construct containing *CpFTSY* (Appendix A), while *tla5* and *tla6* were transformed with a construct containing *CpSRP43* (Appendix A). Figure 28 shows plates of transformed *Chlamydomonas reinhardtii* colonies growing on antibiotic selection media after the respective complementation. On all plates a mixture of dark green and pale green colonies was noted with an approximate 1:1 ratio. Randomly isolated dark green colonies from all plates showed a Chl *a/* Chl *b* ratio similar to that of the wild type strains, ranging between 2.5-3.0, suggesting that these cells in these colonies were successfully complemented. A 50% success rate in complementation is about what is expected considering that the transformed plasmid is randomly integrated into the genomic DNA and thus could be subject to silencing or low transcription rates depending on the locus of integration. The successful cDNA complementation of the *tla4* through *tla7* strains mutants strengthens the notion that *tla4* and *tla7* are *cpftsy* null, and that *tla5* and *tla6* are *cpsrp43* null mutant.
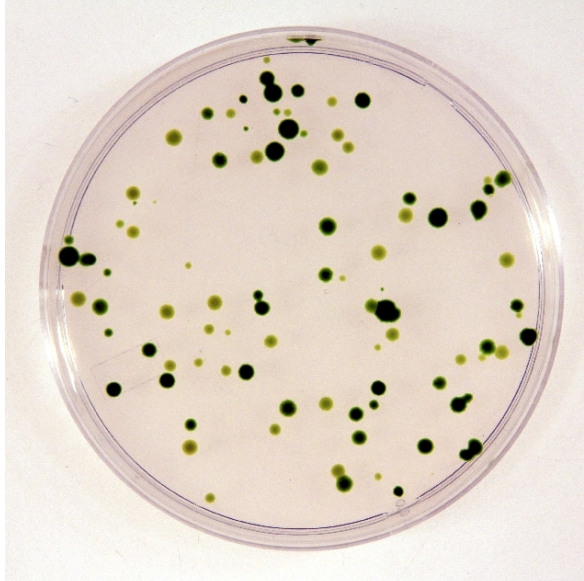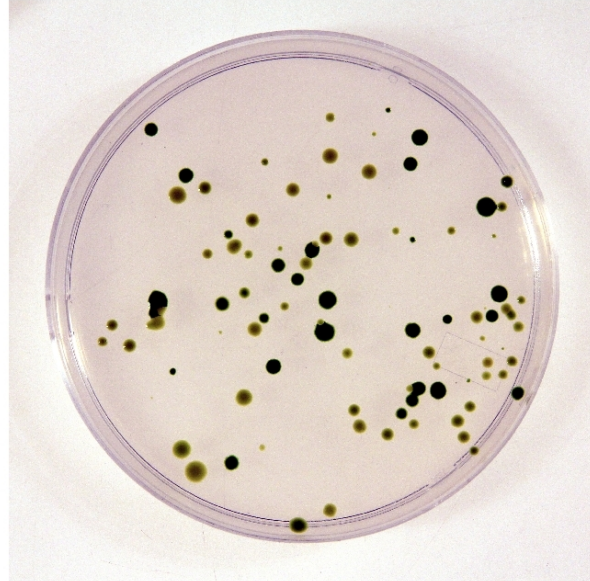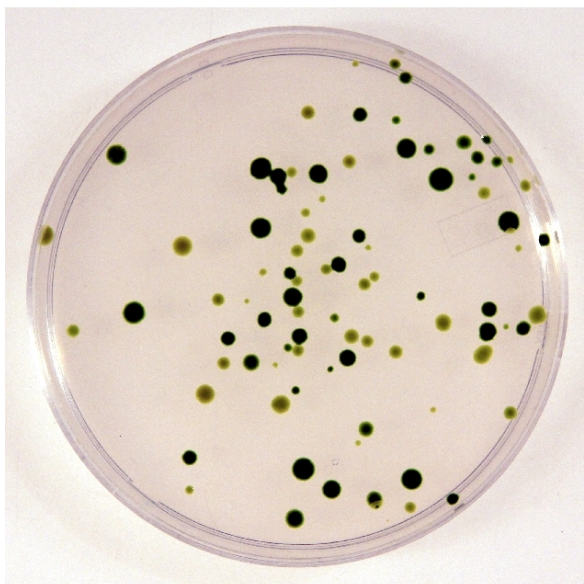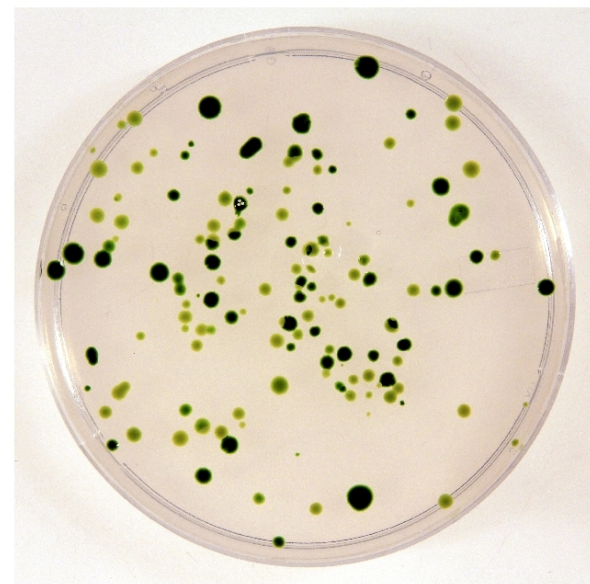
Figure 28: *Chlamydomonas reinhardtii* colonies of transformed *tla4* through *tla7* with their respective construct for complementation growing on antibiotic selection media. Randomly isolated dark green colonies have a Chl *a*/Chl *b* ratio ranging between 2.5 and 3.0.

DISCUSSION

The Ph.D. dissertation research examined six **t**runcated Chl **l**ight-harvesting **a**ntenna (**tla**) mutant strains of the green microalga *Chlamydomonas reinhardtii* with the objective of identifying genes that play a role in the definition of the Chl antenna size of the photosystems. The outcome of this Ph.D. research is cloning and elucidation of the function of two *Chlamydomonas reinhardtii* genes (*CrCpFTSY* and *CrCpSRP43*), specifically involved in the assembly of the Chl *a-b*-containing light harvesting complexes. The *CrCpFTSY* and *CrCpSRP43* genes both are components of the Signal Recognition Particle (CpSRP), which has been identified in bacteria and higher plant chloroplasts as the pathway for the integration of transmembrane proteins into the lipid bilayer of target membranes (Pool, 2005). Thus, it appears that the green microalga *Chlamydomonas reinhardtii,* similar to chloroplasts in the model plants *Zea mays* (Asakura et al., 2004) and *Arabidopsis thaliana* (Klimyuk et al., 1999; Amin et al., 1999; Pilgrim et al., 1998; Asakura et al., 2008; Sundberg et al., 1997), employs the prokaryotic SRP mechanism for the integration of integral thylakoid membrane proteins (Kirst et al., 2012)*.*

The corresponding *crcpftsy* and *crcpsrp43* mutant strains of *Chlamydomonas reinhardtii* both showed a lighter green phenotype, had a lower Chl per cell content and higher Chl *a* / Chl *b* ratios than the corresponding wild type strains. In both cases, detailed physiological analyses revealed a higher intensity for the saturation of photosynthesis and greater Pmax values in the mutants than in the wild type. Biochemical analyses showed that both strains were deficient in the Chl *a-b* light harvesting complex (LHC) proteins, consistent with the notion of a truncated (***tla***) antenna. Although the phenotype was qualitatively similar in the two mutants (*tla2* and *tla3*), there were some quantitative differences between the two types of strains. For example, direct biophysical (spectrophotometric and kinetic) measurements showed a functional Chl antenna size of the photosystems that was about 65% for the *crcpftsy* and about 50% for the *crcpsrp43* mutant compared to that in the wild type.

Initial genetic characterization and attempts to clone the genes in these promising mutants failed. Results obtained during the unsuccessful genetic and molecular analyses suggested that the original DNA insertional mutagenesis strains were severely compromised, both genetically and in terms of cell fitness, with multiple genomic DNA deletions, insertion

of plasmid fragments randomly into loci unrelated to the *tla* lesion, in addition to having a smaller Chl antenna size that compromised their ability to absorb light. It is my conclusion that the plasmid DNA insertional mutagenesis technology in *Chlamydomonas reinhardtii* is not a surgical insertion of an exogenous piece of DNA into the nuclear genome, as it is invariably portrayed. Rather, it is a blunt-force modification of the genomic DNA that occurs in unpredictable ways, which may or may not yield information about genes of interest. It causes considerable lack of fitness in the transformants, many of which cannot easily be maintained or propagated, let alone manipulated and analyzed. This pitfall contributed to the initial inability to clone *tla* genes of interest. After unsuccessfully attempting to do gene cloning with the *tla* strains at hand, I realized the need to clean-up the genotype of the mutants through multiple sequential genetic crosses of the *tla* with wild type *C. reinhardtii* strains, and through careful screening and selection of *tla* daughter cells, in a systematic effort to remove unrelated and unwanted insertions, DNA fragments, and other abnormalities in the genome of the putative *tla* mutants. It was hoped that such effort would help to better define the map of the genomic DNA in the site of plasmid insertion. Indeed, I performed strain(mt+) x strain(mt-) matings, zygospores (2n) generation, isolation and germination, individual tetrad analyses, and isolation of progeny that retained the *tla* property. Multiple sequential crosses of the successively resultant *tla* offspring were thus undertaken. Along the way, it became evident that the resultant *tla* strains from crosses with a wild type gained in robustness, and in some cases the *tla* phenotype also improved. The latter was probably due to elimination of suppressor mutations that partially reverted the phenotype. These suppressor mutations could have accumulated while the strains were maintained and propagated in the Melis-lab, some of them for many years prior to my undertaking this dissertation research. The explanation of interfering suppressor mutations gains credence upon consideration of the low light intensity conditions under which strains are maintained, essentially applying pressure on the *tla* strains to revert to a large Chl antenna size. The systematic effort at cleaning-up the genomic DNA of the mutants was the prerequisite needed to open the way toward successfully mapping the insertion site, enabling the cloning of *tla* genes, and elucidating their function. It was evident that the cleaned-up *tla* strains were genetically and physiologically more fit, thus different from the original mutants.

The *TLA2-CpFTSY* gene, causing the *tla2* phenotype, was cloned by mapping the insertion site and upon complementation with each of the genes that were deleted in the insert site. Successful complementation was achieved with the *Chlamydomonas reinhardtii TLA2-CpFTSY* gene, whose occurrence and function in green microalgae has not hitherto been reported. Functional analysis showed that the nuclear-encoded and chloroplast-localized CrCpFTSY protein specifically operates in the assembly of the peripheral components of the Chl a-b light-harvesting antenna. In higher plants, a cpftsy null mutation inhibits assembly of both the LHC and PS complexes, thus resulting in a seedling lethal phenotype (Asakura et al., 2004; 2008). This Ph.D. research clearly shows that the cpftsy deletion in green algae, but not in higher plants, could be employed to generate viable *tla* mutants. The latter are known to exhibit improved solar energy conversion efficiency and photosynthetic productivity under mass culture and bright sunlight conditions.

The *tla3* mutant of *Chlamydomonas reinhardtii* also exhibited a pale green, low pigmentation and high Chl *a*/Chl *b* ratio phenotype. Biochemical analysis showed substantially lower amounts of the peripheral light-harvesting proteins corresponding to the wild type. The *tla3* mutant did not assemble $PSII_{\alpha}$ supercomplexes, a consequence of the absence of the peripheral LHCB trimers. Photosystem-II units were measured to have a Chl antenna size of about 38% of the average wild type PSII unit, while the Chl antenna size of PSI was reduced to about 50%. Molecular analysis showed a single plasmid insertion in the cleaned-up *tla3* strain. The *TLA3* gene was cloned and annotated as the *Chlamydomonas reinhardtii* homologue to the *CpSRP43* gene earlier reported in the model plants *Arabidopsis thaliana* and *Zea mays* (Klimyuk et al., 1999; Amin et al., 1999; Asakura et al., 2004; 2008). This is the first time the *CpSRP43* gene was cloned and investigated in green algae. Some differences were noted between the *CpSRP43*-null mutants in higher plants and Chlamydomonas. In contrast to the previously described *cpsrp43* mutant in *A. thaliana* (Klimyuk et al., 1999; Amin et al., 1999), the reduction of the light-harvesting complexes in the thylakoid membrane of Chlamydomonas appears to be more severe. Moreover, the phenotype of the *tla3* mutant is similar to that of the *cpftsy* mutant (*tla2*), while in *A. thaliana* the phenotypes differ; the *cpftsy* mutant is seedling lethal (Asakura et al., 2008) while *cpsrp43* is not (Klimyuk et al., 1999; Amin et al., 1999). This suggested a slightly different mode of action of the CpSRP pathway for the integration of transmembrane proteins into the thylakoid membrane of higher plants *versus* that in green algae, a

difference that can be exploited to increase the efficiency of mass cultivation of green algae. This work suggests that the smaller (truncated) light-harvesting antenna of the *tla2* and *tla3* mutants would improve the productivity of chlorophyll under light intensities equivalent to bright sunlight, when compared to that of the wild type.

CrCpFTSY

The *Chlamydomonas reinhardtii tla2* locus encodes for one of the components of the chloroplast Signal Recognition Particle (CpSRP), namely the nuclear-encoded and chloroplast-localized CpFTSY protein. This conclusion is based on the successful complementation of the *tla2* mutant with a cDNA construct of the newly cloned *CrCpFTSY* gene. The product of the *CrCpFTSY* gene shares a sequence identity of about 46% with the CpFTSY protein of *Arabidopsis thaliana* and *Zea mays*, while the sequence identity of CpFTSY of these two plant species to each other is even greater, at 74%. This is not surprising considering the evolutionary distance between higher plants and green algae, but can explain differences in the plant *versus* algal phenotype of *CpFTSY*-deletion mutants. Earlier work in higher plants, i.e., pea (Tu et al., 1999), maize (Asakura et al., 2004) and *Arabidopsis* (Asakura et al., 2008) indicated that CpFTSY is either associated with the thylakoid membrane or equally partitioned between the soluble stroma and thylakoid membrane in the chloroplasts. However, the CrCpFTSY in this study was localized exclusively in the soluble chloroplast stroma fraction of *Chlamydomonas reinhardtii*. This discrepancy could be explained in part by slightly different properties of the plant *versus* algal CpFTSY, as evidenced by their amino acid sequence divergence. Another source of the discrepancy could be traced to differences in cell fractionation and thylakoid membrane isolation protocols between plants and unicellular green algae. In the latter, powerful sonication or French-press methods are employed in order to rupture the cell wall, an approach that invariably breaks the continuity of the thylakoid membrane in the chloroplast. Under these harsh mechanical fractionation conditions, it is possible that loosely bound CpFTSY proteins separate from the nascent thylakoid membranes.

It has been reported that CpFTSY of higher plants is essential not only for the assembly of the Chl *a-b* light-harvesting complexes, but also for the assembly of the PS-core complexes and the biogenesis of thylakoid membranes (Asakura et al., 2004; 2008). CpFTSY was thus assumed to play a role in the correct integration of all these transmembrane

complexes in developing thylakoid membranes. Accordingly, *cpftsy* null mutants of higher plants could not grow photoautotrophically, as they lacked not only the LHC but also functional PSII and PSI core complexes (Asakura et al., 2004; 2008). The deletion mutant of *cpftsy* in *Chlamydomonas*, however, as evidenced in this work, showed a significantly different phenotype: most of the peripheral light-harvesting antenna complexes of PSI and PSII did not accumulate in the thylakoid membrane. However, and contrary to the observation of seedling-lethal *cpftsy* mutants in higher plants (Asakura et al., 2004; 2008), the *tla2* mutant of *C. reinhardtii* grew well photoautotrophically with a quantum yield of photosynthesis similar to that of the wild type. This substantially different property of the *CrCpFTSY* gene in green microalgae will permit application of the *CrCpFtsY* gene in the generation of green microalgal strains with a truncated light-harvesting antenna (**tla**) phenotype, useful in commercial applications comprising biomass, biofuels, and industrial chemicals production.

CrCpSR43

This Ph.D. research also showed that the *tla3* locus of *Chlamydomonas reinhardtii* encodes for the nuclear-encoded and chloroplast-localized light-harvesting chaperon protein known as CpSRP43. This annotation for the *tla3* locus was based on the successful complementation of the *tla3* mutant with the cDNA construct of the *CrCpSRP43* gene. The work provided, for the first time, experimental evidence for the occurrence and functional role of the CpSRP43 protein in green algae. The CpSRP43 protein of *C. reinhardtii* shares a sequence identity of 27.6% and similarity of 38.3% with the *A. thaliana* AtCpSRP43 protein. Even though these numbers are relatively high, the phenotype of the CpSRP43-null mutants differs between *C. reinhardtii* and *A. thaliana,* at least in terms of the pigments accumulating in the chloroplast. The chlorophyll content dropped to about 15% of that of the wild type in *C. reinhardtii*, while the *A. thaliana* retained 50% of its chlorophyll content (Klimyuk et al., 1999; Amin et al., 1999). Consequently, the CpSRP43-null mutation appears to have a more severe effect on the assembly of the light-harvesting proteins, which are nearly absent in the *tla3* mutant, while their abundance is not so adversely affected in the corresponding *A. thaliana* mutant (Klimyuk et al., 1999; Amin et al., 1999).

The CrCpSRP43 protein has a very similar domain configuration with that of the AtCpSRP43 protein. Both proteins contain an ankyrin repeat domain and three

chromodomains, one in front of the ankyrin domain and two immediately after it. Ankyrin repeats are among the most common protein motifs and function in protein-protein interactions (Mosavi et al., 2004). The ankyrin repeats are responsible for binding the L18 motif of light-harvesting complexes (DeLille et al., 2000 and Tu et al., 2000, Stengel et al., 2008) and thereby prevent mis-folding or precipitation of the hydrophoblic LHCB and LHCB apoproteins in the stroma phase (Falk and Sinning, 2010), a likely outcome in the absence of this molecular chaperon that could occur as the nascent LHCB and LHCA apoproteins are targeted to the thylakoid membrane.

The chromodomains are commonly found in proteins manipulating or remodeling chromatin. However, Goforth et al. (2004) and Funke et al. (2005) showed that the chromodomain 2 (CD2) is involved in the binding of CpSRP43 to CpSRP54 to form the Signal Recognition Particle. Due to the high similarity of the AtCpSRP43 and CrCpSRP43 proteins, and their similar domain structure, it can be inferred that they perform similar functions.

Low respiration rate and lower PSII and PSI content in *CrCpSRP43* and *CrCpFTSY* mutants

It is of interest that rates of cellular respiration in the *tla2* and *tla3* mutants were substantially lower, on a per cell basis down to about 30% of those measured in the wild type. A truncated Chl antenna in the photosynthetic apparatus should not *a priori* affect the cell's respiration capacity (Polle et al., 2000; Polle et al., 2003). Rather, loss of respiration fitness in the *tla2* and *tla3* mutants could be attributed to the loss of a number of genes flanking the pJD67 insertion sites, which were deleted or rearranged in the genomic DNA. The deleted genes and the 358 kb genomic DNA 180° flip are proximal to the insertion site in *tla2* and, therefore, could not be recovered in spite of the many crosses of the original *tla2* strain with a wild type counterpart. The deleted genes, and those contained in the 358 kb 180 degree flip, are predicted open reading frames of unknown function, and were not further analyzed in this work. Accordingly, the possibility could not be excluded that one of these deleted or rearranged genes in the *tla2* mutant adversely affected properties of respiration, PSII and PSI content, and/or cell size.

The possibility of gene deletions in the *tla3* mutant, beside the genes investigated in this work, also cannot be excluded. It is likely that the *tla3* mutant has other mutagenesis-related genes that were affected by the insertion process, in a way similar to the events

described for the *tla2* strain. These anomalies may contribute to the slower cellular respiration rate. An additional consideration is that **tla** strains, by necessity due to their diminished ability to absorb enough light, cannot generate photosynthate sufficient to saturate the respiratory rate of the cells, thus attenuating the respiratory capacity of the mutants. The latter explanation gains credence upon consideration of the low light intensity (about 100 µmol photons m^{-2} s^{-1}) to which all strains are grown and acclimated in the Melis-lab, and also upon consideration that such a growth light-intensity is well below the saturation of photosynthesis in the mutants (Fig. 6 and Fig. 17).

The lower photosystem content of *tla2* and *tla3* compared to a wild type is an indication of overall lower thylakoid membrane development and abundance in the chloroplast of the mutants. Inability to assemble the imported light-harvesting proteins in these *tla* mutants may trigger a feedback inhibition in chlorophyll biosynthesis, indirectly affecting the chlorophyll supply and lowering the chloroplast ability to assemble the full complement of PSII and PSI units. Another possible consideration is that deficiency of light-harvesting proteins may have had an adverse effect on the thylakoid morphology. It has been proposed that the light-harvesting proteins are needed to form the grana stacking in the appressed thylakoid membranes (reviewed by Allen and Forsberg, 2001). Absence of the light-harvesting proteins in the *tla2* und *tla3* mutants would thus prevent grana stacking, substantially lowering the thylakoid membrane surface area in which PSII can be placed. The amount of PSI is by consequence negatively adjusted to meet the needs of the chloroplast in terms of an efficient and coordinated electron transport through the thylakoid membranes.

In spite of the total absence of the CpFTSY, the *tla2* mutant retained assembly activity for some of the photosystem inner light-harvesting proteins. It has been reported that the chaperon protein CpSRP43, alone is sufficient to form a complex with the translocase ALB3 (Tzvetkova-Chevolleau et al., 2007; Bals et al., 2010;) and this could suffice to explain the observation that some light-harvesting antenna proteins can still become incorporated into the thylakoid membrane of Chlamydomonas, albeit with a much lower efficiency. The *tla3* mutant retained some LHC assembly activity as well, but to a much lesser extend. In this respect, Moore et al. (2003) showed that CpSRP43 is not required for the interaction of the CpSRP54-CpFTSY with the insertase protein ALB3. This observation could explain how some light-harvesting complexes could be integrated into the thylakoid membrane. The missing

chaperon function of the CpSRP43 protein presumably leads to the precipitation and removal of most of the light-harvesting proteins upon their import into the stroma, but some of them are apparently correctly integrated in the PS superstructures.

Role of CpFTSY and CpSRP43 in LHC assembly

The CpFTSY protein in green microalgae, as evinced for the analysis in this work, plays a role in the integration of the photosystem-peripheral light-harvesting complexes into the thylakoid membrane. It presumably functions together with the other CpSRP pathway proteins, such as CpSRP54, CpSRP43 and ALB3 (Fig. 29). CpSRP43 was also shown in this work to be a specific chaperon for light-harvesting proteins, needed to prevent and/or unfold aggregation of the hydrophobic domains of the light-harvesting proteins after import into the chloroplast (Falk and Sinning, 2010; Jaru-Ampornpan et al., 2010). CpSRP43 binds with the Ankyrin repeat domains to the L18 domain of the light-harvesting complexes (DeLille et al, 2000; Tu et all 2000). CpSRP54 is thought to bind to this LHC-protein/CpSRP43 complex by interaction of a positively charged domain with the chromodomain 2 (CD2) of the CpSRP43 protein (Goforth et al., 2004; Funke et al., 2005). CpFTSY recognizes this complex by an as yet unknown mechanism and guides it to the membrane-bound translocase ALB3. I propose that the ALB3 translocase is specifically localized in the "polar" regions of the chloroplast, where the thylakoid membrane biogenesis takes place. This suggestion is based on the observation that photosystem complexes and their antenna size cannot be altered once assembly has occurred, and once transmembrane complexes become components of the developed thylakoid membrane (Melis, 1991; Kim et al. 1993). According to this model, it is in the polar regions of the chloroplast where the simultaneous assembly of the photosystems, their antenna size, and formation of the thylakoid membrane take place. The nascent thylakoid membrane receives via the ALB3 protein the LHC-CpSRP43-CpSRP54-CpFTSY complex and guides the transmembrane LHC in the developing thylakoid membrane lipid bilayer. Upon GTP hydrolysis, the LHC-protein is integrated into the thylakoid membrane (Tu et al., 1999). The CpSRP-proteins CpSRP54 and ALB3 are apparently needed for the proper integration of other transmembrane proteins, as evident by the phenotype generated in the corresponding knockout mutants (Amin et al. 1999; Bellafiore et al. 2002).
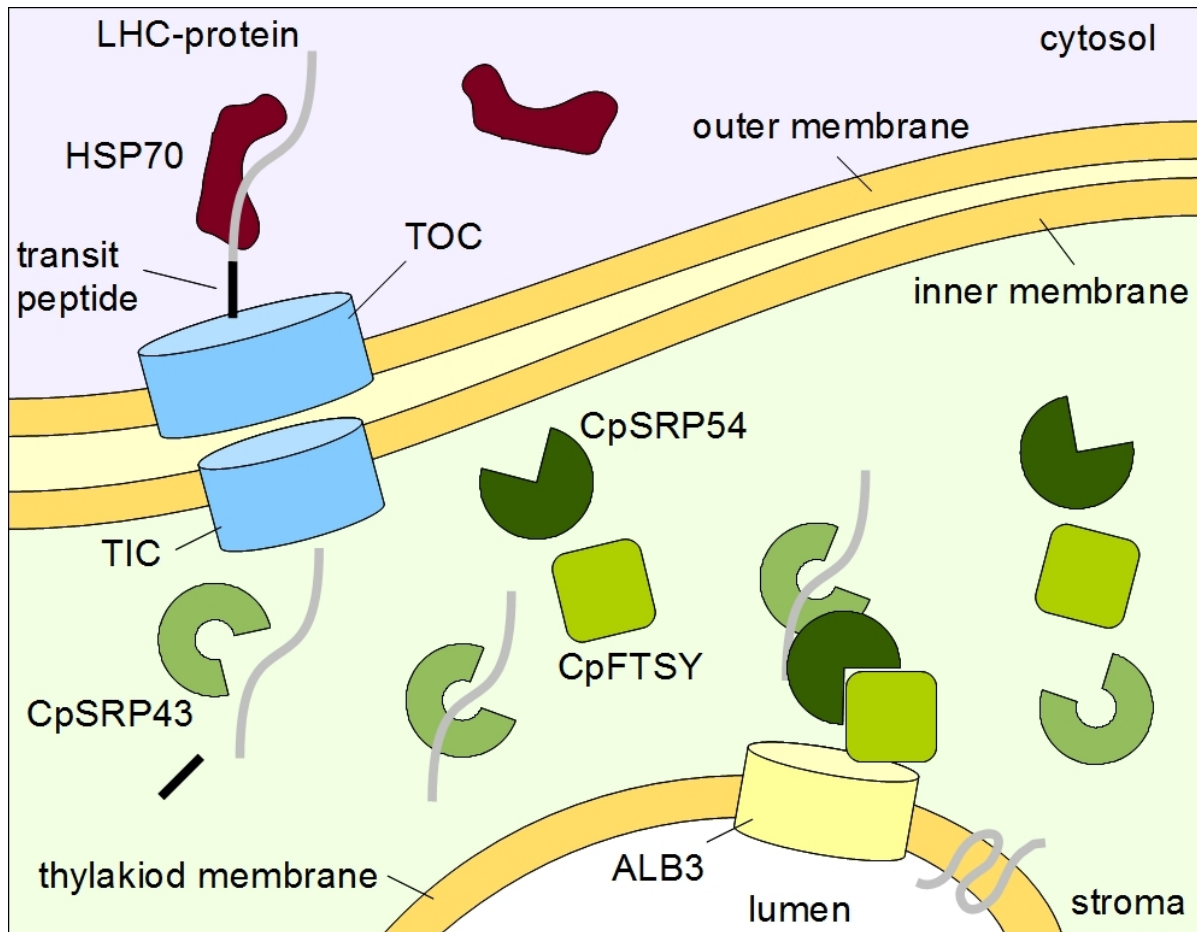
Figure 29: Working model of the function of the CrCpSRP transmembrane complex assembly system in the model green algae *C. reinhardtii*. Precursor light-harvesting proteins (LHCprotein) are targeted to the chloroplast via the transit peptide and the heat shock protein HSP70, which functions as a molecular chaperon to prevent aggregation of the preassembled proteins. Chloroplast protein import is facilitated by the envelope-localized TOC and TIC complexes, which catalyze protein import through the outer and inner envelope membranes of the chloroplast. The transit peptide is cleaved off and the molecular chaperon CpSRP43 binds to the incoming light-harvesting protein to prevent its aberrant misfolding. CpSRP54 and CpFTSY guide this CpSRP43-LHC complex to the membrane-bound translocase ALB3. Upon integration of the light-harvesting protein into the nascent thylakoid membrane, the LHC-CPSRP43-CPSRP54-CpFTSY complex disassembles, making the SRP subunits available for another carry-andassembly cycle.

It is concluded that there is a dichotomy in the function of the CpFTSY protein between green microalgae (e.g. *Chlamydomonas reinhardtii*) and higher plants (e.g. *Arabidopsis thaliana* and *Zea mays*), where absence of the CpFTSY in *C. reinhardtii* impacts the assembly of the LHC-II only, versus the evidence in higher plants, where absence of the CpFTSY impacts the assembly of the entire photosystems (Asakura et al., 2004; Asakura et al., 2008). This is clearly supported by the fact that the *tla2* mutant grew well under autotrophic conditions and had fully functional PSII and PSI reaction centers.

Proteins of the CpSRP pathway are tools for the regulation of the Chl antenna size specifically in microalgae

There is current interest and on-going efforts to renewably generate fuel and chemical products for human consumption, through the process of microalgal photosynthesis. Such bio-products include H_2 and other suitable biofuel molecules (Melis, 2007; Hankamer et al., 2007; Greenwell et al., 2010; Hu et al., 2008; Mata et al., 2010), antigens (Dauvillée et al., 2010, Michelet et al., 2011) and high value bio-products (Mayfield, 2007). For this effort, sunlight energy conversion in photosynthesis must take place with the utmost efficiency, as this would help to make renewable fuel and chemical processes economically feasible. In plants and algae, the solar energy conversion efficiency of photosynthesis is thus a most critical factor for the economic viability of renewable fuel and chemical production (Melis, 2009).

Green microalgae tend to develop large arrays of light-harvesting complexes, especially when cultivated in high-density mass-cultures. This physiological response of the cell reflects an effort to absorb as much sunlight as possible, as they compete in a light-limited environment (Naus and Melis, 1991). However, in such a mass culture with cells possessing large Chl antennae, cells at the surface of the reactor would absorb incident sunlight (intensity of 2,500 μmol photons m^{-2} s^{-1}) with rates that far exceed the capacity of the photosynthetic apparatus to utilize them (saturation of photosynthesis at less than 500 μmol photons m^{-2} s^{-1}). The excess absorbed sunlight-energy is dissipated in the process of non-photochemical quenching (NPQ) to prevent photodamage or photoinhibition phenomena in the thylakoid membrane (reviewed by Müller et al., 2001**)**. It has been shown

that high-density cultures of algae with a truncated Chl antenna size are photosynthetically more productive under bright sunlight, due to the elimination of over-absorption and wasteful dissipation of excess energy (Nakajima and Ueda, 1997; 1999; Melis et al., 1999; Polle et al., 2002; 2003; Melis, 2009). The *tla2* and *tla3* mutants have a permanently truncated light-harvesting antenna size phenotype and in spite of some collateral damage, i.e., mutations or deletions in the plasmid insert region, they showed a greater per chlorophyll photosynthetic productivity than the wild type cells. The DNA insertional mutagenesis, in spite of the blunt force consequences, is thus preferred over the random chemical or UV-induced mutagenesis, where dozens, if not hundreds of mutations adversely impact cell fitness and productivity (Huesemann et al., 2009). In high-density cultures, at light intensities greater than 700-800 µmol photons $m^{-2} s^{-1}$, the *tla2* and *tla3* mutant strains would collectively show greater culture productivity than their wild type counterparts. This would be due to elimination of over-absorption and wasteful dissipation of sunlight at the surface of the culture, and also because of avoidance of shading, permitting sunlight to penetrate deeper in the culture and sensitize many more cells. Accordingly, application of the CpFTSY and CpSRP43 genes in *tla2*-type and *tla3*-type mutations in microalgae can serve to minimize the ability of individual cells to over-absorb sunlight but at the same time helping to substantially improve the productivity of the overall mass culture.

On the basis of the Chl antenna size considerations above, the *tla3* mutant would outperform the *tla2* mutant in terms of photosynthetic productivity under bright sunlight conditions. It was calculated that whereas the *tla2* strain would result to an about 25% increase in mass culture productivity relative to the wild type, the *tla3* strain could double photosynthetic productivity of a green algae mass-culture under bright sunlight conditions. However, the pigmentation properties and Chl antenna size of the *tla3* mutant are not optimal yet, as evident by the light-saturation of photosynthesis measurements. An even greater productivity could be achieved in mass cultures with a green algal strain in which photosynthesis does not begin to saturate, even at an intensity of bright sunlight. Thus, there is room for improvements, meaning isolation of **tla** strains with no LHC proteins at all.

The above analysis and discussion is based on the assumption of bright sunlight at 2,500 µmol photons $m^{-2} s^{-1}$, which is attained in the sunbelt regions of the US and Europe, and other close-to-the equator geographic locations. At more northern latitudes, e.g.

Germany and Scandinavia, and also during the winter season, where and when the intensity of the sunlight is attenuated, consideration could be given to strains with intermediate antenna size between the fully truncated (PSII=37 and PSI=95 Chl molecules) and that of the fully pigmented photosystems (PSII=300 and PSI=250 Chl molecules). This Ph.D. dissertation research showed that a possible approach to such intermediate antenna requirements could be the partially complemented *tla2* and *tla3* strains. Indeed*,* my complementation efforts with both the *tla2* and *tla3* mutants yielded strains with quite a variable degree of functional complementation. Even though the precise number of Chl molecules associated with each reaction center has not been measured in these partially-complemented strains, the measured Chl *a* / Chl *b* ratios indicated that they have intermediate sizes of the light-harvesting complexes, which would be anywhere between the truncated antenna mutant and the fully pigmented wild type. Thus, partial complementation promises to be a useful tool by which to generate strains with optimal light utilization properties for different solar intensity ecotypes.

Frequency of the *tla2-Δcpftsy* and *tla3-Δcpsrp43* mutations

The Ph.D. dissertation research examined six *tla* strains, as Professor Melis assigned these to me (*tla2* through *tla7*). Surprisingly, three of these mutants from the Melis-lab **tla** mutant collection (*tla2, tla4,* and *tla7*) proved to be Δ*cpftsy* mutants, while the remainder three (*tla3, tla5,* and *tla6*) proved to be Δ*cpsrp43* mutants. One possible explanation for this presumably high frequency of Δ*cpftsy* and Δ*cpsrp43* mutations may be sought in the screening and selection processes employed during isolation of putative *tla* strains (see Materials and Methods). Another possibility is that, for reasons unknown, there is a far greater probability of plasmid DNA insertions in the genomic DNA of the *CpFTSY* and *CpSRP43* genes, than that encountered for other Chl antenna size defining genes. The DNA insertional mutagenesis of 15,000 strains assumed that such a number of transformants would statistically satisfy the requirement that each *C. reinhardtii* genes would be interrupted by the mutagenesis process at least once. This assumption would be incorrect if the DNA insertional mutagenesis is not as random a phenomenon as currently believed but, rather, there are regions of the *C. reinhardtii* genome where there is preferential incorporation of exogenous plasmids.

However, as yet another alternative, the possibility cannot be excluded that the six analyzed *tla* strains in this work are not independent of one another but, rather, have been the result of cross-contamination among the original isolates. This possibility needs to be considered, as the required obligate continuous live cell maintenance and monthly propagation of Chlamydomonas on agar plates, over prolonged periods of time, could possibly permit such cross contamination, e.g. due to human error. Delineation between the two alternatives and resolution of this issue could be provided in comparative mapping of the plasmid insertion site in the three Δ*cpftsy* mutants and, independently, in the three Δ*cpsrp43* mutants. This approach would illuminate the origin of the triplicate Δ*cpftsy* and triplicate Δ*cpsrp43* mutant strains (*tla2* through *tla7*). If these strains arose as independent insertional transformants they ought to have different genomic DNA insert site maps. If they arose via cross contamination due to human error, they would show identical genomic DNA insert site maps. This genetic mapping analysis remains to be done, hopefully in the near future.

It is of interest in this respect to note that farmers have isolated multiple and independent spontaneous "Chl-deficient" mutants in tobacco, maize, barley, soybean, pea, and possibly others. These strains were noted in the field by their pale-green or yellow-green phenotype. Cultivation in the laboratory and analysis has shown that all these mutants had a truncated Chl antenna size for the photosystems (reviewed in Melis, 1991). Unfortunately, affected genes could not be cloned from these crop plant mutants, as the lesions were not marked and the state of the art in genetic and molecular analysis was not at the time as advanced as it is today. Nevertheless, the frequent and spontaneous occurrence of such *tla* mutants in crop plants may corroborate the notion above that one or more specific genes (*CpFTSY* and *CpSRP43* ?) defining the Chl antenna size in green plants and algae may be subject to easier of more frequent mutagenesis than that affecting other genes.

Considerations upon the potential release of *tla* strains in the environment

The smaller light-harvesting Chl antenna size in the *tla2* and *tla3* mutant requires a higher intensity to saturate photosynthesis than that in the wild type. Thus, under limiting irradiance conditions, as those that prevail in the natural ecotype, individual *tla2* and *tla3*

cells would be at a survival disadvantage over their wild type counterparts, as their ability to absorb sunlight has been compromised. It follows that *tla* mutant strain, if and when released in the environment, would not be able to compete with fully pigmented strains and thus cannot survive.

MATERIALS AND METHODS

Cell cultivation

Chlamydomonas reinhardtii strains CC-503 cw92 mt+, CC-425 arg2 cw15 sr-u-2-60 mt+, CC-125 wild type mt+ 137C, obtained from the Chlamydomonas Center (http://www.chlamy.org/), and laboratory strains 4A+ and *tla2* were maintained under orbital shaking in 100 ml liquid cultures in Erlenmeyer flasks at 25 °C under continuous illumination at low light (30 µmol photons $m^{-2} s^{-1}$). Irradiance was provided by balanced cool-white and warm-white fluorescent lamps. Cells were grown photo-heterotrophically in TAP medium (Gorman and Levine, 1965), or photo-autotrophically in HS medium (Harris, 1989) under a combination of cool-white, warm-white fluorescent, and incandescent irradiance at a light intensity of 450 µmol photons $m^{-2} s^{-1}$. For physiological measurements, cultures were harvested during the logarithmic growth phase (~1-3x10^6 cells/ml).

Cell count and chlorophyll determination

Cell density was measured using an improved Neubauer ultraplane hemacytometer and a BH-2 light microscope (Olympus, Tokyo). Pigments from intact cells or thylakoid membranes were extracted in 80% acetone and cell debris removed by centrifugation at 20,000 g for 5 min. The absorbance of the supernatant was measured with a Shimadzu UV-1800 spectrophotometer, and the chlorophyll concentration of the samples was determined according to Arnon (1949), with equations corrected as in Melis et al. (1987).

Generation of a *Chlamydomonas reinhardtii* DNA insertional mutagenesis library for the isolation of *tla* (truncated light-harvesting antenna) mutants

To identify genes in green microalgae specifically involved in the regulation of the size of the auxiliary chlorophyll *a-b* light-harvesting antenna of photosystem I, and photosystem II, DNA insertional mutagenesis libraries of the model green algae *Chlamydomonas reinhardtii* were generated (Polle et al. 2003). Specifically, transformants of *Chlamydomonas reinhardtii* were obtained upon DNA insertional transformation by the glass-bead method, as described in Debuchy et al. (1989). Parental strain CC-425 was transformed with linearized

plasmid pJD67, containing a functional copy of the argininosuccinate lyase (*ARG7*) gene, which complements the arg2 locus of the native but inactive argininosuccinate lyase in the CC-425 strain (Davies et al. 1994, 1996). Since a truncated Chl antenna size would result in lower yields of chlorophyll fluorescence in vivo, or in pale green phenotype, *C. reinhardtii* transformants were screened for aberrant Chl fluorescence yield properties via a fluorescence video imaging apparatus, as described in Polle et al. (2001a, 2003). Other DNA insertional mutagenesis libraries were screened visually, seeking to identify pale green lines for further analysis. Mutants showing lower Chl fluorescence or pale green coloration were isolated and analyzed for their Chl *a*/Chl *b* ratio (second screening step). The resulting isolates were more systematically screened by physiological, biochemical, genetic and molecular approaches (Kirst et al., 2012) to identify **t**runcated **l**ight-harvesting **a**ntenna (*tla*) mutants from which to clone the antenna defining gene(s). To clarify, not all of the mutants employed in this Ph.D. research have been generated and isolated by me personally, in fact only the *tla4* and *tla7* strain have been generated by myself. Co-workers in the Melis laboratory at UC Berkeley contributing to the mutant generation process and isolation have been recognized in the list of acknowledgments. University of California regulations define that all strains, as these employed in this work, are the property of the Melis laboratory. They have been assigned to my Ph.D. dissertation research by Professor Melis, and have so been utilized under the direct supervision of Prof. Melis.

The random mutagenesis approach required that enough mutant strains be generated to statistically be confident that all *C. reinhardtii* nuclear genes have been mutated. The genome of *Chlamydomonas reinhardtii* contains 15,256 genes (Merchant et al. 2007). Thus, for a complete genome mutagenesis library, a minimum of 15,000 mutant strains must be generated and screened. In this approach, plasmid DNA containing a selectable marker will be inserted into the genomic DNA of *Chlamydomonas reinhardtii* at random location. Ideally, the mutagenesis would knock out a different gene in each of the 15,000 mutant strains, so that, statistically, every nuclear gene would be inactivated upon the insertion of an exogenous plasmid. The inserted plasmid DNA functions as a tag allowing the identification of the insertion locus on the genomic DNA and, thus, cloning of the gene interruption of which resulted in a specific mutant phenotype.

Critical in the application of the DNA insertional mutagenesis approach is the design

and execution of a stringent screening protocol, by which to identity a handful of strains with the desirable phenotype out of the 15,000+ mutant strains generated. A screening protocol for the identification of *tla* strains was developed and applied to enable a high throughput screening for mutants with an altered light-harvesting chlorophyll antenna size. Measurement the Chl *a / Chl b* ratio provides indirect information of the developmental status of the light-harvesting Chl antenna complex. The lower the amount of Chl *b*, relative to Chl *a*, i.e., the higher the Chl *a / Chl b* ratio, the less developed the light-harvesting chlorophyll of the photosystems would be. This measurement is independent of the cell density or total pigment content in the sample, and thus independent of differences in growth rate due to the mutations or sample volume. Chl *a* and Chl *b* can be extracted form the cells by incubating the cells in the presence of 80% acetone, and Chl can be quantified by absorption spectroscopy and upon application of Beer's law. Using equations derived by Arnon (1951) for Chl *a* and Chl *b* concentration in 80% acetone (below), the Chl *a*/Chl *b* ratio of individual DNA insertional mutagenesis strains was determined.

$$\text{Chl } a \text{ (µg/ml)} = 12.7(A_{663} - A_{710}) - 2.69(A_{645} - A_{710})$$

$$\text{Chl } b \text{ (µg/ml)} = 22.9(A_{645} - A_{710}) - 4.68(A_{663} - A_{710})$$

To avoid scattering of the measuring beam light (resulting in erroneous absorbance readings) and in order to avoid background noise in the absorbance measurement, cell debris were separated from the pigment containing acetone solution by centrifugation. Strains with a lower or higher than the wild type Chl *a / Chl b* ratio were tested in a secondary screening step for photo autotrophy by growing them without any organic carbon source on HS (high salt) medium (Sueoka 1960) under medium light conditions (450 µmol photons m^{-2} s^{-1}). This secondary screening ensures that the selected mutants assemble functional photosystems, and suggest that differential pigmentation of mutant and wild type strains is not an artifact caused by a deficiency in photosynthesis.

Figure 30 shows a flow chart of the mutant generation and screening process. In the process of this work over 15,000 mutant strains have been generated and screened, leading to the isolation of a total of six *tla* type mutants, which successfully passed both screening steps enumerated above. These putative *tla* strains were termed *tla2* through *tla7*. All six mutants had a higher Chl *a / Chl b* ratio than wild type strains (Table 1), suggesting the possibility of a smaller Chl light-harvesting antenna size than the wild type. No strain could

81

be identified, comprising a larger Chl light-harvesting antenna than the wild type.
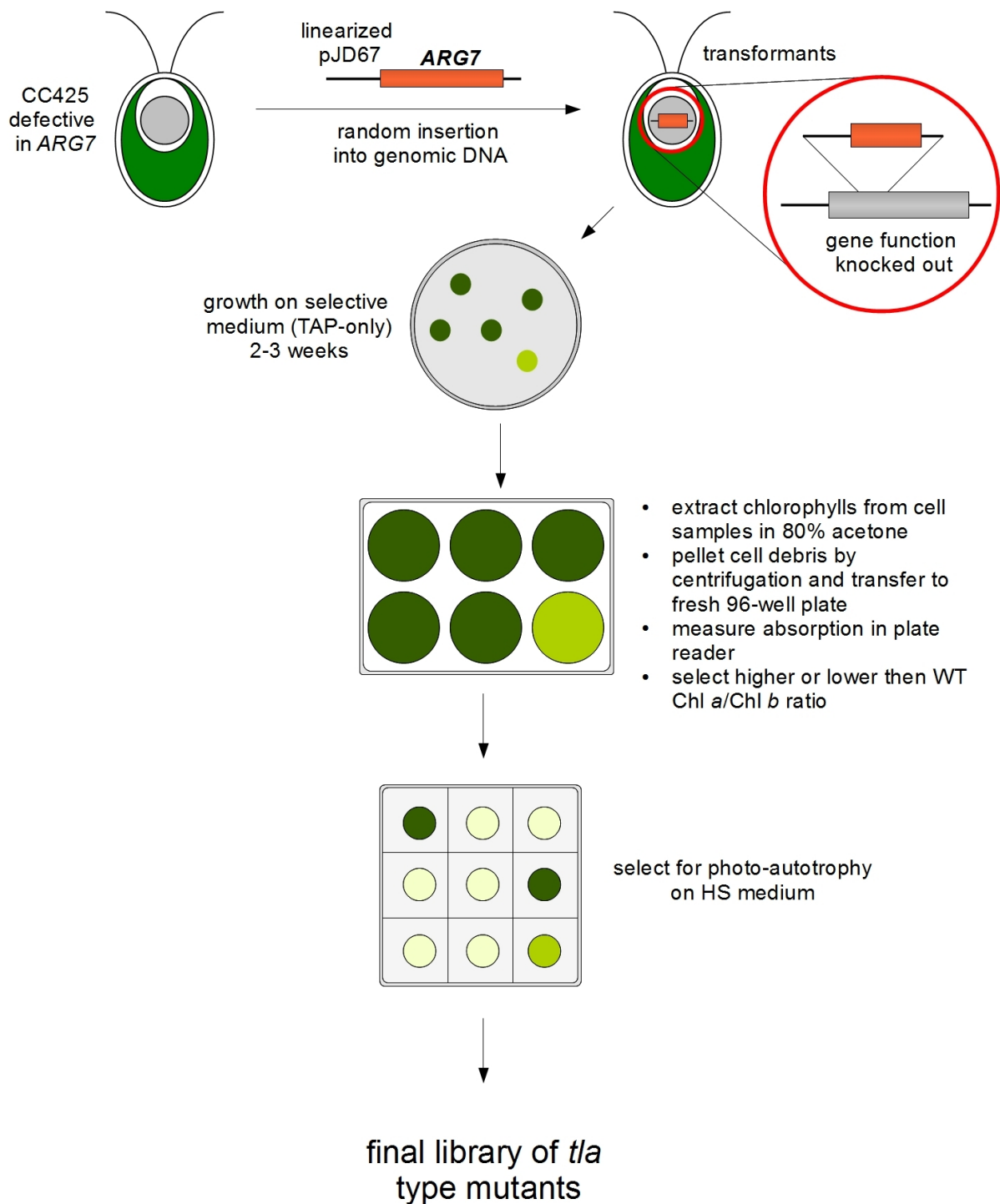
Figure 30: Flow chart of the mutant generation and screening process employed in this work.

Nucleic acid extractions

Chlamydomonas reinhardtii genomic DNA was isolated for PCR analysis using Qiagen's Plant DNA purification kit. For Southern blot analysis, genomic DNA was isolated by harvesting cells from a 50 ml aliquot of the culture upon centrifugation at 5000 g for 5 min, followed by re-suspension of the pellet in 500 μl sterile water. Cells were lysed upon addition of 500 μl lysis buffer containing 2% SDS, 400 mM NaCl, 40 mM EDTA, 100 mM Tris/HCl (pH 8.0) and upon incubation for 2 h at 65°C. To this mix, 170 μl of 5 M NaCl solution was added. SDS and carbohydrates where precipitated upon addition of 135 μl 10% CTAB in 0.7 M NaCl and incubation for 10 min at 65°C. They were extracted by mixing with Chloroform:Isoamylalcohol 24:1 followed by centrifugation at 20,000g for 5 minutes. Proteins were removed by extraction with Phenol:Chloroform:Isoamylalcohol 25:24:1 solution. RNA in the water-phase was digested using 10 ng/ml RNase A and upon incubation at 37°C for 20 min. RNase A was removed by extraction with Phenol:Chloroform:Isoamylalcohol 25:24:1 solution. Desalting of the DNA solution was achieved upon precipitation with Isopropanol and resuspension in 10 mM Tris-HCl (pH 8.0).

Southern blot analysis

Approximately 5 μg genomic DNA was digested by various restriction enzymes (NEB) in a 500 μl volume at 37°C with overnight incubation (16 h). The digested DNA was precipitated with isopropanol, washed in 70% ethanol and resuspended in 20 μl buffer containing 5 mM Tris, pH 8.0. DNA fragments were separated on a 0.6% agarose gel, transferred on a positively charged nylon membrane (Hybond-N[+]; Amersham) and UV cross-linked. Probes were obtained upon PCR reactions using specific primers (Appendix B) and the pJD67 plasmid as template DNA, and labeled with alkaline phosphatase using the "Gene Images AlkPhos Direct Labeling and Detection System" kit (Amersham). The manufacture's protocol was used for labeling, hybridization, washing and signal detection with the following modifications: hybridization temperature and primary washing buffer temperature was maintained at 72°C.

Genetic crosses and analyses

All genetic crosses and strain matings were performed according to the protocol of Harris (1989). Prior to any physiological analysis, putative truncated light-harvesting antenna (***tla)*** mutants were crossed four times to a laboratory-generated *Chlamydomonas* strain 4A+ (*arg2*). For co-segregation analysis of the *tla2* phenotype with the pJD67 insert, *tla2* was crossed to AG1x3.24 (ARG7-8⁻). Progeny were plated on TAP medium containing arginine (TAP+Arg) and also on regular TAP-only medium (-Arg). Moreover, PCR reactions were used to test for co-segregation of the *tla2* phenotype with the pJD67 insert, using the HK128/HK126 (Appendix B) insertion flanking sequence specific primers set and a DNA isolation control HK135/HK134 (Appendix B).

Measurements of photosynthetic activity

The oxygen evolution activity of the cultures was measured at 22°C with a Clark-type oxygen electrode illuminated with light from a halogen lamp projector. A Corning 3-69 filter (510 nm cut-off filter) defined the yellow actinic excitation via which photosynthesis measurements were made. Samples of 5 ml cell suspension contained 1.3 μM Chl were loaded into the oxygen electrode chamber. Sodium bicarbonate (100 μl of 0.5 M solution, pH 7.4) was added to the cell suspension prior to the oxygen evolution measurements to ensure that oxygen evolution was not limited by the carbon supply available to the cells. After registration of the rate of dark respiration by the cells, samples were illuminated with gradually increasing light intensities. The rate of oxygen exchange (uptake or evolution) under each of these irradiance conditions was recorded continuously for a period of about 5 min.

Isolation of thylakoid membranes

Cells were harvested by centrifugation at 1,000 g for 3 min at 4°C, the pellet was stored frozen at -80°C until all samples were ready for processing. Samples were thawed on ice and resuspended with ice-cold sonication buffer containing 50 mM Tricine (pH 7.8), 10 mM NaCl, 5 mM MgCl₂, 0.2% polyvinylpyrrolidone 40, 0.2% sodium ascorbate, 1 mM aminocaproic acid, 1 mM aminobenzamidine and 100 μM phenylmethylsulfonyl fluoride (PMSF). Cells were broken by sonication in a Branson 250 Cell Disrupter operated at 4°C, three times for 30 s each time (pulse mode, 50% duty cycle, output power 5) with 30 s

cooling intervals on ice. Unbroken cells and starch grains were removed by centrifugation at 3,000 g for 4 min at 4°C. Thylakoid membranes were collected by centrifugation of the first supernatant at 75,000 g for 30 min at 4°C. The thylakoid membrane pellet was resuspended in a buffer containing 50 mM Tricine (pH 7.8), 10 mM NaCl, 5 mM $MgCl_2$ for spectrophotometric measurements, or 250 mM Tris–HCl (pH 6.8), 20% glycerol, 7% SDS and 2 M urea for protein analysis.

Spectroscopic and kinetic methods

A laboratory-constructed split-beam spectrophotometer (Melis and Hart, 1980) was employed for the quantitative measurements of PSII (Q_A), PSI (P700) and also for the measurements of the PSII and PSI Chl antenna size.

Quantification of PSII in thylakoid membranes

Isolated thylakoid membrane samples were treated in the dark with 15 μM DCMU (3-(3,4-dichlorophenyl)-1,1-dimethylurea) to block the electron transport step from Q_A to Q_B. The spectrophotometer was set with the measuring beam at 320 nm, designed to specifically monitor the reduction of the PSII Q_A primary electron acceptor. Dark-adapted samples (Q_A oxidized) were illuminated with weak green actinic light, provided by a projector lamp and filtered by a combination of CS 4-96 and CS 3-69 Corning glass filters. This quality of actinic illumination is designed to excite Chl a and Chl b molecules equally (Melis and Anderson, 1983; Ghirardi and Melis, 1984). Measuring the actinic light-induced absorbance increase at 320 nm (ΔA_{320}) provided a direct measurement of the reduction of Q_A from 100% oxidized to 100% reduced form. The amplitude of the ΔA_{320} change provided, upon application of Beer's law, the concentration of Q_A in the thylakoid membrane sample, based on the known differential extinction coefficient of 13 $mM^{-1} cm^{-1}$ for Q_A at 320 nm (Van Gorkom, 1974). A typical light-induced absorbance change signal at 320 nm is shown in Fig. 31. The amplitude of the ΔA_{320} measured from the baseline before illumination and from the steady-state line at the saturation of the signal reflects the number of total Q_A molecules in the sample able to undergo photoreduction. After measuring the total Chl content of the sample, the number of total Chl molecules per functional PSII reaction center was calculated (Chl/Q_A). Note, that the total number of Chl molecules thus calculated, includes molecules associated with PSII and also those associated with PSI, thus Chl/Q_A gives a statistical ratio of

total Chl to total PSII in the sample. It does not immediately provide a direct measure of the PSII light-harvesting antenna size.
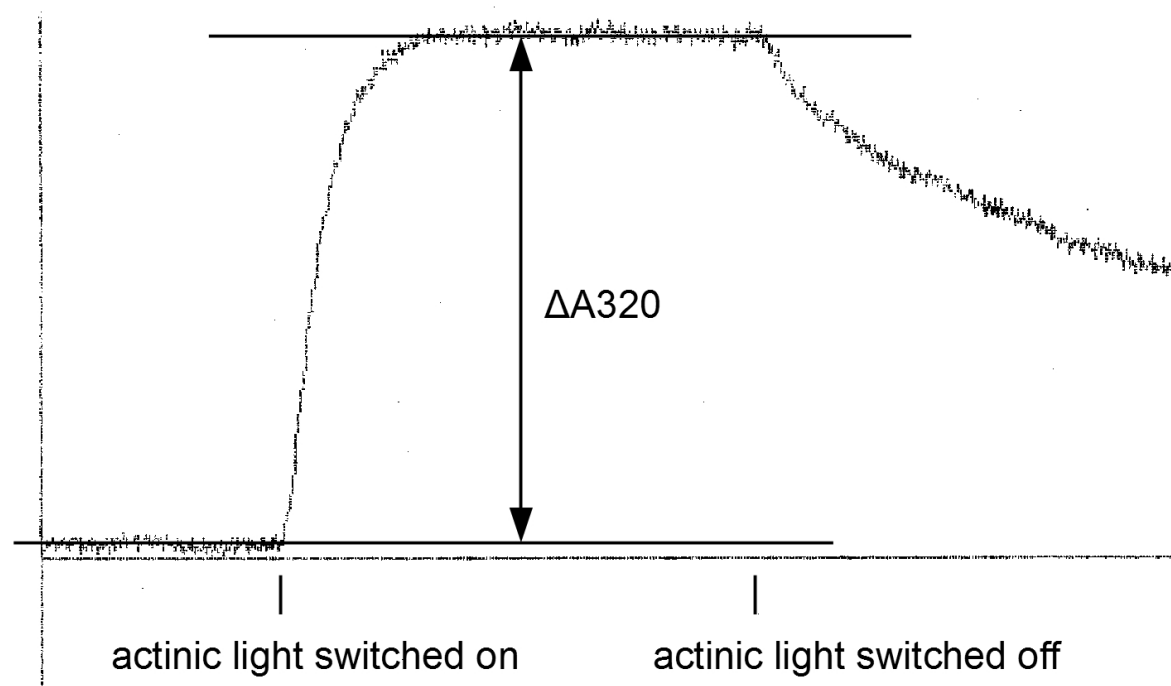
Figure 31: Typical light induced absorbance change at 320 nm wavelength for quantification of Q_A. The absorbance difference $\Delta A320$ before illumination and at the saturation of the signal reflects the number of total Q_A molecules in the sample that are able to undergo photoreduction. After the actinic light is switched off, orders of magnitude slower oxidation of Q_A occurs.

Quantification of PSI in thylakoid membranes

The quantification of PSI is based on the light-induced absorbance different spectrum at 700 nm (ΔA_{700}) measuring the oxidized-minus-the reduced form of the PSI reaction center (Melis, 1989). Dark-adapted thylakoid membrane samples (P700 reduced) were treated with 2 mM ascorbate (Asc) to ensure that P700 was in the reduced form, 0.02% SDS was added to partially break the lipid bilayer of the thylakoid membranes and to make P700 accessible for ascorbate. The concentration of SDS was calibrated to bring about a disrupting the continuity of the thylakoid membrane and of inactivating the labile PSII, thus completely inhibiting its function and ensuring that no electrons originating from PSII can reach PSI upon illumination of the sample. Since this treatment also removed the ferredoxin electron

acceptor from PSI, 0.2 mM methyl viologen was used to accept electrons from the reducing side of the PSI complex. Methylviologen thus served to inhibit a back flow of electrons to $P700^+$. The amplitude of the light-*minus*-dark absorbance difference signal at 700 nm (ΔA_{700}) was measured upon illumination of the sample with broadband blue actinic light, defined by a Corning CS 4-96 filter. This filter provides strong actinic illumination to ensure that all P700 molecules in the sample will become oxidized regardless of (the slow) electron donation to $P700^+$ from ascorbate. The P700 quantity in the sample was calculated from the amplitude of the ΔA_{700} signal and Beer's law, based on the known differential extinction coefficient of 64 mM^{-1} cm^{-1} for $P700^+$ minus P700 (Hiyama and Ke, 1972). A typical trace of the absorbance change at 700 nm upon illumination, reflecting the oxidation of P700, is shown in Fig. 32. The reduction kinetics of $P700^+$ by Asc in this case is much slower than the photo-oxidation of P700 by the strong blue actinic light, thus the equilibrium redox reaction upon illumination lies quantitatively on the side of the oxidized $P700^+$.
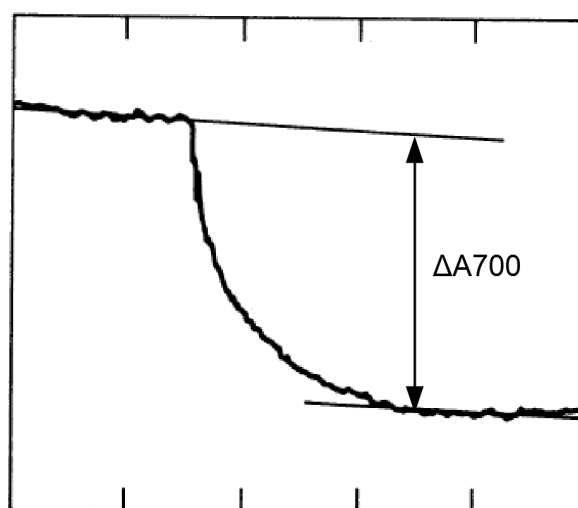
Figure 32: Typical light induced absorbance change at 700 nm wavelength adopted from (Melis, 1989). The absorbance difference ΔA700 before illumination and at the saturation of the signal reflects the number of total Pheo molecules in the sample that are able to undergo photoreduction.

Photosystem kinetic and antenna size measurements

The rate of photoreduction of Q_A, or photooxidation of P700, induced under limiting light, is directly proportional to the number of Chl molecules associated with each photosystem (Melis and Anderson, 1983). In the presence of DCMU, Q_A^- can not be re-

oxidized and the light-energy absorbed by the antenna of thus closed reaction centers is dissipated as fluorescence. In addition to direct ΔA_{320} absorbance change kinetics, the Chl fluorescence induction kinetics can also (and more easily) used to provide a measure of the PSII Chl antenna size (Melis and Duysens 1978). In this case, the area above the fluorescence induction kinetics is a measure of the Q_A reduction rate, which is proportional to the rate of light capture by the light-harvesting antenna (Duysens and Sweers, 1963). The PSII reduction kinetics of plant and algal chloroplasts show biphasic reduction kinetics due to the existence of two types of PSII units differing in the size of the light-harvesting antenna complexes, namely $PSII_\alpha$ and $PSII_\beta$ (Melis and Homann, 1976). The initial slope of a semi-logarithmic blot defines the rate constant K_α of $PSII_\alpha$ reduction (Fig. 31), which has a larger antenna and thus faster reduction kinetics. The rate constant K_β of $PSII_\beta$ reduction (Fig. 33), is determined from the slope of the slower kinetics (Melis, 1989). This measurement also contains information about the relative abundance of $PSII_\alpha$ to $PSII_\beta$. The contribution of each PSII-type to the signal intensity is correlated with their relative abundance to each other in the sample and can be determined by the intercept of the slower kinetics with the y-axsis (Melis, 1989).
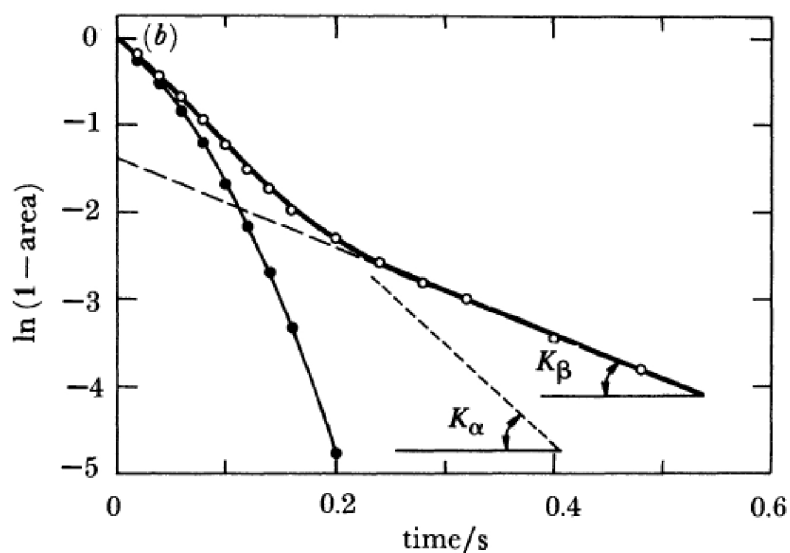
Figure 33: A representative semi logarithmic plot of the kinetics of the area over the fluorescence induction curve (open circles). The slope of the slower linear phase defined the rate constant K_β of $PSII_\beta$ photoreduction. The semi logarithmic plot of the kinetics of PSII, photoreduction (solid circles) deviated from linearity. The rate constant K_α was determined from the slope of the nonlinear curve (solid circles) at zero time (Figure curtsey: Melis, 1989).

In the presence of DCMU the electron transport chain is interrupted at the Q_A-Q_B site of PSII, thus electron donation from PSII to $P700^+$ is prevented. P700 oxidation kinetics in the light were measured by the differential absorption at 700 nm (ΔA_{700}). Under limiting light, the ΔA_{700} kinetics (Fig. 34), reflect the rate of P700 oxidation, which depend on the size of the light-harvesting antenna of PSI. The slope of semi-logarithmic plots of the ΔA_{700} kinetics define the reduction rate constant K_l of PSI, (Melis, 1989).
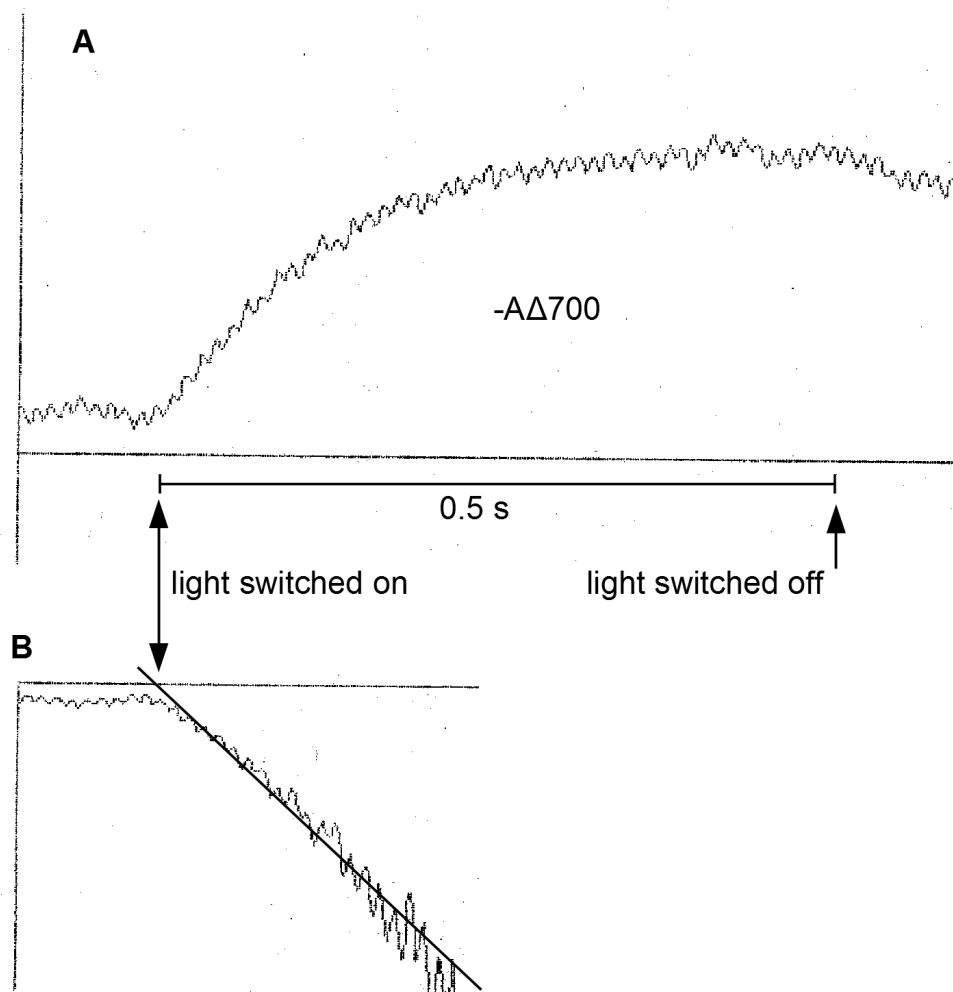
Figure 34: Typical light induced absorbance change at 700 nm wavelength for kinetic measurements of PSI. **A**: The rise of the -Δ700 absorbance is directly proportional to the size of the size of LHCI. **B**: semi logarithmic blot of the signal shown in A. The reduction kinetics K_l of PSI can be determined by the slope of the reduction in the semi logarithmic blot.

Calculating the functional Chl antenna size of the photosystems

The total number of Chl molecules in the sample (*Chl*) is the sum of the Chl

molecules associated with a given-type type of a photosystem (N_i), times the relative concentration of that photosystem in the sample (PS_i):

$$Chl = \sum_{i=1}^{n} N_i \cdot PS_i \qquad \textbf{(3)}$$

Thylakoid samples of the green algae *C. reinhardtii* contain both photosystems, PSI and PSII, while PSII has two distinct subpopulations, namely PSII$_\alpha$ and PSII$_\beta$. Thus,

$$Chl = N_\alpha \cdot PSII_\alpha + N_\beta \cdot PSII_\beta + N_I \cdot PSI \qquad \textbf{(4)}$$

The experimentally determined rate constants from the photosystem conversion kinetics (K_i) is directly proportional to the number of Chl molecules associated with a given reaction center times a constant (c_i) that depends on the quantum yield of photochemistry for the given photosystem:

$$K_i = c_i \cdot N_i \qquad \textbf{(5)}$$

For *C. reinhardtii*:

$$K_\alpha = c_\alpha \cdot N_\alpha \qquad \textbf{(6)}$$

$$K_\beta = c_\beta \cdot N_\beta \qquad \textbf{(7)}$$

$$K_I = c_I \cdot N_I \qquad \textbf{(8)}$$

The quantum yield of photochemistry for the photosystems are greater then 0.8 and thus similar (Avron and Ben-Hayyim, 1969; Sun and Sauer, 1971 ; Thielen and Van Gorkom, 1981 ; Ley and Mauzerall, 1982). For a solution of equation (4) we assumed *c* to be the same for all photosystems in the thylakoid membrane of *C. reinhardtii*:

$$c_\alpha = c_\beta = c_I = c \qquad \textbf{(9)}$$

$$K_\alpha = c \cdot N_\alpha \qquad \textbf{(10)}$$

$$K_\beta = c \cdot N_\beta \qquad \textbf{(11)}$$

$$K_I = c \cdot N_I \qquad \textbf{(12)}$$

By introducing (12) into the equations (10) and (11):

$$N_\alpha = \frac{K_\alpha \cdot N_I}{K_I} \qquad \textbf{(13)}$$

$$N_\beta = \frac{K_\beta \cdot N_I}{N_I} \qquad \textbf{(12)}$$

Equation (4) can now be solved using (13) and (14):

$$\frac{1}{N_I} = \frac{PS_I}{Chl} + \frac{K_\alpha}{K_I} \cdot \frac{PSII_\alpha}{Chl} + \frac{K_\beta}{K_I} \cdot \frac{PSII_\beta}{Chl} \qquad \textbf{(15)}$$

With the solution of N_I the equations (13) and (14) can be solved and thus the Chl molecules associated with each reaction center type is known.

5' and 3' RACE analysis

Total RNA was isolated from CC-503 cells in the early log phase of growth (0.5×10^6 cells ml^{-1}) using the Trizol reagent (Invitrogen, USA). Genomic DNA in these samples was digested according to the protocol provided by the Turbo DNA-free kit (Ambion, USA). The RNA sample was used immediately for the 5' and 3' RACE analysis using the FirstChoice RLM-RACE kit (Ambio, USA) and with suitable primers (HK297/HK298 outer/inner for 3' RACE; HK289/HK290 outer/inner for 5' RACE; Appendix B). The manufacture's protocol was followed in all procedures.

Transformation of *Chlamydomonas reinhardtii*

Complementation of the *tla2* strain was achieved by co-transformation of the mutant with BAC clones 08N24 and 36L15 and pBC1 plasmid (conferring paromomycin resistance) using the highly efficient electroporation method (Shimogawara et al., 1998). pBC1 contains a paromomycin resistance gene (selectable marker) operated under the control of the *C. reinhardtii Hsp70A* and *RbcS2* promoters (Sizova et al., 2001). Further, *CpFTSY* cDNA was cloned into pSL18 and incorporated into the genomic DNA of the *tla2* mutant using the conventional glass bead transformation protocol (Kindle, 1990). pSL18 also contains a paromomycin resistance gene (selectable marker) operated under the control of the C. reinhardtii *Hsp70A* and *RbcS2* promoters (Sizova et al., 2001) and linked to the PsaD promoter and terminator that was used to express the *CpFTSY* gene. Transformants were isolated upon screening independent cell lines on the basis of the measured the Chl *a/* Chl *b* ratio of the cells.

H6-CpFTSY and H6-CpSRP54 recombinant protein expression and purification

Standard procedures were employed for isolation of plasmid DNA, restriction analysis, PCR amplification, ligation and transformation (Sambrook et al. 1989). Plasmid DNA was prepared with a plasmid purification kit supplied by Qiagen (USA). Restriction enzymes were purchased from New England Biolabs (USA). They were used according to the recommendation of the vendors. Oligonucleotides were purchased from Bioneer (USA) and sequence details are given in Appendix B.

E. coli Rosetta (DE3) cells were transformed with plasmid pET28-H$_6$*FtsY* and pET28-H$_6$-*SRP54* and grown in 1 L of LB medium in 2 L Fernbach flasks on a rotary shaker at 37°C to a density of about OD$_{600}$=0.8. Protein expression was induced by the addition of 0.2 mM isopropyl β-D-thiogalacto-pyranoside (IPTG), and growth was continued for 4 h at 37°C. Cells were harvested by centrifugation at 4,500 g for 10 min at 4°C. Cells were resuspended in 10 ml of buffer I (50 mM Tris/HCl, pH 8.0, 400 mM NaCl, 10 mM b-ME) and lysed in a French pressure cell operated at 1,000 psi. To remove cell debris, the cell lysate was centrifuged at 13,000 g for 10 min at 4 °C. The supernatant was mixed with 4 ml of Ni^{2+}-NTA agarose resin (Qiagen, USA), equilibrated with buffer I, and incubated for 1 h at 4°C. The slurry was poured into a column, the flow-through was discarded and the slurry washed at 4°C with buffer I^5 (buffer I supplemented with 5 mM imidazole) and buffer I^{25} (buffer I supplemented with 25 mM imidazole). H$_6$-FtsY was eluted with buffer I^{200} (buffer I supplemented with 200 mM imidazole). Protein fractions were analyzed by SDS-PAGE and fractions containing H$_6$-FtsY were pooled. The purified protein was concentrated with Amicon Ultra 15, 30 kDa cut-off devices (Millipore, USA) to a final volume of 3 ml (2 - 3 mg/ml). The concentrate was centrifuged at 15,000 g for 5 min to remove precipitated protein. The resulting proteins were pure as judged by SDS-PAGE analysis and migrated to the expected molecular mass of about 39 kDa for the CpFTSY and 54 kDa for the CpSRP54 proteins, respectively (results not shown). Specific polyclonal antibodies were generated in rabbit against the recombinant purified H6-CpFtsY and H6-CpSRP54 protein (ProSci Incorporated, USA).

Analysis of genomic DNA flanking the plasmid insert site

Chlamydomonas reinhardtii genomic DNA flanking the plasmid insertion site was amplified using a TAIL-PCR protocol (Liu et al., 1995), optimized for Chlamydomonas genomic DNA, as recently described (Chen et al., 2003; Dent et al., 2005). Primers used for the TAIL-PCR are listed in Appendix B. Briefly, flanking genomic DNA was amplified by PCR from the region adjacent to the inserted pJD67 plasmid that was used for DNA insertional mutagenesis. Specific primers for primary, secondary, and tertiary reactions were designed (Appendix B). Two arbitrary degenerate primers were tested for amplification, HK030 and HK031, as previously described (Dent et al., 2005). The general TAIL-PCR protocol of Liu et al., (1995) was used with minor modifications for the various PCR amplification reactions. Nucleotide sequences of the resulting PCR products were obtained via an ABI3100 sequence analyzer. Chlamydomonas genomic DNA sequence information was obtained from the Chlamydomonas Genome Project website:

(http://genome.jgi-psf.org/Chlre4/Chlre4.home.html

and/or http://www.phytozome.net/chlamy/).

Cell fractionation of *Chlamydomonas reinhardtii*

Chlamydomonas reinhardtii strain CC-503 (cw92 mt+) was cultured photo-heterotrophically in Tris-Acetate-Phosphate (TAP) medium (Harris, 1989) upon illumination of 30 µmol photons $m^{-2}s^{-1}$ at 25°C. Cultures were grown to the early logarithmic phase with a maximum optical density of OD_{750} = 0.5 (~ $6X10^6$ cells ml^{-1}) in 250 ml Erlenmeyer flasks and harvested by centrifugation at 1,500 g for 5 min in a swinging bucket rotor (Eppendorf 5810 R centrifuge) prior to cell fractionation approaches. Cells were resuspended in cell lysis buffer (20 mM Hepes-KOH pH 7.5, 5 mM $MgCl_2$, 5 mM β-mercaptoethanol and 1 mM PMSF) at 4°C and broken in a French press chamber (Aminco, USA) at 600 psi. Total supernatant and total membrane were separated by centrifugation at 17,900 g for 30 min at 4°C. Total membranes were washed twice and resuspended to a final chlorophyll concentration of 1 mg/ml with thylakoid membrane buffer (20 mM Hepes-KOH pH 7.5, 300 mM sorbitol, 5 mM MgCl2, 2.5 mM EDTA, 10 mM KCl and 1 mM PMSF). Total cell pellets were resuspended to 1 mg Chl per mL with 1 volume of lysis buffer and 1 volume of 2x denaturing cell extraction buffer (0.2 M Tris, pH 6.8, 4% SDS, 2 M Urea, 1 mM EDA and 20% glycerol). In addition, all

denaturing samples were supplemented with a 5% (v/v) of β-mercaptoethanol and centrifuged at 17,900 g for 5 min prior to gel loading. Chloroplast enriched fractions were isolated from synchronized cultures with 12 h light/dark cycles of cell wall-deficient strain CC-503 (cw92 mt+) as in Zerges and Rochaix (1998).

Western blot analysis

Western blot analysis were performed with total protein from cell extracts, resolved in precast SDS-PAGE Any KDTM (BIO-RAD, USA). Loading of samples was based on equal protein, quantified by colorimetric Lowry-based Dc protein assay (BIO RAD, USA) and transferred to a polyvinylidene difluoride (PVDF) membrane (Immobilon-FL 0.45 μm, Millipore, USA) by a tank transfer system. Specific polyclonal antibodies raised against the LHCB(1-5), PSBO, CP43 and PSAL from *Arabidopsis thaliana* and CrCpFTSY, CrCpSRP54, D2, RBCL and ATPβ from *Chlamydomonas reinhardtii* were visualized by Supersignal West Pico Chemiluminiscent substrate detection system (Thermo Scientific, USA). The NIH Image 1.62 software was employed for the deconvolution and quantification of the Western blot bands.

Non-denaturing Deriphat-PAGE

Non-denaturing Deriphat-PAGE was performed following the method developed by Peter and Thornber (1991) with the following modifications; continuous native resolving PAGE gradients (4 to 15% final concentration of acrylamide) with no stacking gel were prepared. Isolated thylakoid membranes, from wild type, *tla2* mutant and *tla2-*complemented lines C1, C2, C3, and C4 were prepared with thylakoid membrane buffer and solubilized at a Chl concentration of 2, 1 and 0.4 mg/ml, respectively, with an equal volume of surfactant 10% n-Dodecyl-β-D-Maltoside (SIGMA). Thus, a 50:1 weight ratio of surfactant to Chl was used for the wild type. Thylakoid membranes were incubated on ice for 30 min and centrifuged at 17,900 g for 10 min in order to precipitate unsolubilized material. The amounts loaded per lane correspond to 10 μl of solubilized samples. Non-denaturing deriphat-PAGE was run for 2 h in the cold room at 5 mA constant current.

One-dimension non-denaturing deriphat PAGE strips were solubilized in the presence of Laemmli denaturing buffer (Laemmli et al. 1970) for 15 min and resolved in a denaturing 2 M Urea 12% SDS-PAGE second dimension. Acrylamide gels were stained with Coomassie (Fast gelTM Blue R, GE Healthcare, USA) or silver nitrate gel staining according to Wray et al.

(1981).

ACKNOWLEDGEMENTS

LITERATURE CITED

Aldridge C, Cain P, Robinson C (2009) Protein transport in organelles: Protein transport into and across the thylakoid membrane. FEBS J **276**: 1177-86

Allen JF, Forsberg J (2001) Molecular recognition in thylakoid structure and function. Trends Plant Sci **6**: 317–326

Amin P, Sy DAC, Pilgrim ML, Parry DH, Nussaume L, Hoffman NE (1999) Arabidopsis Mutants Lacking the 43- and 54-Kilodalton Subunits of the Chloroplast Signal Recognition Particle Have Distinct Phenotypes. Plant Physiol **121**: 61-70

Amunts A, Toporik H, Borovikova A, Nelson N (2010) Structure determination and improved model of plant photosystem I. J Biol Chem **285**: 3478–3486

Anderson JM (1986) Photoregulation of the composition, function and structure of thylakoid membranes. Annu Rev Plant Physiol **37**: 93-136

Arnon D (1949) Copper enzymes in isolated chloroplasts. Polyphenol oxidase in *Beta vulgaris*. Plant Physiol **24**: 1–15

Asakura Y, Hirohashi T, Kikuchi S, Belcher S, Osborne E, Yano S, Terashima I, Barkan A, Nakai M (2004) Maize mutants lacking chloroplast FtsY exhibit pleiotropic defects in the biogenesis of thylakoid membranes. Plant Cell **16**: 201–214

Asakura Y, Kikuchi S, Nakai M (2008) Non-identical contributions of two membrane-bound cpSRP components, cpFtsY and Alb3, to thylakoid biogenesis. Plant J **56**: 1007–1017

Ballottari M, Dall'Osto L, Morosinotto T, Bassi R (2007) Contrasting behavior of higher plant photosystem I and II antenna systems during acclimation. J Biol Chem **282**: 8947-8958

Bellafiore S, Ferris P, Naver H, Göhre V, Rochaix JD (2002) Loss of Albino3 leads to the specific depletion of the light-harvesting system. Plant Cell **14**: 2303–2314

Bals T, Dünschede B, Funke S, Schünemann D (2010) Interplay between the cpSRP pathway components, the substrate LHCP and the translocase Alb3: an *in vivo* and *in vitro* study. Febs Lett **584**: 4138-41441

Barber J (2003) Photosystem II: the engine of life. Q Rev Biophys **36**: 71–89

Buick R (2008) When did oxygenic photosynthesis evolve? Philos Trans R Soc Lond B Biol Sci **363**: 2731–2743

Castelletti S, Morosinotto T, Robert B, Caffarri S, Bassi R, Croce R (2003) Recombinant Lhca2

and Lhca3 subunits of the photosystem I antenna system. Biochemistry **42**:4226–4234

Chaddock AM, Mant A, Karnauchov I, Brink S, Herrmann RG, Klösgen RB, Robinson C (1995). A new type of signal peptide: central role of a twin-arginine motif in transfer signals for the DpH-dependent thylakoidal protein translocase. EMBO J. **14**: 2715–2722

Clark SA, Theg SM (1997) A folded protein can be transported across the chloroplast envelope and thylakoid membranes. Mol Biol Cell **8**: 923–934

Cline K, Ettinger WF, Theg SM (1992) Protein-specific energy requirements for protein transport across or into thylakoid membranes. Two lumenal proteins are transported in the absence of ATP. J Biol Chem **267**: 2688–2696

Croce R, Morosinotto T, Castelletti S, Breton J, Bassi R (2002) The Lhca antenna complexes of higher plants photosystem. Biochim Biophys Acta **1556**:29–40

Dauvillée D, Delhaye S, Gruyer S, Slomianny C, Moretz SE, d'Hulst C, Long CA, Ball SG, Tomavo S (2010) Engineering the chloroplast targeted malarial vaccine antigens in Chlamydomonas starch granules. PLoS One **5**: e15424

Davies JP, Yildiz F, Grossman AR (1994) Mutants of *Chlamydomonas* with aberrant responses to sulfur deprivation. Plant Cell **6**: 53–63

Davies JP, Yildiz F, Grossman AR (1996) Sac1, a putative regulator that is critical for survival of *Chlamydomonas reinhardtii* during sulfur deprivation. EMBO J **15**: 2150–2159

Debuchy R, Purton S, Rochaix JD (1989) The arginosuccinate lyase gene of *Chlamydomonas reinhardtii:* an important tool for nuclear transformation and for correlating the genetic and molecular maps of the ARG7 locus. EMBO J **8**: 2803–2809

DeLille J, Peterson EC, Johnson T, Moore M, Kight A, Henry R (2000) A novel precursor recognition element facilitates posttranslational binding to the signal recognition particle in chloroplasts. Proc Natl Acad Sci U.S.A. **97**: 1926–1931

Dent RM, Haglund CM, Chin BL, Kobayashi MC, Niyogi KK (2005) Functional genomics of eukaryotic photosynthesis using insertional mutagenesis of *Chlamydomonas reinhardtii*. Plant Physiol **137**: 545-56

Dewez D, Park S, García-Cerdán JG, Lindberg P, Melis A (2009) Mechanism of the REP27 protein action in the D1 protein turnover and photosystem-II repair from photodamage. Plant Physiol **151**: 88-99

Duysens LNM and Sweets HE (1963) Mechanisms of the two photochemical reactions in algae as studied by means of fluorescence. In: Studies on Microalgae and Photosynthetic

Bacteria, pp 353-372, Japan Society of Plant Physiology, Univ of Tokyo Press, Tokyo

Elrad D, Grossman AR (2004) A genome's-eye view of the light-harvesting polypeptides of *Chlamydomonas reinhardtii*. Curr Genet **45**: 61–75

Escoubas JM, Lomas M, LaRoche J and Falkowski PG (1995) Light intensity regulation of cab gene transcription is signalled by the redox state of the plastoquinone pool. Proc Nat Acad Sci **92**: 10237-10241

Falk S, Sinning I (2010) cpSRP43 Is a Novel Chaperone Specific for Light-harvesting Chlorophyll a,b-binding Proteins. J Biol Chem **285**: 21655–21661

Ferreira KN, Iverson TM, Maghlaoui K, Barber J, Iwata S (2004) Architecture of the photosynthetic oxygen-evolving center. Science **303**: 1831–1838.

Finazzi G, Chasen C, Wollman FA, de Vitry C (2003) Thylakoid targeting of Tat passenger proteins shows no delta pH dependence in vivo. EMBO J **22**: 807–815

Funke S, Knechten T, Ollesch J, Schuenemann D (2005) A unique sequence motif in the 54-kDa subunit of the chloroplast signal recognition particle mediates binding to the 43-kDa subunit. J Biol Chem **280**: 8912–8917

Ghirardi ML, Melis A (1984) Photosystem electron-transport capacity and light-harvesting antenna size in maize chloroplasts. Plant Physiol **74**:993 - 998

Glick RE, Melis A (1988) Minimum photosynthetic unit size in system-I and system-II of barley chloroplasts. Biochim Biophys Acta **934**: 151–155

Goforth RL, Peterson EC, Yuan J, Moore MJ, Kight AD, Lohse MB, Sakon J, Henry RL (2004) Regulation of the GTPase cycle in post-translational signal recognition particle-based protein targeting involves cpSRP43. J Biol Chem **279**: 43077–43084

Göhre V, Ossenbühl F, Crèvecoeur M, Eichacker LA, Rochaix JD (2006) One of two alb3 proteins is essential for the assembly of the photosystems and for cell survival in Chlamydomonas. Plant Cell **18**: 1454–1466

Gorman DS, Levine RP (1965) Cytochrome f and plastocyanin: their sequence in the photosynthetic electron transport chain of *Chlamydomonas reinhardtii*. Proc Natl Acad Sci USA **54**: 1665-1669

Greenwell HC, Laurens LML, Shields RJ, Lovitt RW, Flynn KJ (2010) Placing microalgae on the biofuels priority list: a review of the technological challenges. J R Soc Interface **7**: 703–726

Guenther JE, Melis A (1990) The physiological significance of photosystem II heterogeneity

in chloroplasts. Photosynth Res **23**: 105–109

Guskov A, Kern J, Gabdulkhakov A, Broser M, Zouni A, Saenger W (2009) Cyanobacterial photosystem II at 2.9 Å resolution and the role of quinones, lipids, channels and chloride". Nat Struct Mol Biol **16** (3): 334–42

Hageman J, Robinson C, Smeekens S, Weisbeek P (1986) A thylakoid processing protease is required for complete maturation of the lumen protein plastocyanin. Nature **324**: 567–569

Hankamer B, Lehr F, Rupprecht J, Mussgnug JH, Posten C, Kruse O (2007) Photosynthetic biomass and H2 production by green algae: from bioengineering to bioreactor scale-up. Physiol Plant **131**: 10-21

Harris EH (1989) The *Chlamydomonas* source book: a comprehensive guide to biology and laboratory use. Academic Press, San Diego

Harrison MA, Melis A (1992) Organization and stability of polypeptides associated with the chlorophyll *a-b* light-harvesting complex of photosystem-II. Plant Cell Physiol **33**: 627-637

High S, Henry R, Mould RM, Valent Q, Meacock S, Cline K, Gray JC, Luirink J (1997) Chloroplast SRP54 interacts with a specific subset of thylakoid precursor proteins. J Biol Chem **272**: 11622–11628

Hiyama T, Ke B (1972) Difference spectra and extinction coefficients of P700. Bioehim Biophys Acta **267**: 160 - 171

Hu Q, Sommerfeld M, Jarvis E, Ghirardi M, Posewitz M, Seibert M, Darzins A (2008) Microalgal triacylglycerols as feedstocks for biofuel production: perspectives and advances. Plant J. **54**: 621-39

Huesemann MH, Hausmann TS, BarthaR, Aksoy M, Weissman JC, Benemann JR (2009) Biomass productivities in wild type and pigment mutant of *Cyclotella sp.* (Diatom). Appl Biochem Biotechnol **157**: 507–526

Huner NPA, Oquist G, Sarhan F (1998) Energy balance and acclimation to light and cold. Trends in Plant Science **3**: 224-230

Hynds PJ, Robinson D, Robinson C (1998) The Sec-independent twin-arginine translocation system can transport both tightly folded and malfolded proteins across the thylakoid membrane. J Biol Chem **273**: 34868–34874

Jansson S, Pichersky E, Bassi R, Green BR, Ikeuchi M, Melis A, Simpson DJ, Spangfort M, Staehelin LA Thornber JP (1992) A nomenclature for the genes encoding the chlorophyll

a-b-binding proteins of higher plants. Plant Mol Biol Rep **10**: 242-253

Jaru-Ampornpan P, Shen K, Lam VQ, Ali M, Doniach S, Jia TZ, Shan SO (2010) ATP-independent reversal of a membrane protein aggregate by a chloroplast SRP subunit. Nat Struct Mol Biol **17**: 696-702

Jarvis P, Robinson C (2004) Mechanisms of Protein Import and Routing in Chloroplasts. Curr Biol 14: R1064–R1077

Jarvis P, Soll J (2002). Toc, Tic, and chloroplast protein import. Biochim Biophys Acta **1590**: 177–189.

Jonas-Straube E, Hutin C, Hoffman NE, Schuenemann D (2001) Functional Analysis of the Protein-interacting Domains of Chloroplast SRP43 J Biol Chem **276**: 24654–24660

Kim JH, Nemson JA, Melis A (1993) Photosystem-II reaction center damage and repair in the green alga Dunaliella salina: analysis under physiological and adverse irradiance conditions. Plant Physiol **103**: 181-189

Kim SJ, Robinson C, Mant A (1998) Sec/SRP-independent insertion of two thylakoid membrane proteins bearing cleavable signal peptides. FEBS Lett **424**: 105–108

Kindle KL (1990) High-frequency nuclear transformation of *Chlamydomonas reinhardtii*. Proc Natl Acad Sci USA **87:** 1228-1232

Kirk JTO (1994) Light and photosynthesis in aquatic ecosystems, 2nd edn. Cambridge University Press, Cambridge

Kirst H, Garcia-Cerdán JG, Zurbriggen A, Melis A (2012) Assembly of the light-harvesting chlorophyll antenna in the green alga *Chlamydomonas reinhardtii* requires expression of the *TLA2-CpFTSY* gene. Plant Physiol doi: http://dx.doi.org/10.1104/pp.111.189910

Klimyuk VI, Persello-Cartieaux F, Havaux M, Contard-David P, Schuenemann D, Meiherhoff K, Gouet P, Jones JD, Hoffman NE, Nussaume L (1999) A chromodomain protein encoded by the Arabidopsis CAO gene is a plant-specific component of the chloroplast signal recognition particle pathway that is involved in LHCP targeting. Plant Cell **11**: 87–99

Klostermann E, Droste Gen Helling I, Carde JP, Schuenemann D (2002) The thylakoid membrane protein ALB3 associates with the cpSecY-translocase in Arabidopsis thaliana. Biochem J **368**: 777–781.

Klösgen RB, Brock IW, Herrmann RG, Robinson C (1992) Proton gradient-driven import of the 16 kDa oxygen-evolving complex protein as the full precursor protein by isolated thylakoids. Plant Mol Biol **18**: 1031–1034.

Ko K, Cashmore AR (1989). Targeting of proteins to the thylakoid lumen by the bipartite transit peptide of the 33 kd oxygenevolving protein. EMBO J. **8:** 3187–3194.

Kok B, Forbush B, McGloin M (1970) Cooperation of charges in photosynthetic oxygen evolution. A linear four step mechanism. Photochem Photobiol **11:** 457–475

Laemmli UK (1970) Cleavage of structural proteins during the assembly of the head of bacteriophage T4. Nature **227**: 680–685

Laidler V, Chaddock AM, Knott TG, Walker D, Robinson C (1995) A SecY homolog in Arabidopsis thaliana. Sequence of a full-length cDNA clone and import of the precursor protein into chloroplasts. J Biol Chem **270**: 17664–17667

Ley AC, Mauzerall DC (1982) Absolute absorption cross sections for the photosystem II and the minimum quantum requirement for photosynthesis in *Chlorella vulgaris*. Biochim Biophys Acta **680**: 95-106

Liu YG, Mitsukawa N, Oosumi T, Whittier RF (1995) Efficient isolation and mapping of *Arabidopsis thaliana* T-DNA insert junctions by thermal asymmetric interlaced PCR. Plant J. **8**: 457–463

Liu Z, Yan H, Wang K, Kuang T, Zhang J, Gui L, An X, Chang W (2004) Crystal structure of spinach major light-harvesting complex at 2.72 A resolution. Nature **428**(6980):287-92.

Luirink J, Sinning I (2004) SRP-mediated protein targeting: structure and function revisited, BBA Mol Cell Res **1694**: 17-35

Mant A, Woolhead CA, Moore M, Henry R, Robinson C (2001) Insertion of PsaK into the thylakoid membrane in a "Horseshoe" conformation occurs in the absence of signal recognition particle, nucleoside triphosphates, or functional albino3. J Biol Chem **276**: 36200–36206

Masuda T, Tanaka A and Melis A (2003) Chlorophyll antenna size adjustments by irradiance in Dunaliella salina involve coordinate regulation of chlorophyll a oxygenase (CAO) and Lhcb gene expression. Plant Mol. Biol. **51**: 757-771

Mata TM,Martins AA, Caetano NS (2010) Microalgae for biodiesel production and other applications: a review. Renew Sust Energy Rev **14**: 217–232

Mawson BT, Morrissey PJ, Gomez A, Melis, A (1994). Thylakiod membrane development and differentiation: assembly of the chlorophyll a-b light-harvesting antenna complex and evidence for the origin of Mr = 19, 17.5 and 13.4 kDa proteins. Plant Cell Physiol **35**:341-351

Mayfield SP, Manuell AL, Chen S, Wu J, Tran M, Siefker D, Muto M, Marin-Navarro J (2007) Chlamydomonas reinhardtii chloroplasts as protein factories. Curr Opin Biotech **18**: 126-33

Melis A (1989) Spectroscopic methods in photosynthesis: photosystem stoichiometry and chlorophyll antenna size. Phil Trans R Soc London B **323**: 397–409

Melis A (1991) Dynamics of photosynthetic membrane composition and function Biochim Biophys Acta **1058:** 87-106

Melis A (1999) Photosystem-II damage and repair cycle in chloroplasts: what modulates the rate of photodamage *in vivo?* Trends in Plant Science **4**: 130-135

Melis A (2007) Photosynthetic H2 metabolism in *Chlamydomonas reinhardtii* (unicellular green algae). Planta **226**: 1075-1086

Melis A (2009) Solar energy conversion efficiencies in photosynthesis: minimizing the chlorophyll antennae to maximize efficiency. Plant Science **177**: 272-280

Melis A, Brown JS (1980) Stoichiometry of system I and system II in different photosynthetic membranes. Proc Natl Acad Sci USA **77**: 4712-4716

Melis A, Anderson JM (1983) Structural and functional organization of the photosystems in spinach chloroplasts: Antenna size, relative electron transport capacity, and chlorophyll composition. Biochim Biophys Acta **724**: 473-484

Melis A, Duysens LNM (1979) Biphasic energy conversion kinetics and absorbance difference spectra of PS II of chloroplasts. Evidence for two different PS II reaction centers. Photochem Photobiol **29**: 373-382

Melis A, Hart RW (1980) A laboratory-constructed sensitive difference spectrophotometer for the ultraviolet, visible, and far-red region of the spectrum. Carnegie Inst Wash Yb **19**: 170-173

Melis A, Homann PH (1976) Heterogeneity of the photochemical centers in system 11 of chloroplasts. Photochem Photobiol **23**: 343-350

Melis A, Neidhardt J, Benemann JR (1999) *Dunaliella salina* (Chlorophyta) with small chlorophyll antenna sizes exhibit higher photosynthetic productivities and photon use efficiencies than normally pigmented cells. J Appl Phycol **10**: 515–525

Melis A, Spangfort M, Andersson B (1987) Light-absorption and electron transport balance between photosystem-II and photosystem-I in spinach chloroplasts. Photochem Photobiol **45**: 129–136

Merchant SS, Prochnik SE, Vallon O, Harris EH, Karpowicz SJ, Witman GB, Terry A, Salamov A, Fritz-Laylin LK, Maréchal-Drouard L, et al. (2007) The Chlamydomonas genome reveals the evolution of key animal and plant functions. Science **318**: 245–250

Michelet L, Lefebvre-Legendre L, Burr SE, Rochaix JD, Goldschmidt-Clermont M. (2011) Enhanced chloroplast transgene expression in a nuclear mutant of Chlamydomonas. Plant Biotechnol J **9**: 565-574

Michl D, Robinson C, Shackleton JB, Herrmann RG, Klösgen RB (1994) Targeting of proteins to the thylakoids by bipartite presequences: CFoII is imported by a novel, third pathway. EMBO J **13**: 1310–1317

Mitchell P (1961) Coupling of phosphorylation to electron and hydrogen transfer by a chemi-osmotic type of mechanism". Nature **191** (4784): 144–148

Mitra M, Melis A (2010) Genetic and biochemical analysis of the TLA1 gene in *Chlamydomonas reinhardtii*. Planta **231**:729-740

Montané MH, Kloppstech K (2000) The family of light-harvesting-related proteins (LHCs, ELIPs, HLIPs): was the harvesting of light their primary function? Gene **258**: 1–8

Moore M, Goforth RL, Mori H, Henry R (2003) Functional interaction of chloroplast SRP/FtsY with the ALB3 translocase in thylakoids: Substrate not required. J Cell Biol **162**: 1245–1254

Mosavi LK, Cammett TJ, Desrosiers DC, Peng ZY (2004) The ankyrin repeat as molecular architecture for protein recognition. Protein Sci **13:** 1435–1448

Mould RM, Robinson C (1991) A proton gradient is required for the transport of two lumenal oxygen-evolving proteins across the thylakoid membrane. J Biol Chem **266**: 12189–12193

Müller P, Li XP, Niyogi KK (2001) Non-photochemical quenching: a response to excess light energy. Plant Physiol **125**: 1558–1566

Mussgnug JH, Wobbe L, Elles I , Claus C, Hamilton M, Fink A, Kahmann U, Kapazoglou A, Mullineaux CW, Hippler M, Nickelsen J, Nixon PJ, Kruse O (2005) NAB1 Is an RNA Binding Protein Involved in the Light-Regulated Differential Expression of the Light-Harvesting Antenna of *Chlamydomonas reinhardtii*. Plant Cell **17**: 3409-3421

Nakada E, Asada Y, Arai T, Miyake J (1995) Light penetration into cell suspensions of photosynthetic bacteria and relation to hydrogen production. J Ferment Bioengin **80**: 53-57

Nakajima Y, Ueda R (1997) Improvement of photosynthesis in dense microalgal suspension by reduction of light harvesting pigments. J Appl Phycol **9**: 503-510

Nakajima Y, Ueda R (1999) Improvement of microalgal photosynthetic productivity by reducing the content of light harvesting pigments. J Appl Phycol **11**: 195-201

Naus J, Melis A (1991) Changes of photosystem stoichiometry during cell growth in *Dunaliella salina* cultures. Plant Cell Physiol **32**: 569-575

Nilsson R, van Wijk K (2002) Transient interaction of cpSRP54 with elongating nascent chains of the chloroplast-encoded D1 proteins: cpSRP54 caught in the act. FEBS Lett **524**: 127–133

Nixon PJ, Diner BA (1992) Aspartate 170 of the photosystem II reaction center polypeptide D1 is involved in the assembly of the oxygen-evolving manganese cluster. Biochemistry **31:** 942-948

Ossenbühl F, Göhre V, Meurer J, Krieger-Liszkay A, Rochaix JD, et al. (2004) Efficient assembly of photosystem II in *Chlamydomonas reinhardtii* requires Alb3.1p, a homolog of *Arabidopsis* ALBINO3. Plant Cell **16**: 1790–1800

Pan X,Li M, Wan T, Wang L, Jia C, Hou Z, Zhao X, Zhang J, Chang W (2011) Structural insights into energy regulation of light-harvesting complex CP29 from spinach Nat Struct Mol Biol **18:** 309–315

Pasch JC, Nickelsen J, Schuenemann D (2005) The yeast split-ubiquitin system to study chloroplast membrane protein interactions. Appl Microbiol Biotechnol **69**: 440–447

Peter GF, Thornber PJ (1991) Biochemical composition and organization of higher plant photosystem I1 light-harvesting pigment proteins, J Biol Chem **266**: 16745-16754

Pilgrim ML, van Wijk KJ, Parry DH, Sy DA, Hoffman NE (1998) Expression of a dominant negative form of cpSRP54 inhibits chloroplast biogenesis in *Arabidopsis*. Plant J **13**: 177–186

Polle JE, Benemann JR, Tanaka A, Melis A (2000) Photosynthetic apparatus organization and function in wild type and a Chl *b*-less mutant of *Chlamydomonas reinhardtii*. Dependence on carbon source. Planta **211**: 335–344

Polle JEW, Kanakagiri S, Benemann JR, Melis A (2001) Maximizing photosynthetic efficiencies and hydrogen production in microalga cultures. In: Miyake J, Matsunaga T, San Pietro A (eds) BioHydrogen II. Pergamon/Elsevier Science, Oxford, pp 111–130

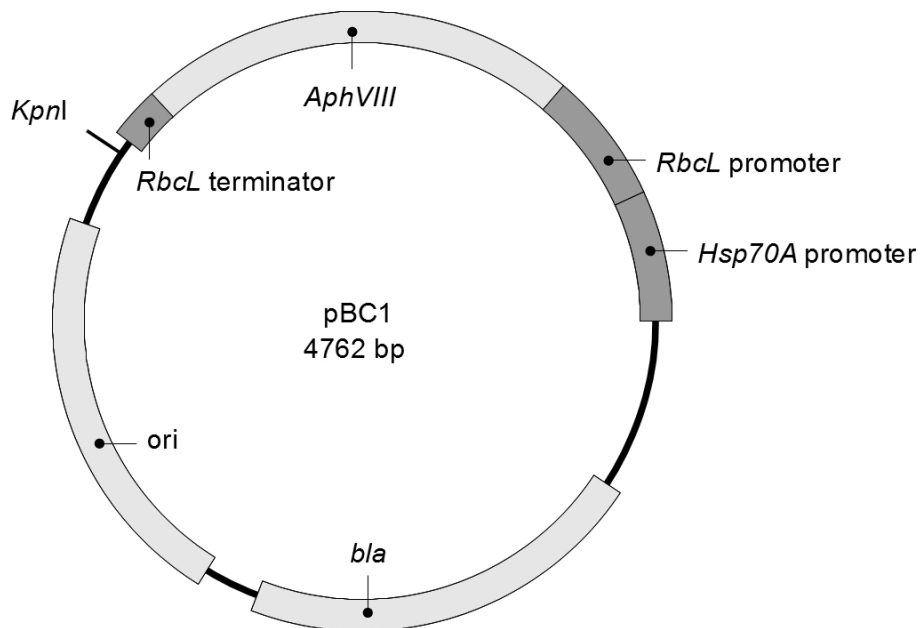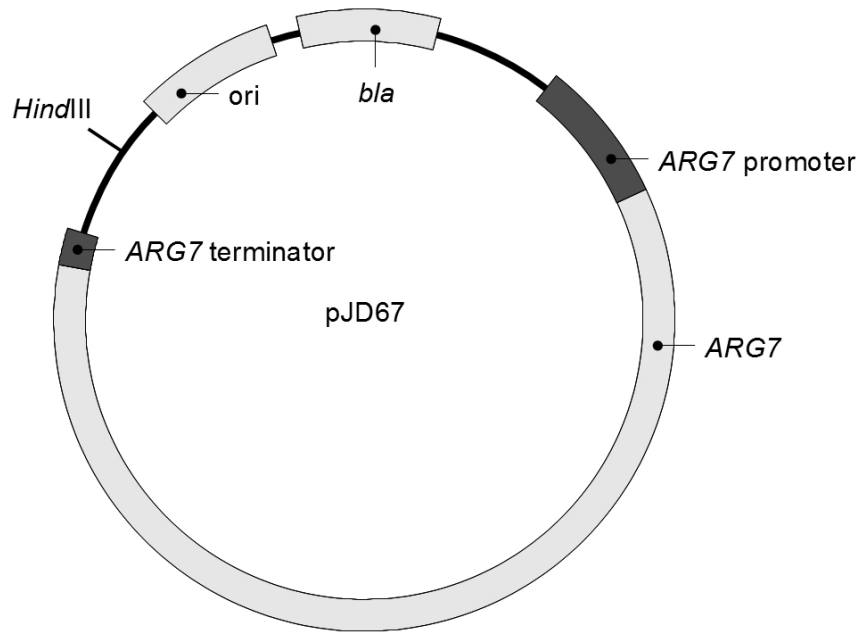**Polle JEW, Kanakagiri S, Jin E, Masuda T, Melis A** (2002) Truncated chlorophyll antenna size

of the photosystems: a practical method to improve microalgal productivity and hydrogen production in mass culture. Int J Hydrogen Energy **27**: 1257–1264

Polle JE, Kanakagiri SD, Melis A (2003) *tla1*, a DNA insertional transformant of the green alga *Chlamydomonas reinhardtii* with a truncated light-harvesting chlorophyll antenna size. Planta **217**: 49–59

Pool MR (2005) Signal recognition particles in chloroplasts, bacteria, yeast and mammals. Mol Membr Biol **22**: 3–15

Powles SB, Critchley C (1980) Effect of light intensity growth on photoinhibition of intact attached bean leaflets. Plant Physiol **65**: 1181-1187

Rodríguez-Ezpeleta N, Brinkmann H, Burey SC, Roure B, Burger G, Löffelhardt W, Bohnert HJ, Philippe H, Lang BF (2005) Monophyly of primary photosynthetic eukaryotes: green plants, red algae, and glaucophytes. Curr Biol **15**: 1325–1330

Sambrook J, Fritsch EF, Maniatis T (1989) Molecular Cloning: A Laboratory Manual. Cold Spring Harbor, NY: Cold Spring Harbor Laboratory Press

Shimogawara K, Fujiwara S, Grossman A, Usuda H (1998) High-efficiency transformation of *Chlamydomonas reinhardtii* by electroporation. Genetics **148**: 1821–1828

Schuenemann D, Amin P, Hartmann E, Hoffman NE (1999) Chloroplast SecY is complexed to SecE and involved in the translocation of the 33-kDa but not the 23-kDa subunit of the oxygen-evolving complex. J Biol Chem **274**: 12177–12182

Sizova IA, Fuhrmann M, Hegemann P (2001) A Streptonyces rimosus aphVIII gene coding for a new type phosphotransferase provides stable antibiotic resistance to *Chlamydomonas reinhardtii*. Gene **277**: 221-229

Smeekens S, Bauerle C, Hageman J, Keegstra K, Weisbeek P (1986). The role of the transit peptide in the routing of precursors toward different chloroplast compartments. Cell **46**: 365–375

Smith BM, Morrissey PJ, Guenther JE, Nemson JA, Harrison MA, Allen JF, Melis A (1990) Response of the photosynthetic apparatus in *Dunaliella salina* (green algae) to irradiance stress. Plant Physiol **93**: 1433–1440

Stengel KF, Holdermann I, Cain P, Robinson C, Wild K, Sinning I (2008) Structural basis for specific substrate recognition by the chloroplast signal recognition particle protein cpSRP43. Science **321**: 253–256

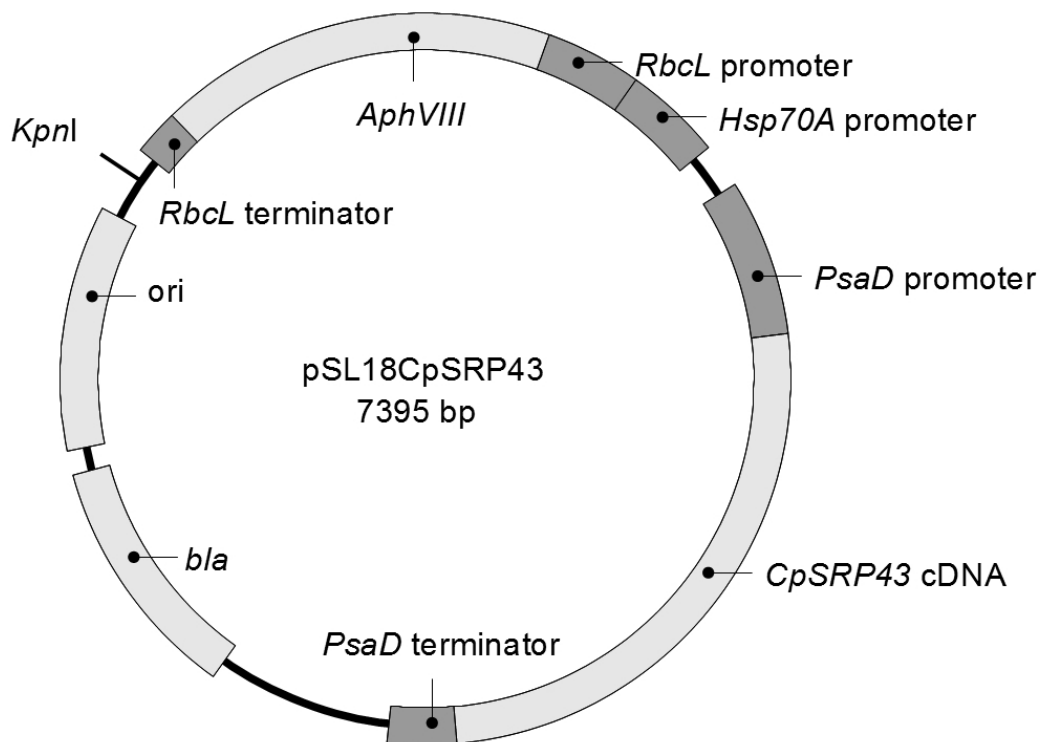**Sueoka N, Chiang KS, Kates JR** (1967) Deoxyribonucleic acid replication in meiosis of

Chlamydomonas reinhardtii.I. Isotopic transfer experiments with a strain producing eight zoospores. J Mol Biol **25**: 44-67

Sugiura M (1989) The chloroplast chromosomes in land plants. Annu Rev Cell Biol **5**: 51–70.

Sundberg E, Slagter JG, Fridborg I, Cleary SP, Robinson C, et al. (1997) ALBINO3, an *Arabidopsis* nuclear gene essential for chloroplast differentiation, encodes a chloroplast protein that shows homology to proteins present in bacterial membranes and yeast mitochondria. Plant Cell **9**:717–730

Tetali SD, Mitra M, Melis A (2007) Development of the light-harvesting chlorophyll antenna in the green alga *Chlamydomonas reinhardtii* is regulated by the novel Tla1 gene. Planta **225**: 813–829

Tu CJ, Schuenemann D, Hoffman NE (1999) Chloroplast FtsY, chloroplast signal recognition particle, and GTP are required to reconstitute the soluble phase of light-harvesting chlorophyll protein transport into thylakoid membranes. J Biol Chem **274:** 27219–27224

Tu CJ, Peterson EC, Henry R, Hoffman NE (2000) The L18 domain of light-harvesting chlorophyll proteins binds to chloroplast signal recognition particle 43. J Biol Chem 2**75**: 13187–13190

Tzvetkova-Chevolleau T, Hutin C, Noel LD, Goforth R, Carde JP, Caffarri S, Sinning I, Groves M, Teulon JM, Hoffman NE, Henry R, Havaux M, Nussaume L (2007) Canonical Signal Recognition Particle Components Can Be Bypassed for Posttranslational Protein Targeting in Chloroplasts. Plant Cell **19:** 1635–1648

Van Gorkom HJ (1974) Identification of the reduced primary electron acceptor of photosystem II as a bound semiquinone anion. Biochm Biophys Acta **347**:439-442

Webb MR and Melis A (1995) Chloroplast response in Dunaliella salina to irradiance stress. Effect on thylakoid membrane assembly and function. Plant Physiol **107**: 885-893

Woolhead CA, Thompson SJ, Moore M, Tissier C, Mant A, Rodger A, Henry R, Robinson C (2001) Distinct Albino3-dependent and -independent pathways for thylakoid membrane protein insertion. J Biol Chem **276**: 40841–40846

Wray W, Boulikas T, Wray VP, Hancock R (1981) Silver staining of proteins in polyacrylamide gels. Anal Biochem **118**: 197-203

Yakovlev AG, Taisova AS, Fetisova ZG (2002) Light control over the size of an antenna unit building block as an efficient strategy for light harvesting in photosynthesis. FEBS Lett **512**: 129-132

Yi L, Dalbey RE (2005) Oxa1/Alb3/YidC system for insertion of membrane proteins in mitochondria, chloroplasts and bacteria (review). Mol Membr Biol **22**: 101–111

Yuan J, Henry R, McCaffery M, Cline K (1994) SecA homolog in protein transport within chloroplasts: evidence for endosymbiont-derived sorting. Science **266**: 796–798

Zhang L, Aro EM (2002) Synthesis, membrane insertion and assembly of the chloroplast-encoded D1 protein into photosystem II. FEBS Lett **512**: 13–18

Zhang L, Paakkarinen V, Suorsa M, Aro EM (2001) A SecY homologue is involved in chloroplast-encoded D1 protein biogenesis. J Biol Chem **276**: 37809–37814

Zerges W, Rochaix JD (1998). Low-Density membranes are associated with RNA-binding proteins and thylakoids in the chloroplast of *Chlamydomonas reinhardtii*. J Cell Biol **140**: 101-110

Zouni A, Witt HT, Kern J, Fromme P, Krauss N, Saenger W, Orth P (2001) Crystal structure of photosystem II from *Synechococcus elongatus* at 3.8 A resolution. Nature **409**: 739–743

APPENDIX

Appendix A: plasmid maps

*Kpn*I

RbcL promoter

Hsp70A promoter

AphVIII

PsaD promoter

RbcL terminator

ori

pSL18CpFTSY
7248 bp

CpFTSY cDNA

bla

PsaD terminator

*Kpn*I

RbcL promoter

Hsp70A promoter

AphVIII

PsaD promoter

RbcL terminator

ori

pSL18CpSRP43
7395 bp

CpSRP43 cDNA

bla

PsaD terminator
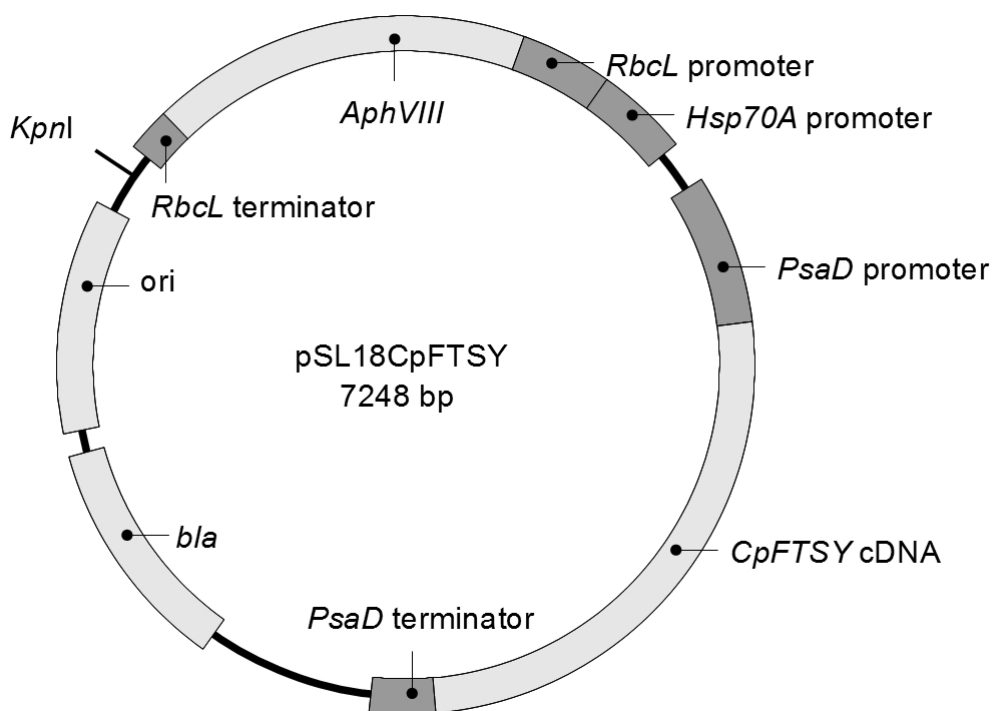
Appendix B: primer

Primer	Sequence	description	restriction site	anneal. temp. (°C)
HK001	ATTGGGCGCTCTTCCGCTTC	generates with HK002 and pJD67 as template DNA probe 1 in Fig. 3		60.7
HK002	GCCTCACTGATTAAGCATTGG	generates with HK001 and pJD67 as template DNA probe 1 in Fig. 3		54.0
HK003	TATGAGTAAACTTGGTCTGACAG	generates with HK004 and pJD67 as template DNA probe 2 in Fig. 3		52.0
HK004	AGGAAGAGTATGAGTATTCAAC	generates with HK003 and pJD67 as template DNA probe 2 in Fig. 3		49.3
HK081	GGAATAAGGGCGACACGGAAATGTT	generates with HK082 and pJD67 as template DNA probe 3 in Fig. 3		59.6
HK082	CTCCTTTCGCTTTCTTCCCTTCCTTTC	generates with HK081 and pJD67 as template DNA probe 3 in Fig. 3		59.4
HK094	CTAGAACTAGTGGATCCCCCGAAC	generates with HK095 and pJD67 as template DNA probe 4 in Fig. 3		58.2
HK095	CTCATCCTCCTCGCACTCGTG	generates with HK094 and pJD67 as template DNA probe 4 in Fig. 3		59.5
HK096	GTTACAAGCGACGAATGCGTG	generates with HK097 and pJD67 as template DNA probe 5 in Fig. 3		57.0
HK097	CTGTGCCGCACCTTGATGTC	generates with HK096 and pJD67 as template DNA probe 5 in Fig. 3		59.1
HK038	GTTTGTGCAGGAGTGTTGGGAG	generates with HK039 and pJD67 as template DNA probe 6 in Fig. 3		58.5
HK039	AACGTTCGATAGCTCTCACAAC	generates with HK038 and pJD67 as template DNA probe 6 in Fig. 3		54.9
HK120	CCACTACGTGAACCATCACCCTAATC	fine mapping of pJD67 sequence in *tla2*, generates a product with *tla2* gDNA template with HK082		58.8
HK119	AGACCGAGATAGGGTTGAGTGTTGT	fine mapping of pJD67 sequence in *tla2*, generates a product with *tla2* gDNA template with HK082		59.3
HK118	CAAATAGGGGGTTCCG	fine mapping of pJD67 sequence in		59.2

	CGCAC	*tla2*, generates a product with *tla2* gDNA template with HK082	
HK081	GGAATAAGGGCGAC ACGGAAATGTT	fine mapping of pJD67 sequence in *tla2*, generates no product with *tla2* gDNA template with HK082	59.6
HK082	CTCCTTTCGCTTTCTT CCCTTCCTTTC	fine mapping of pJD67 sequence in *tla2*	59.4
HK030	NTCGWGWTSCNAG C	arbitrary degenerate primers for TAIL PCR	
HK031	WGNTCWGNCANGC G	arbitrary degenerate primers for TAIL PCR	
HK121	GACGGTTTTTCGCCC TTTGACGTTGGAGTC	TAIL PCR primary reaction, between *bla* and and *ARG7* of pJD67	64.4
HK122	CACGTTCTTTAATAGT GGACTCTTGT	TAIL PCR secondary reaction, between *bla* and and *ARG7* of pJD67	54.9
HK123	CCAAACTGGAACAAC ACT	TAIL PCR tertiary reaction, between *bla* and and *ARG7* of pJD67	50.1
HK124	AACGCGAATTTTAAC AAAATATTAACGCTTA CAATTTAGG	TAIL PCR primary reaction, between *bla* and and *ARG7* of pJD67	58.8
HK125	TGGCACTTTTCGGGG AAATGT	TAIL PCR secondary reaction, between *bla* and and *ARG7* of pJD67	57.6
HK126	GGAACCCCTATTTGT TTATTTTTC	TAIL PCR tertiary reaction, between *bla* and and *ARG7* of pJD67	50.6
HK169	GTCCAACATGGGCGA CCGCATCTG	TAIL PCR primary reaction, chromosome 5, 5' of insertion	64.4
HK170	CATGCCGGACCCGTT AACATC	TAIL PCR secondary reaction, chromosome 5, 5' of insertion	58.5
HK171	CTCCACCAACGTCAC CATC	TAIL PCR tertiary reaction, chromosome 5, 5' of insertion	55.8
HK214	GTTTATCAGATTGAG AGTGAAACTGGCGCT TTAC	generates with HK215 and WT *C. reinhardtii* gDNA as template DNA 3' probe in Fig. 4	60.5
HK215	CATGACCTACTCGGC TCGCATTC	generates with HK214 and WT *C. reinhardtii* gDNA as template DNA 3' probe in Fig. 4	59.7
HK131	CAAAACCTCACCGTG	generates with HK132 and WT *C.*	59.6

	GATTTCGTCAA	*reinhardtii* gDNA as template DNA 5' probe in Fig. 4	
HK132	GGGTTGTAATACCGT GGGGATTTTAAGC	generates with HK131 and WT *C. reinhardtii* gDNA as template DNA 5' probe in Fig. 4	59.5
HK172	GTAGACTATCCTCCG CTTTGAATCAAGGTG	generates with HK173 and WT *C. reinhardtii* gDNA as template DNA deletion probe in Fig. 4	60.0
HK173	CACGAGGTGTTTGAC AGTTTGACTGAAG	generates with HK172 and WT *C. reinhardtii* gDNA as template DNA deletion probe in Fig. 4	59.6
HK193	GCTTACGTGGAGCGT GCAG	crude deletion mapping on chromosome 5 in *tla2,* 10.1 kb downstream of insertion. No product with HK194 using *tla2* gDNA.	59.1
HK194	CAGTTTACTGGTGTC GTGGTGCAC	crude deletion mapping on chromosome 5 in *tla2,* 10.1 kb downstream of insertion. No product with HK193 using *tla2* gDNA.	60.2
HK216	CACCCAACCTCACGA CCACAC	crude deletion mapping on chromosome 5 in *tla2,* 11.7 kb downstream of insertion. No product with HK216 using *tla2* gDNA.	60.5
HK217	CACCCCTCCGTGTTGT AACCTATACAACTAC	crude deletion mapping on chromosome 5 in *tla2,* 11.7 kb downstream of insertion. No product with HK216 using *tla2* gDNA.	61.1
HK220	GTGGCACTTTTAGTG TCAAGCATACTGTG	crude deletion mapping on chromosome 5 in *tla2,* 13.8 kb downstream of insertion. Gives product with HK216 using *tla2* gDNA.	59.7
HK221	GGATGCGGAATCCAC CCACAATG	crude deletion mapping on chromosome 5 in *tla2,* 13.8 kb downstream of insertion. Gives product with HK216 using *tla2* gDNA.	60.7
HK220	GTGGCACTTTTAGTG TCAAGCATACTGTG	fine deletion mapping on chromosome 5 in *tla2*. Gives product with HK240 using *tla2* gDNA.	59.7
HK238	CCTGAACAAGGGTG CATGCATG	fine deletion mapping on chromosome 5 in *tla2*. Gives product	59.2

		with HK240 using *tla2* gDNA.	
HK237	GTCGTGCGCGTTTCA GGTC	fine deletion mapping on chromosome 5 in *tla2*. No product with HK240 using *tla2* gDNA.	59.5
HK236	CTTCGGAACCATTGT TGATTACACTTCTATA AAGCAG	fine deletion mapping on chromosome 5 in *tla2*. No product with HK240 using *tla2* gDNA.	60.1
HK240	CACCTTATCATTCCTT ACAGCACAAATAAAG ACTGAG	fine deletion mapping on chromosome 5 in *tla2*.	59.9
HK128	GCTTTCTACCGCCTGT CTCAATACC	testing for co-segregation of the insertion with the *tla2* phenotype; on chromosome 5, next to insertion, if used with HK126 will only generate a product if insertion is present, expected size: 1.1 kb	59.3
HK126	GGAACCCCTATTTGT TTATTTTTC	testing for co-segregation of the insertion with the *tla2* phenotype; in pJD67 between bla and *ARG7*. If used with HK128 will only generate a product if insertion is present, expected size 1.1 kb	50.6
HK134	GCAGCCTTGCCAATC CCAAATAAGG	positive control for co-segregation PCR analysis. on chromosome 5 downstream of insertion, is present in *tla2* and WT, if used with HK135 expected size is 0.5 kb	60.8
HK135	CTCCGCACATTCACAT TAGGAGGTTC	positive control for co-segregation PCR analysis. on chromosome 5 downstream of insertion, is present in *tla2* and WT	59.4
HK289	GATGCGGTCCACGAT CTTCAGAG	outer 5' RACE for *CpFTSY*	59.5
HK290	GAGATGAGCACCTCC TCCAGCTC	inner 5' RACE for *CpFTSY*	61.0
HK297	CTGTGGTGCTGATTG TGGGAGTGAAC	outer 3' RACE for *CpFTSY*	61.6
HK298	CAAGATCGCGTACAA GTACGGCAAG	inner 3' RACE for *CpFTSY*	59.8

HK345	GGAATTCCATATGCAGACGACCGTGGGGCGCAAGTG	cloning of *CpFTSY* cDNA into pSL18	NdeI	68.8
HK346	GGAATTCCGTTCATTTACTTGGTGCCGGCAGTGG	cloning of *CpFTSY* cDNA into pSL18	EcoRI	65.1
pET28-ftsY_up	GGGAATTCCATATGGCCAACGCGGGCGGC	cloning *CpFTSY* cDNA into pET28	NdeI	70.7
pET28-ftsY_down	CCGGAATTCTTACTTGGTGCCGGCAGTGGC	cloning *CpFTSY* cDNA into pET28	EcoRI	70.2
pET28-srp54_up	GGGAATTCCATATGTCGGCCATGTTCGACAGCCTG	cloning *CpSRP54* cDNA into pET28	NdeI	69.6
pET28-srp54_down	CCGGAATTCCTATTTGGACGATGAGCCGAAGCCG	cloning *CpFSRP54* cDNA into pET28	EcoRI	69.1

Appendix C: SRP1 CpFTSY alignment

```
SRP1      MLDYVLAFERGGAILWALQFTSLRHNPLEAINALIRGCLLEERLGDNTFTFNPKSGAPQT 60
CpFTSY    ------------------------------------------------------------


SRP1      LKWTFHNGLGLVFVAVYQKTLSLLYVDELLSNVKEEFVNVYKPGQRGYRQFDETFNRLLR 120
CpFTSY    ------------------------------------------------------------


SRP1      DAESRADAAKKQPVMRSGPPANAKQGTGSQAVGAQAKKGTQAGKDASGDDDAGAARKGAA 180
CpFTSY    -------------------------MQTTVGRKCVASSAAGRSR----NVTVFRRCSR 29
                                   . :** :.  .: **:.     :. . *: :

SRP1      NGTVGNTSDGSAGGEDGDEDNVRAFDVSKLPKGMAGRGTRGVRGRPVPGAGSAKVSDTGK 240
CpFTSY    GGPVKVVAN--AGGEAG---------------------------------------PGF 47
          .*.*  .::  **** *                                        .*

SRP1      KKEEAPAAKVKKARNWNTMLSGGKGDTPTRIDYTEDGDGPGTSDMDLISGASASATEDEG 300
CpFTSY    LQRLGRVIKEKAAGDFDRFFAG-------------------------------------- 69
           :. . . * * * ::: :::*

SRP1      RGVGVSRMDVEEDEYDDSEFEDDEDLNNGAGGRGGSGAGASGSAAAAPKKQGLLASFVSS 360
CpFTSY    ----------------------------------------TSKTRERLGLVDEMLAL 86
                                                  :: : :: **: .:::

SRP1      LAMNVVGKAALSRADVEPALAEMKRKLMERNVAEEIAAQVCDSVGRNLEGQRLAGFTGVA 420
CpFTSY    WSL---------EDYEDSLEELEEVLISADFGPRTALKIVDRIREGVKAGRVK----SA 132
           ::          * * :* *::. *:. :.. . * :: * : ..::. *:      *

SRP1      AFVRNAFEEALSGILNKRSVDVLLDIKKSQARGKPYVIVFCGVNGVGKSTNLAKIAYWLG 480
CpFTSY    EDIRASLKAAIVELLTARGRSSELKLQ-----GRPAVVLIVGVNGAGKTTTVGKIAYKYG 187
           :* ::: *:  :*. *. .  *.::     *:* *:::  ****.**:*.:.**** *

SRP1      SHNIKVMIAACDTFRAGAVEQLKTHCARLRVPLYERGYEKDPAKVAYEAVRQAEK----- 535
CpFTSY    KEGAKVFLIPGDTFRAAAAEQLAEWSRRAGATIGAFREGARPQAVIASNLDDLRQRTCKD 247
          ... **::  . *****.*.***   . *  ..:        *  *  .: : .:

SRP1      --DGVHVVLVDTAGRMQDNQPLMRALSTLISLNNPNLVLFVGEALVGNDAVDQLTKFNKS 593
CpFTSY    ASDVYDLILVDTAGRLHTAYKLMEELALCKAAVSNALPGQPDETLLVLDGTTGLNMLN-- 305
            *  .::*******::    **. *:   :  .  *    .*:*: *.. *. :*

SRP1      LSDLAPTTAGAGGPGEGTGAVGRGQADGSALTRRHGGVIDGIVLTKFDTIDEKVGAALSM 653
CpFTSY    ---------------------------QAKEFNEAVRLSGLILTKLDGT-ARGGAVVSV 336
                                     .*   ...  :.*::***:*    : **.:*:

SRP1      VYTSGAPVMFVGCGQTYVDLKKLNVKSVVKSLLK---------- 687
CpFTSY    VDQLGLPVKFIGVGETAEDLQPFDPEAFAEALFPKVKEPATAGTK 381
          *    * ** *:* *:*  **: :: ::..::*:
```

CLUSTAL 2.1 multiple sequence alignment of CrSRP1 and CrCpFTSY. ClustalW amino acid sequence analysis of the putative CrCpFTSY identified in this work with the cytoplasmic SRalpha subunit homologue. Noted is the dissimilarity between these two proteins, both in terms of amino acid sequence identity and length of the respective polypeptides.

GLOSSARY

ATP	adenosine-5'-triphosphate
ADP	adenosine-5'-diphosphate
ARG7	argininosuccinate lyase
Asc	ascorbate
A_0	primary electron acceptor in PSI
A_1	phylloquinone, secondary plastoquinone electron acceptor in PSI
BAC	bacterial artificial chromosome
*Bam*HI	restriction enzyme, GGATCC
*Ban*II	restriction enzyme, GRGCYC
BSA	bovine serum albumin
Chl	Chlorophyll
CpSRP	Chloroplast signal recognition partile
CP43	*PSBC*-encoded 43 kDa PSII reaction center protein
CP47	*PSBB*-encoded 47 kDa PSII reaction center protein
CTAB	hexadecyltrimethylammonium bromide
DCMU	3-(3,4-dichlorophenyl)-1,1-dimethylurea
DNA	deoxyribonucleic acid
DNS	Desoxyribonukleinsäure
D1	*PSBA*-encoded 32 kDa PSII reaction center protein
D2	*PSBD*-encoded 34 kDa PSII reaction center protein
dNTP	deoxyribonucleoside triphosphate
DTT	dithiothreitol, reducing agent
DMSO	dimethyl sulfoxide
EDTA	ethylendiaminotetraacetic acid, metalloprotease inhibitor
Fd	ferredoxin
*Fsp*I	restriction enzyme, TGCGCA
GSH	glutathione, $C_{10}H_{17}N_3O_6S$
GST	glutathione-S-transferase
Hepes	(4-(2-hydroxyethyl)-1-piperazineethanesulfonic acid)
*Hind*III	restriction enzyme, AAGCTT
HS	high salt
IPTG	Isopropyl β-D-1-thiogalactopyranoside

*Kpn*I	restriction enzyme, GGTACC
LB	Luria Bertani bacterial medium
LHC	light-harvesting complex
mRNA	messenger ribonucleic acid
NADPH	nicotinamide adenine dinucleotide phosphate
NADP$^+$	oxidized nicotinamide adenine dinucleotide phosphate
*Nco*I	restriction enzyme, CCATGG
*Nde*I	restriction enzyme, CATATG
NPQ	non-photochemical quenching
NTA	nitrilotriacetic acid
ORF	open reading frame
PAGE	polyacrylamide gel-electrophoresis
PCR	polymerase chain reaction
Phe	pheophytin
P$_i$	inorcanic phosphate
Pmax	light-saturated rate of photosynthesis minus respiration
PMSF	phenylmethylsulfonyl fluoride
PQ	Plastoquinone
PQH$_2$	plastohydroquinone
PSI	Photosystem I
PSII	Photosystem II
*Pst*I	restriction enzyme, CTGCAG
PVDF	polyvinylidene difluoride
P680	Photosystem II primary donor
P700	Photosystem I primary donor
Q$_A$	primary plastoquinone electron acceptor in PSII
Q$_B$	secondary plastoquinone electron acceptor in PSII
RACE	rapid amplification of cDNA ends
RC	reaction center
*Sac*I	restriction enzyme, GAGCTC
SDS	sodium dodecylsulfate
*Sma*I	restriction enzyme, CCCGGG
SRP	Signal recognition particle
TAP	tris-acetate-phosphate medium

TAIL-PCR	thermal asymmetric interlaced PCR
tla	truncated light-harvesting antenna
TIC	translocon at the inner envelope membrane of chloroplasts
TOC	translocon at the outer envelope membrane of chloroplasts
Tris	2-amino-2-hydroxymethyl-1,3-propanediol
Triton X-100	polyethylene glycol p-(1,1,3,3-tetramethylbutyl)-phenyl ether
w/v	weight per volume
w/w	weight per weight
*Xma*I	restriction enzyme, CCCGGG
β-ME	β-mercaptoethanol

Curriculum Vitae

Personal information

Name: Henning Kirst
Address: Eiermarkt 15D
                 30938 Burgwedel, Germany
Telephone: +49-5139-2236
E-Mail: henning.kirst@googlemail.com
Birth date: 02. January 1980
Nationality: German

Education

July 2007 – present Leibniz Universität Hannover / UC Berkeley
                 Ph.D. student, "Assembly of the light-harvesting chlorophyll antenna in the green alga *Chlamydomonas reinhardtii* requires expression of the *CpFTSY* and *CpSRP43* genes"
Oct. 2006 – April 2007   Diploma thesis at UC Berkeley, "Aspects of the development of the chlorophyll antenna in photosynthesis"
Sept. 2004 - Mar. 2005   University of California at Berkeley, visiting scholar
Oct. 1999 - April 2007   Leibniz Universität Hannover, student of biochemistry
                 Emphases: • Biophysical-chemistry
                               • Plant physiology
1992 - 1999   High school; Großburgwedel

Teaching

Sept. 2005 - Mai 2006   Medizinische Hochschule Hannover, Teaching assistant

Publications

Kirst H, Garcia-Cerdán JG, Zurbriggen A, Melis A (2012) Assembly of the light-harvesting chlorophyll antenna in the green alga *Chlamydomonas reinhardtii* requires expression of the *TLA2-CpFTSY* gene. Plant Physiol 158: 930-945

Zurbriggen A, Kirst H, Melis A (2012) Isoprene production via the mevalonic acid pathway in *Escherichia coli* (bacteria). Bioenergy Res, in press

Presentations

Kirst H, Melis A (2010), Engineering the light-harvesting chlorophyll antenna size to improve photosynthetic solar energy conversion efficiency. Western photosynthesis conference, Pacific Grove

Kirst H, Melis A (2009), Engineering the light-harvesting chlorophyll antenna size to improve photosynthetic solar energy conversion efficiency. American Society of Plan Biology, Honolulu

Kirst H, Melis A (2008), Isolation and characterization of photosynthetic chlorophyll antenna mutants by DNA insertional mutagenesis, American Society for Photobiology, Burlingame

Erklärung zur Dissertation

gemäß §6(1) der Promotionsordnung der Naturwissenschaftlichen Fakultät der Gottfried Wilhelm Leibniz Universität Hannover für die Promotions zum Dr. rer. nat.

Hierdurch erkläre ich, dass ich meine Dissertation mit dem Titel:

"Assembly of the light-harvesting chlorophyll antenna in the green alga *Chlamydomonas reinhardtii* requires expression of the *CpFTSY* and *CpSRP43* genes"

selbständig verfasst und die benutzten Hilfsmittel und Quellen sowie gegebenenfalls die zu Hilfeleistungen herangezogene Institutionen vollständig angegeben habe.

Die Dissertation wurde nicht schon als Masterarbeit, Diplomarbeit oder andere Prüfungsarbeit verwendet.

Henning Kirst